

Title	有機溶媒を用いない手法での機能性ポリビニルアルコール材料の開発
Author(s)	田岡, 裕輔
Citation	
Issue Date	2024-03
Type	Thesis or Dissertation
Text version	ETD
URL	<a href="http://hdl.handle.net/10119/19070">http://hdl.handle.net/10119/19070</a>
Rights	
Description	Supervisor: 松村 和明, 先端科学技術研究科, 博士

Doctoral Dissertation

Development of Functional Poly(vinyl alcohol) Materials  
Prepared without Organic Solvent

Yusuke Taoka

Supervisor: Kazuaki Matsumura

Graduate School of Advanced Science and Technology

Japan Advanced Institute of Science and Technology

Materials Science

March 2024

Poly(vinyl alcohol) (PVA) is a synthetic polymer with hydroxyl groups. It is used in various fields due to its chemical resistance, biodegradability, and biocompatibility. It is well known that PVA exhibits excellent mechanical properties due to strong intermolecular hydrogen bonds. Another important characteristic of PVA is that it is water soluble, which is unusual for a synthetic resin. Since it is water soluble, there is no need to use organic solvents or other solvents when processing. However, there are currently many challenges to processing using only water as a solvent, and dimethyl sulfoxide (DMSO) and other solvents are often used. In addition, hydrogen bonding in PVA prevents a high degree of molecular orientation, which inhibits the improvement of mechanical properties of PVA fibers and other materials. PVA has several problems: its melting and decomposition points are close to each other, it has almost no thermoplasticity, and it cannot be molded and processed by heat. Previous studies have reported that the addition of lithium salts is an effective way to reduce hydrogen bonds in PVA and slow the crystallization rate. However, few specific studies have been conducted to determine the extent to which these effects are effective in processing PVA.

The present focused on the effect of lithium salt addition on the ductility of PVA fibers and on the mechanical properties, crystal structure, and thermoplasticity of PVA prepared by hot pressing with lithium salt addition. The stretchability of PVA fiber spun by adding lithium iodide (LiI) to PVA was greatly improved and showed high mechanical properties. This is because stretching in a state where hydrogen bonds are reduced by LiI reduces orientation defects during stretching and increases the drawing ratio. The highly stretched fibers have high molecular orientation and exhibit superior mechanical strength compared to fibers without LiI addition. High-strength PVA fibers can be used as reinforcing fibers in fiber reinforced plastics (FRP) and will play an important role in the fiber industry in the future. Lithium salts reduce the crystallinity and melting point of PVA, which may provide thermoplasticity. The physical properties of PVA prepared by adding lithium salt (lithium halide) and hot pressing showed a lower melting point, lower crystallinity and lower mechanical strength compared to No salt PVA. This effect was higher in the order  $\text{LiCl} > \text{LiBr} > \text{LiI}$ . The thermoplasticity was confirmed by the decrease in crystallinity and melting point. There was little difference in the mechanical strength of PVA before and after thermoforming. In other words, lithium salt can improve the processability of PVA.

Syndiotactic PVA (sPVA) was difficult to handle because it hardly dissolves in water or organic solvents. However, sPVA-H could be adjusted by using a hot press. Compared to atactic PVA hydrogel (aPVA-H), sPVA-H exhibited higher mechanical strength and crystallinity at lower water content. This is attributed to the high stereoregularity of sPVA and its easy crystallization.

Keywords: Poly(vinyl alcohol), Lithium salts, Hydrogen bond, Crystallization, Thermoplasticity, Tacticity

## Acknowledgment

In conducting this research, I would like to thank my supervisor, Prof. Dr. Kazuaki Matsumura, for his careful guidance and advice on everything from research preparation to writing and presentation of the paper. Also, if I had any questions, I could always go to him for advice, and he was always available to help me even though he was very busy. It is thanks to Prof. Matsumura guidance that I was able to carry out and complete my research. I would like to express my deepest gratitude and appreciation.

I would like to express my sincere gratitude to Prof. Dr. Masayuki Yamaguchi (JAIST), Prof. Dr. Noriyoshi Matsumi (JAIST), Prof. Dr. Takahiro Hohsaka (JAIST), and Prof. Dr. Makoto Ota (Institute of Fluid Science, Tohoku University) for reviewing my thesis and providing useful advice.

I deeply grateful to Dr. Takumitsu Kida (University of Shiga Prefecture) for his help in many ways, from the use of the measurement equipment to advice in research.

I deeply grateful to Dr. Riza Asmaa Saari for her many helpful suggestions in carrying out the research.

Asst. Prof. Dr. Rajan Robin and Ms. Keiko Kawamoto of the Matsumura Laboratory taught me a lot and enabled me to carry out my research. Also, everyone in the laboratory helped me in various situations. I would like to express my deepest gratitude.

Finally, I would like to thank my family and friends for their support and encouragement during my long student life.

Yusuke Taoka

# Contents

Chapter 1: General Introduction .....	1
1 General Introduction.....	2
1-1 Poly(vinyl alcohol) .....	3
1-1-1 Development and characteristics of poly(vinyl) alcohol .....	3
1-1-2 Molecular chain structure of PVA .....	4
1-1-3 Tacticity of PVA .....	5
1-2 Modification of PVA.....	6
1-2-1 Functionalization of polymer .....	6
1-2-2 Functionalization of PVA with metal salts.....	7
1-2-3 Modification of PVA hydroxyl groups.....	9
1-3 PVA fiber.....	10
1-3-1 PVA fiber.....	10
1-3-2 Wet spinning process .....	10
1-3-3 Mechanical properties enhancement of PVA fiber .....	11
1-4 Composite materials .....	14
1-5 Polyvinyl alcohol hydrogel (PVA-H) .....	15
1-5-1 Hydrogel and structure.....	15
1-5-2 PVA hydrogel methods .....	16
1-6 Applications of PVA-H.....	18
1-6-1 Application as artificial joint cartilage.....	18
1-6-2 Blood vessel biomodel using PVA-H .....	20
1-7 Purpose of this research .....	21
1-8 References .....	22

Chapter 2: Enhancing the mechanical properties of Poly (vinyl alcohol) fibers by lithium iodide addition.....	32
2-1 Introduction.....	33
2-2 Materials and methods.....	35
2-2-1 Materials .....	35
2-2-2 Sample preparation.....	35
2-2-3 PVA fiber spinning.....	35
2-2-4 Secondary stretching and heat-treatment .....	36
2-2-5 Measurements.....	39
2-2-5-1 Differential scanning calorimetry (DSC) .....	39
2-2-5-2 Scanning electron microscope (SEM) .....	39
2-2-5-3 Tensile test.....	39
2-2-5-4 Wide-angle X-ray diffraction (WAXD) .....	40
2-2-5-5 Measurement of lithium concentration.....	40
2-3 Results and Discussion .....	41
2-3-1 Fiber surface observation and fiber diameter measurement by SEM.....	41
2-3-2 Thermal analysis of PVA fiber .....	43
2-3-3 Secondary stretching with LiI addition.....	44
2-3-4 Tensile test.....	45
2-3-5 Orientation analysis by 2D-WAXD.....	54
2-3-6 Measurement of lithium concentration .....	57
2-3-7 Summary of this study .....	58
2-4 Conclusion .....	59
2-5 References.....	60

Chapter 3: Effect of lithium halide on mechanical properties and thermoplasticity of Poly(vinyl alcohol) molded by hot press .....	67
3-1 Introduction.....	68
3-2 Materials and methods.....	70
3-2-1 Materials .....	70
3-2-2 Preparation of PVA-H.....	70
3-2-3 Washing of salts.....	71
3-2-4 Thermal melt forming.....	71
3-2-5 Measurements.....	71
3-2-5-1 Measurement of light transmittance .....	71
3-2-5-2 Fourier transform infrared spectroscopy (FT-IR).....	71
3-2-5-3 Tensile test.....	72
3-2-5-4 Dynamic mechanical analysis (DMA) .....	72
3-2-5-5 Measurement of water content .....	72
3-2-5-6 Differential Scanning Calorimetry (DSC) .....	73
3-2-5-7 Measurement of residual lithium concentration.....	73
3-3 Results and Discussion .....	74
3-3-1 Appearance of PVA with lithium salt added .....	74
3-3-2 FT-IR.....	75
3-3-3 DSC .....	80
3-3-4 Tensile test.....	83
3-3-5 Dynamic mechanical analysis .....	88
3-3-6 Measurement of water content .....	90
3-3-7 Testing thermoplasticity by hot press .....	92

3-3-8 Measurement of lithium concentration .....	94
3-3-9 Summary of this study .....	95
3-4 Conclusion .....	95
3-5 References.....	96
<b>Chapter 4: Effect of gelation and heat-treatment of syndiotactic-rich Poly(vinyl alcohol) on Mechanical Properties.....</b>	<b>100</b>
4-1 Introduction.....	101
4-2 Materials and methods.....	104
4-2-1 Materials .....	104
4-2-2 Gelation of PVA .....	104
4-2-3 Heat-treatment and swelling .....	105
4-2-4 Measurements.....	106
4-2-4-1 Fourier transform infrared spectroscopy (FT-IR) .....	106
4-2-4-2 Water content.....	106
4-2-4-3 Fourier transform infrared spectroscopy (FT-IR) .....	106
4-2-4-4 Differential Scanning Calorimetry (DSC) .....	107
4-2-4-5 Tensile test.....	107
4-2-4-6 Wide-angle X-ray diffraction (WAXD) .....	108
4-2-4-6 Small-angle X-ray scattering (SAXS) .....	108
4-3 Results and Discussion .....	109
4-3-1 Syndiotacticity.....	109
4-3-2 Water content.....	111
4-3-3 FT-IR.....	112
4-3-4 DSC .....	115

4-3-5 Tensile test.....	117
4-3-6 WAXD .....	119
4-3-7 SAXS .....	120
4-4 Conclusion .....	122
4-5 References.....	123
<b>Chapter 5: General Conclusion .....</b>	<b>126</b>
5-1 General Conclusion .....	127
5-2 Future Scope .....	129
<b>Achievements.....</b>	<b>130</b>

# *Chapter 1: General introduction*

# Chapter 1: General Introduction

## 1. General Introduction

In this thesis, I present a study focusing on the enhancement of mechanical properties in polyvinyl alcohol (PVA) fibers through the utilization of lithium salts, the functionalization of PVA hydrogels, and the gelation of highly stereoregular PVA as the foundational material. The concept of this study is without using dimethyl sulfoxide (DMSO). DMSO is often used as a good solvent for PVA, but it has problems such as high skin penetration and strong oxidizing activity. In particular, its permeability is dangerous because of the possibility of introducing toxic substances into the body. Recently, the Sustainable Development Goals (SDGs) have been mentioned on various occasions, and there is a movement to minimize the use of organic solvents that tend to cause environmental pollution. In addition, the need for biodegradable materials is also important, given the serious marine pollution problems caused by microplastics. In this regard, PVA has a number of advantages, such as being water soluble and biodegradable. However, deficiencies such as lack of mechanical strength are a practical obstacle. In this study, we used "DMSO free" as a solvent for PVA fiberization and gelation, aiming at modification and higher functionality of PVA. Figure 1 shows an image of the research outline.

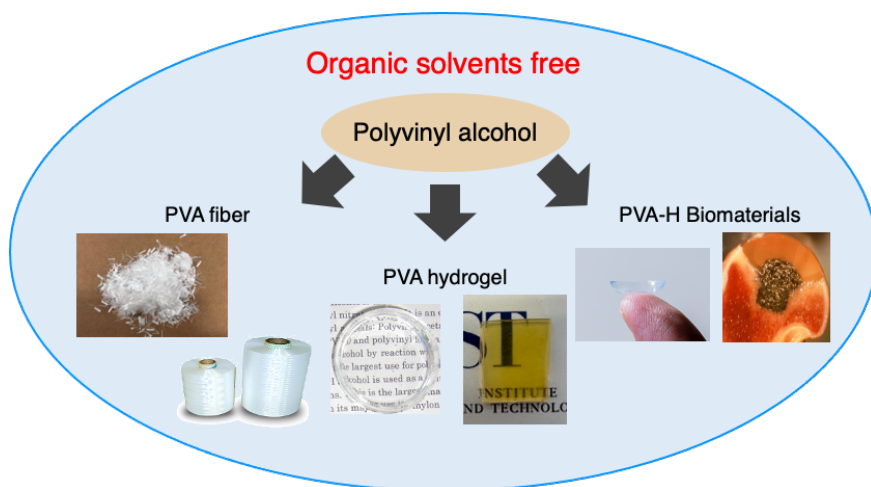


Figure 1-1 Schematic diagram of this research.

## 1-1. Poly(vinyl) alcohol

### 1-1-1. Development and characteristics of poly(vinyl) alcohol

Polyvinyl alcohol (PVA) is, by its name, a polymer of vinyl alcohol. However, the vinyl alcohol monomer is so unstable that it cannot exist by itself and is immediately converted to acetaldehyde by keto-enol tautomerism (Figure 1-2). Therefore, PVA is known to be a special polymer that cannot be synthesized by polymerization due to the absence of the monomer precursor.

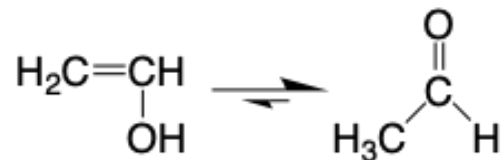


Figure 1-2 Keto-enol tautomerism of vinyl alcohols.

PVA was prepared by H. Heahnel and W. O. Herrmann in Germany in 1924 by mixing polyvinyl acetate (PVAc) with an alkaline solution to saponify the ester [1]. This method is still used today to synthesize PVA. A typical production method is shown in Figure 1-3. PVAc is obtained by synthesizing vinyl acetate monomer from ethylene, oxygen, and acetic acid, and then polymerizing the resulting vinyl acetate to form PVAc, which is saponified with an alkali such as sodium hydroxide [2].



Figure 1-3 Production process of polyvinyl alcohol.

PVA has a hydroxyl group, which makes it uniquely water soluble among synthetic resins. It is also characterized by high stability due to its strong resistance to organic solvents and alkaline substances. Other features include biodegradability, low toxicity, and high biocompatibility. Its various applications include paper processing agents, emulsion dispersants, films, and

polymerization stabilizers for vinyl chloride resin. In particular, the processing of PVA into textiles is well known, and W. O. Herrmann and H. Heahnel, who discovered the alkali saponification of PVAc, showed that PVA could be made into fiber by wet spinning [3]. Subsequently, Sakurada et al. in Japan improved the water resistance of PVA fiber by acetalization and mass-produced it as Vinyon. Recently, research as a biomaterial has also been conducted extensively [4].

#### 1-1-2. Molecular chain structure of PVA

In the industrial polymerization process of PVA, monomer units are oriented in the same direction to produce polymer chains with substituents on their carbon atoms. The result is known to be the formation of head-to-tail or 1,3-glycol structures [5, 6]. The arrangement of such structures reflects the selectivity of monomer addition in free radical polymerization: despite the predominance of 1,3-glycol structures, head-to-head or tail-to-tail structures with regularly alternating pairs of substituents on successive carbon atoms are also possible. It has been shown that head-to-head or tail-to-tail structures are also possible. These arrangements result in 1,2-glycol structures. The marketed PVA products contain about 2% of the head-to-head or tail-to-tail type with 1,2-glycol structural units, but this is thought to have little effect on the properties of PVA [7]. Figure 1-4 shows the head-to-head and head-to-tail structures of PVA.

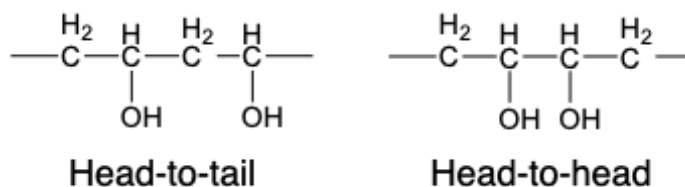


Figure 1-4 Head-to-head and head-to-tail structures of PVA.

### 1-1-3. Tacticity of PVA

The three tacticity of PVA (atactic, syndiotactic, and isotactic) are determined by the type of vinyl ester monomer used in the production of PVA. The PVA commonly used is atactic PVA, which has a random structure in which the side chains with hydroxyl groups are arranged relative to the main chain of the polymer. Atactic PVA is obtained by polymerization and saponification of vinyl acetate. To obtain PVA with high syndiotactic and isotactic stereo-regularity, vinyl ester monomers such as vinyl pivalate, vinyl benzoate, and vinyl formate, and vinyl ether monomers such as benzyl vinyl ether and *tert*-butyl vinyl ether are used [8-13]. These monomers are characterized by having bulky substituents. Monomers with these bulky substituents can polymerize polymers with predominant stereo-regularity by inducing steric hindrance between neighboring substituents upon polymerization [14, 15]. High molecular weight PVA with high syndiotacticity can be tailored from the polymerization and saponification of vinyl pivalate.

It is well known that when the stereo-regularity of PVA is high, it has a significant impact on physical properties due to its easy crystallization and increased crystallinity. It has been reported that increased syndiotacticity affects physical properties such as solvent solubility, melting point, heat resistance, and mechanical strength [16, 17]. For example, PVA, which is water soluble, can be dissolved in water or hot water, but syndiotactic PVA is almost insoluble in water; it is also almost insoluble in dimethyl sulfoxide (DMSO), which is often used as a good solvent for PVA, except under heating conditions. Figures 1-5 show the stereoregularity of atactic, syndiotactic, and isotactic PVA.

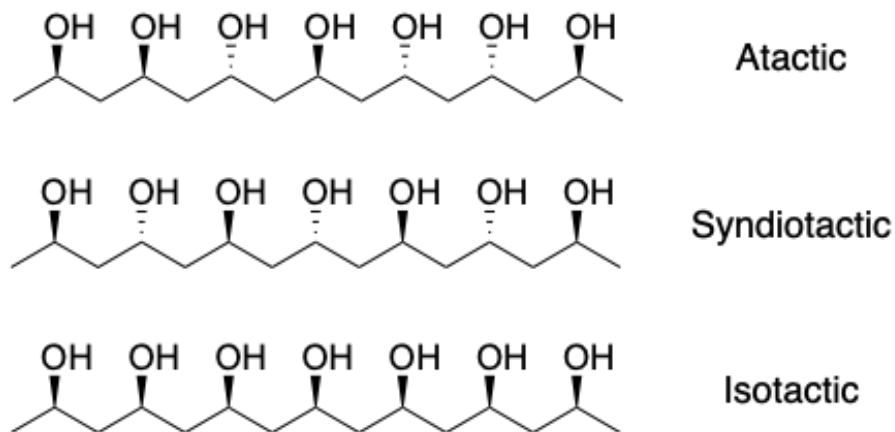


Figure 1-5 Tacticity of PVA.

## 1-2. Modification of PVA

### 1-2-1. Functionalization of polymer

The use of a single plastic material is often limited by its physical properties and other issues. For this reason, the use of plasticizers and additives to improve physical properties is used in a variety of plastic products. Improvement by additives is superior to synthesizing new materials in terms of cost. On the other hand, many plasticizers are carcinogenic, and their use is a cause for concern. However, it is true that modifications have improved glass transition temperature, heat resistance, crystallinity, molecular orientation, and mechanical strength, and have improved functional aspects [18-20]. For example, the addition of lithium halide such as lithium bromide (LiBr) to polyamide 6 (PA6) and polymethyl methacrylate (PMMA) was reported to improve optical and mechanical properties [21, 22]. These effects have also been confirmed by addition to PVA, and there are actually several research reports as described in 1-2-2.

## 1-2-2. Functionalization of PVA with metal salts

The addition of alkali metal salts, including lithium halides, to PVA is known to affect the melting point, crystallinity, and mechanical properties. O.N. Tretinnikov and S.A. Zagorskaya investigated the crystallinity of PVA films prepared by adding lithium chloride (LiCl), sodium fluoride (NaF), and other alkali halides of metals were added to aqueous PVA solutions and the crystallinity of the films prepared by the casting method was investigated using Fourier transform infrared spectroscopy (FT-IR). The results showed that the crystallinity of PVA increased for the salts excluding LiCl, while the films containing LiCl showed a significant decrease in crystallinity. They also reported that the maximum value of the stretching vibration of the hydroxyl groups was shifted compared to the film without salt, and that the magnitude and direction of this shift depended on the type and radius of the ions [23]. They further investigated PVA films with lithium bromide (LiBr) and lithium iodide (LiI) in addition to LiCl by FT-IR. The results showed that the crystallinity of the films containing lithium salts decreased to 0~7% compared to the films containing non-lithium salts. In addition, the crystallinity increased in films containing non-lithium salts. This is because as water evaporates from the film during formation, the hydroxyl groups of PVA become free and can form hydrogen bonds with each other. At this time, competition for water molecules occurs between the non-lithium salt and the hydroxyl group, which increases according to water evaporation. As a result, the hydroxyl group passes the bound water molecules to the salt ion. This process of  $\text{-OH}\cdots\text{H}_2\text{O}$  hydrogen bond cleavage and  $\text{-OH}$  to  $\text{-OH}$  hydrogen bond formation is more likely to result in higher crystallinity due to higher water content and therefore easier molecular chain migration compared to a solution without salt. For films containing lithium salt, it can be assumed that lithium ions are bonded not only with water molecules but also with hydroxyl groups. We concluded that these suppression of crystallinity and the high affinity of lithium salt to hydroxyl groups are due to the high affinity of hydroxyl

groups to oxygen atoms and lithium ions [24]. The high affinity of lithium ions with alcohols such as -OH is well known, as reported by N. L. Ma et al. in their study of alkali metal cations containing lithium ions interacting with short-chain alcohols [25].

When PVA is processed into films or fibers, it is generally used as a solution dissolved in water or DMSO. This is because the melting point and decomposition point of PVA are close to each other, and PVA has almost no thermoplastic, making it difficult to be molded by heat. We have discussed the crystallinity of PVA films with metal salts (especially lithium salts), and here we describe the rheological properties of PVA aqueous solutions with lithium salts. R. A. Saari et al. evaluated the rheological properties of aqueous PVA solutions with LiCl, LiBr, and LiI with respect to frequency dependence [26]. In their report, they found that the plateau modulus in the low-frequency range was reduced by the addition of lithium salts and increasing temperature. Among the lithium salts, LiI showed the most significant effect. This was explained by the Hofmeister series (HS), which indicated that this was due to the iodide ion acting as a water-structure breakers. In other words, LiI acts as a water-structure breakers in a PVA solution because it reduces hydrogen bonds between hydroxyl groups and affects rheological properties. As mentioned above, lithium ions have a high affinity for alcohols such as -OH, and  $\text{Li}^+\cdots\text{OH}$  bonds are easily formed. However, they revealed that it is not only cations that inhibit hydrogen bonds between hydroxyl groups, but also anions that are strongly affected. The ability of anions to inhibit hydrogen bonds can also be explained by HS [27]. Figure 1-6 show the cations and anions arranged according to HS. The ions on the left have low solubility of the polymer in the solvent and have a salting-out (aggregation) effect and are called water structure-forming ions. The ions on the right have high solubility in the polymer and have a salting-in (solubilization) effect [28].

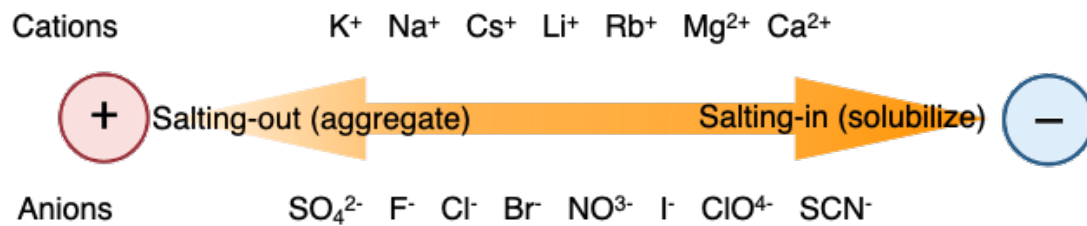


Figure 1-6 Hofmeister series.

The relationship between PVA film and HS was further investigated by R. A. Saari et al. using lithium perchlorate (LiClO<sub>4</sub>) and lithium sulfate (Li<sub>2</sub>SO<sub>4</sub>) in addition to lithium halide [27]. LiClO<sub>4</sub> affected PVA crystals more strongly than LiI. In other words, ClO<sub>4</sub><sup>-</sup> suppressed hydrogen bonding more significantly than I<sup>-</sup> according to HS. Since the suppression of hydrogen bonding decreases the crystallinity of PVA, it can be expected that the decrease in salt will temporarily create a low crystallinity state and improve the processing performance of PVA.

### 1-2-3. Modification of PVA hydroxyl groups

Modification of polymer side chains is a common study to improve their properties and add new functions; in the case of PVA, some hydroxyl groups have been replaced with other functional groups to add hydrophobicity and photocrosslinkability. Photocrosslinking PVA has been investigated as a scaffold material in fields such as tissue engineering, taking advantage of its advantages such as low toxicity [29-31]. Scaffolding materials serve as temporary substitutes for extracellular matrices and other materials, and are intended for tissue repair by anchoring cells and supporting their growth [32]. The addition of methacryl groups is often used as the main synthetic method for photocrosslinked PVA [33]. One example of its synthesis is shown in Figure 1-7.

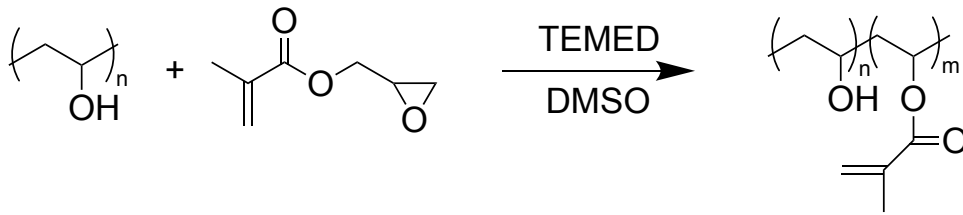


Figure 1-7 Synthesis of PVA methacrylate.

### 1-3. PVA fiber

#### 1-3-1. PVA fiber

PVA fiber is made by spinning PVA into fiber, which is widely used as a reinforcing agent for cement due to PVA's alkali resistance and other characteristics. PVA fiber can be made by wet spinning or dry spinning. Recently, gel spinning using organic solvents to produce high-strength PVA fibers has become popular. The melt-spinning method is not an appropriate spinning method due to the low thermoplasticity of PVA. Therefore, it is generally produced by wet spinning method using PVA aqueous solution. Unlike other synthetic fibers, PVA fiber is water soluble and can be dissolved in water even after the spinning process. Therefore, PVA fibers are subjected to heat treatment and formaldehyde formalization to enhance their water resistance. Figure 1-8 shows the manufacturing process of PVA fibers.

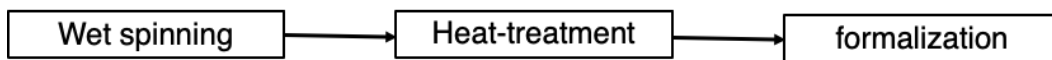


Figure 1-8 Flow to formalization of PVA fiber.

#### 1-3-2. Wet spinning process

The wet spinning process is a manufacturing method in which fibers are extruded from a solution tank through a nozzle into a coagulation bath. In the wet spinning process, PVA is completely dissolved in hot water to create an aqueous PVA solution. Impurities that can cause

problems in the spinning process are removed from the PVA solution by filtration and used in the spinning process. The spinning solution is then discharged through narrow holes in the discharge nozzle into the coagulation bath and wound to form fibers. The coagulation bath is filled with a saturated sodium sulfate solution, which rapidly dehydrates and solidifies due to osmotic pressure differences. The fiber is then stretched, washed, dried, heat-treated, and finally formalized. The wet spinning process is shown in Figure 1-9.

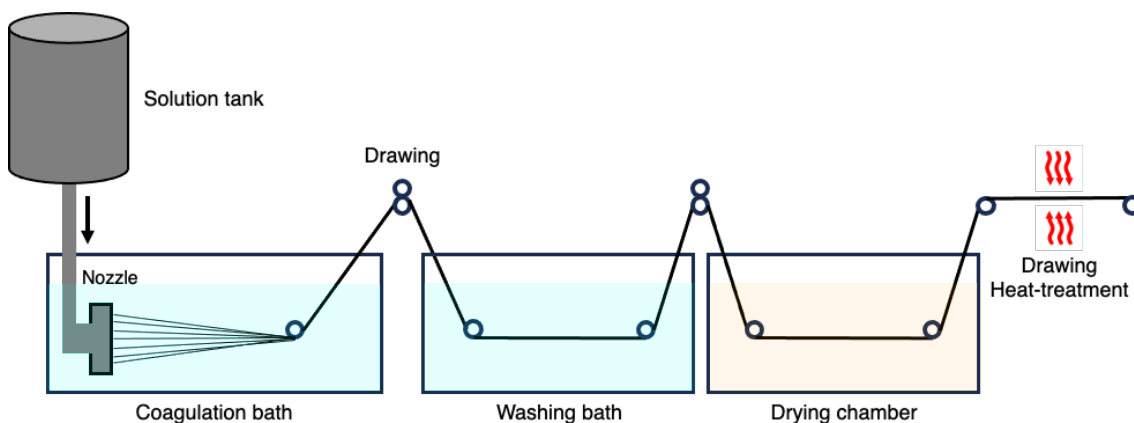


Figure 1-9 Wet spinning process for PVA fiber.

### 1-3-3. Mechanical properties enhancement of PVA fiber

Although PVA fibers are known to exhibit high mechanical strength, their properties are limited and their use is restricted. Improvements have been made to increase the strength of PVA fibers by improving the spinning method and using additives. For example, gel spinning has been used as a spinning method. PVA is dissolved in DMSO, and the PVA solution is spun by discharging it into cold methanol. This is commercialized as “KURALON K-II” by Kuraray Co. However, there are concerns about the use of organic solvents and other factors, so ideally, wet spinning is used to increase strength. Boric acid is a well-known additive, which is also added to industrially produced PVA fiber. Boric acid forms mono diol, double diol, and hydrogen bonds with PVA molecules [34, 35]. This reduces hydrogen bonds between hydroxyl groups and

decreases the entanglement of PVA molecular chains. Furthermore, the mechanical strength of PVA fibers can be increased by increasing the drawing ratio. Figure 1-10 shows a schematic diagram of the reaction of PVA and boric acid.

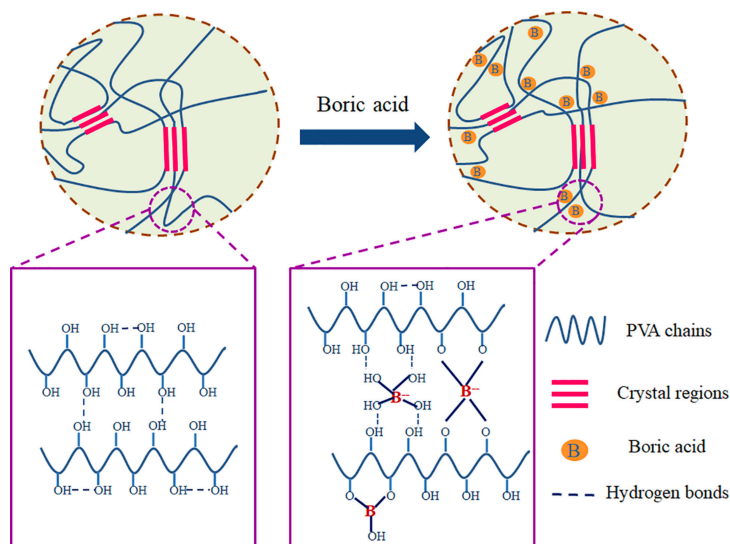


Figure 1-10 Reaction of PVA hydroxyl groups with boric acid [34].

Recently, a new method for increasing the strength of PVA fibers using metal salts was reported by R. A. Saari et al [36]. This method reduces hydrogen bonds in PVA by adding LiBr to a PVA solution, and wet spinning and drawing are performed in this state. The reasons for the difficulty in increasing the strength of PVA is the strong hydrogen bonding between the hydroxyl groups. When hydrogen bonds are strong, it is difficult to increase molecular orientation by stretching PVA fibers. However, the addition of lithium salt has the effect of reducing hydrogen bonding. Therefore, spinning and drawing with reduced hydrogen bonding resulted in improved mechanical properties compared to the case without salt addition. In particular, the improvement of molecular orientation of PVA fibers was achieved by reducing orientation defects by adding LiBr and by increasing the drawing ratio. In addition, the addition of LiI has enabled drawing at a higher drawing ratio than LiBr, further increasing the strength of the material [37]. Figure 1-11 shows the effect of salt addition on the molecular chains of PVA fibers and the state of molecular

orientation after stretching. Crystals are formed by hydrogen bonding between hydroxyl groups when PVA is wet-spun into fibers and rapidly dehydrated. However, in the presence of salt, the amount of crystals formed is reduced due to the reduction of hydrogen bonds. When fibers in both states are stretched, if there are no salts and strong interaction of PVA are present, the drawing ratio cannot be improved and molecular orientation is reduced due to the formation of orientation defects. When salts are added, the low interaction of the PVA fiber allows it to be easily stretched, which improves its molecular orientation. PVA fibers with high molecular orientation have very high mechanical strength, which opens up applications as reinforcing fibers for composite materials.

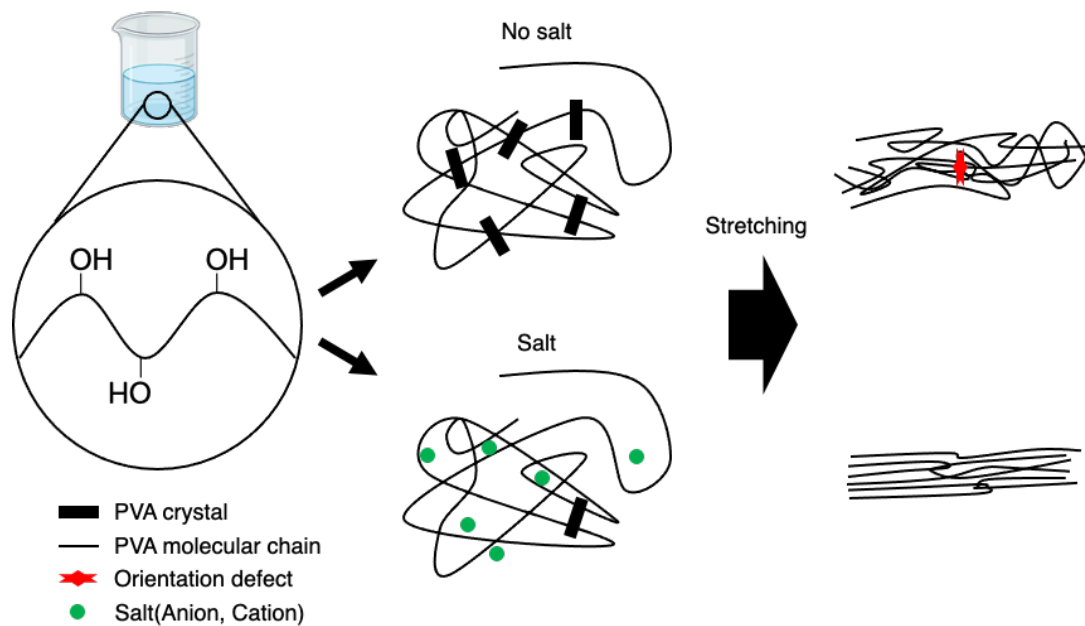


Figure 1-11 Schematic of molecular orientation of PVA by stretching.

## **1-4. Composite materials**

A composite material (CM) is a material that combines two or more materials for the purpose of improving material properties, and these materials have clear boundaries within the material. Among them, fiber-reinforced plastics (FRP) are well known and used in various fields. There are several types of FRP depending on the reinforcing fibers, with carbon fiber reinforced plastic (CFRP) and glass fiber reinforced plastic (GFRP) being the main types. FRP is often used in the aerospace industry, automobiles, and infrastructure facilities because of its light weight and high strength [38-41]. The mechanical properties of FRP are due to the strong anisotropy of the fibers. In general, the strength of FRP is proportional to the fiber content, since the strength of the matrix can be neglected compared to the strength of the fibers in FRP. However, in practice, it is difficult to achieve the theoretical strength due to factors such as fiber orientation disorder. Furthermore, when the fiber content exceeds 70%, it becomes difficult to make the matrix uniform and the strength decreases [42].

Carbon fiber, the reinforcing fiber of FRP, is lightweight and shows excellent performance in terms of tensile strength and Young's modulus, but it has serious drawbacks in terms of energy consumption and treatment problems during manufacturing. As a result, carbon fiber is expensive and has a high environmental impact. Solving these problems is the most important issue for the future composites industry. Recently, cellulose nanofibers and PVA fibers have been investigated as new reinforcing fibers [43-45]. PVA, in particular, has high mechanical properties and low environmental impact, making it a promising candidate for use as a reinforcing fiber. PVA fiber is already commonly used as a cement reinforcing agent, for example, due to its alkali resistance and other properties [46-48]. However, PVA fibers have low molecular orientation due to strong hydrogen bonds that inhibit stretching and cause orientation defects, and they do not exhibit inherent strength. These problems must also be solved for use as reinforcing fibers. The

application of PVA fiber as a reinforcing fiber is a means to solve the environmental impact and price issues in FRP. In other words, increasing the strength of PVA fiber is likely to be one of the major roles in the fiber industry in the future.

## **1-5. Polyvinyl alcohol hydrogel (PVA-H)**

### 1-5-1. Hydrogel and structure

PVA can form hydrogels when its cross-linked structure is hydrated. Hydrogel is a substance with a three-dimensional network structure that holds water inside and is insoluble in solvents, as well as its swollen form. Hydrogels are known to exhibit the properties of elastic solids because their structure makes them soft and easily deformable [49]. Hydrogels are classified into physically crosslinked and chemically crosslinked gels based on the type of crosslinking. The cross-linking points of physically crosslinked gels are bonded by ionic bonding, hydrogen bonding, and dipole interactions. On the other hand, chemically crosslinked gels are composed of crosslink points formed by covalent bonding, and thus have excellent mechanical properties and degradation resistance. Schematic diagrams of physical and chemical gels are shown in Figure 1-12. Unlike metals and ceramics, hydrogels have a moisture content similar to that of living tissue. In addition, the Young's modulus of hydrogel can be adjusted by adjusting the water content. Hydrogels have been studied in a wide range of fields such as tissue engineering, drug delivery systems, artificial muscles, and artificial cartilages [49-58].

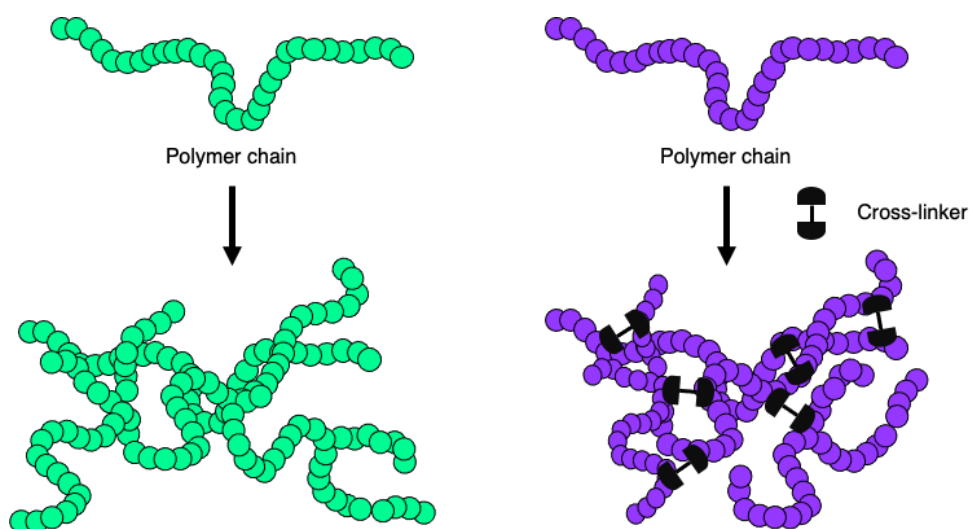


Figure 1-12 Schematic diagram of physical and chemical gels.

PVA forms a physical cross-linked gel by microcrystallization through hydrogen bonding. PVA hydrogels (PVA-H) formed by physical cross-linking are considered to be excellent as artificial cartilage because they exhibit frictional behavior and physical properties similar to those of cartilage [58, 60, 61]. However, PVA-H is a bioinert material and has problems with adhesion to joint surfaces, etc. Furthermore, PVA-H lacks mechanical strength and lubricity, and cannot be applied for the clinical use as a substitute for articular cartilage at present [62].

#### 1-5-2. PVA gelation methods

There are several methods for gelation of PVA. Typical methods for forming physical cross-links include ultraviolet and gamma ( $\gamma$ ) ray irradiation. In the former, molecules are joined together via free radicals produced by thermal decomposition of initiators, while in the latter, cross-linking occurs via ions produced from water by irradiation. Simpler and most commonly used is the freeze-thaw method [63-66]. This method improves the gel fraction and strength by freezing PVA-H at  $-20\text{ }^{\circ}\text{C}$  for about 1 day and thawing it at  $4\text{ }^{\circ}\text{C}$  or room temperature for 2~3 times. However, PVA-H prepared by the freeze-thaw method contains both microcrystalline and

amorphous regions due to phase separation that occurs during freezing, resulting in a non-uniform network structure and a white, cloudy appearance. Also, sufficient mechanical strength cannot be obtained [65]. S.-H. Hyon et al. reported PVA-H with transparent, high mechanical strength and high water content by dissolving PVA in a mixed solvent of DMSO and water and crystallizing at  $-20\text{ }^{\circ}\text{C}$  at low temperature [67]. This low-temperature crystallization method is commonly used as a preparation method for PVA-H in research fields such as biomaterials. For example, the high transparency of the material has been used for contact lens applications [68]. However, DMSO also has toxic properties such as high skin penetration and oxidizing power, making its use as a biomaterial unprofitable.

T. Sakaguchi et al. reported a hot press (HP) method that can prepare transparent PVA-H with high mechanical strength using only water and PVA [69]. HP method can be prepared by mixing water/PVA = 50/50 weight ratio and then heating and pressing it in a press. Since PVA does not need to be dissolved, PVA-H can be made at high concentrations, which was not possible, and organic solvents such as DMSO do not need to be used. It also exhibits an extremely high Young's modulus, which makes it promising for use as artificial cartilage and joint prostheses. The process of making PVA-H by the HP method is shown in Figure 1-13.

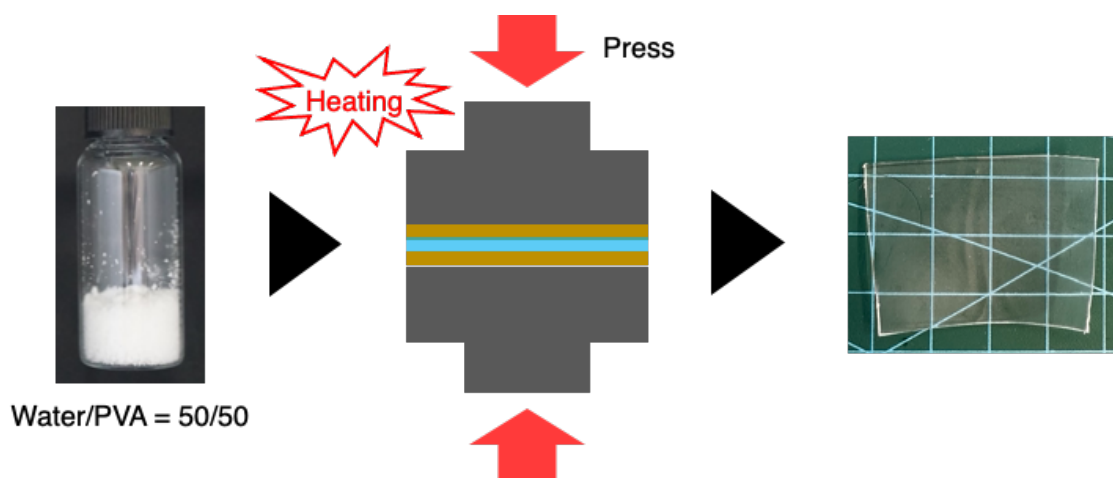


Figure 1-13 Gelation of PVA by hot press (HP) method.

## **1-6. Applications of PVA-H**

### **1-6-1. Application as artificial joint cartilage**

Numerous studies have been conducted on articular cartilage prostheses, and their performance has evolved over the years. Recently, artificial articular cartilage materials utilizing high-strength gels such as hydrogels and double network (DN) gels have been studied [70-73]. In particular, cartilage repair materials based on DN gel have high mechanical properties and excellent frictional properties. However, joints must be highly reliable materials because they are subjected to very high long-term loads. Because of its high mechanical and frictional properties, water content similar to that of living organisms, and biocompatibility, PVA-H shows promise for use as artificial articular cartilage, and many studies have been conducted. Kobayashi et al. fabricated PVA-H artificial cartilage and evaluated it by replacing the femoral head of a dog, and reported the problems and future improvements of PVA-H artificial cartilage [74]. The authors concluded that there are still some problems regarding adhesion to biological tissues and long-term effects, but that improvements in these areas will lead to promising future developments. The following is a brief description of hip joint replacements, which are frequently applied to artificial articular cartilage replacements.

This section describes the structure of the artificial articular cartilage currently in use. There are many hip prostheses on the market. Many joint prostheses can also be classified by shape and material, and can be divided into total hip replacement (THR) and resurfaced hip replacement (RHR) structures [75]. A comparison of their structures is shown in Figures 1-14. The THR consists of a stem, femoral head, acetabular cup and cement or metal shell; the RHR consists of an articulating surface covered by a conventional cup and head liner.

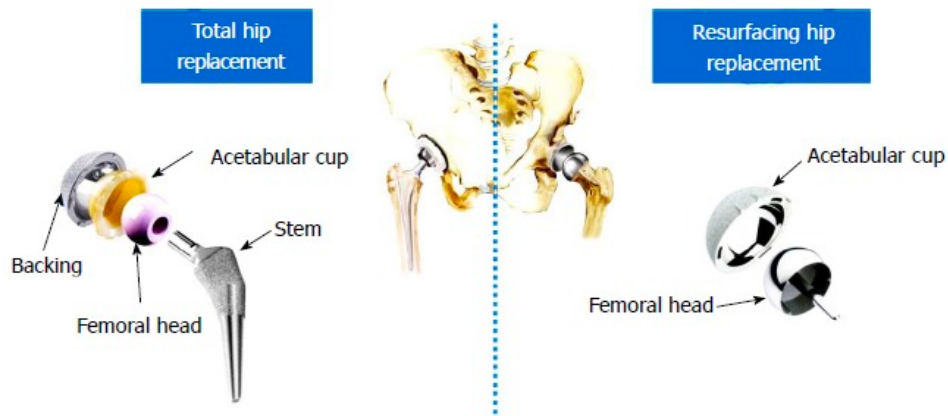


Figure 1-14 Total and resurfacing hip arthroplasty [75].

Plastics, metals, and ceramics are used as materials for THR and RHT (implants). Plastic is used only for the socket, while other materials are used for both the head and cup. Common material combinations include the following. Metal-on-Plastic (MoP), Ceramic-on-Plastic (CoP), Ceramic-on-Ceramic (CoC), and Metal-on-Metal (MoM) (Figure 1-15). Although these hip prostheses are very good and widely used, they also have several problems such as aseptic loosening and wear. As a result, damaged hip prostheses must be replaced by revision surgery, which places a heavy burden on the patient [76].



Figure 1-15 Coupling of materials for artificial hip implants [75].

## 1-6-2. Blood vessel biomodel using PVA-H

In recent years, endovascular treatment, in which a medical device such as a catheter is used to treat a diseased area from the inside of a blood vessel, has been increasing as a means of treating cardiovascular diseases in particular. This technique is less invasive and less burdensome to patients than surgical procedures. However, because endovascular treatment is performed inside complex blood vessels, it requires a high level of skill and experience. For this reason, bio-models that mimic blood vessels are used for training to improve the surgeon's technique. It is also expected to be applied to the evaluation of medical devices for endovascular treatment, evaluation of treatment strategies (preoperative conferences), development of surgical techniques, and informed consent [77-79].

Silicon used to be the most common material for biomodels, and it is still used today. However, the surface frictional resistance and elastic modulus of silicon models are not very similar to those of human blood vessels. Therefore, attention was focused on PVA-H biomodels, whose mechanical properties are very similar to those of human blood vessels. PVA-H is also highly transparent, making it possible to directly view medical devices during actual training. Currently commercially available PVA-H biomodels are shown in Figures 1-16.



Figure 1-16 Commercially available PVA-H biomodel [80].

As mentioned above, the common preparation methods for PVA-H are freeze-thaw or low-

temperature crystallization. The former method is not suitable for biomodels because it produces a cloudy gel. Therefore, PVA-H biomodels currently available on the market are produced by cryocrystallization using DMSO. Since the biomodel is not actually placed in a living organism, there is no problem with the use of organic solvents. However, it is reasonable to refrain from using DMSO because of concerns about toxicity, considering environmental pollution and the need to improve the handling of the biomodel.

## **1-7. Purpose of this research**

This study is based on the concept of "DMSO free" and is to modify it by improving metal salts, solvents, and fabrication methods, and by using PVA with different tacticity. In Chapter 2, we present research on the creation of high-strength PVA fibers for composite materials with low orientation defects and high molecular orientation through advanced stretching with suppressed hydrogen bonding by adding LiI. In Chapter 3, we present research on the changes in properties and thermo-plasticization of PVA-H prepared by the HP method using lithium salts for application to artificial joint cartilage. In Chapter 4, we present a study on the establishment of a gelation method by the HP method using syndiotactic PVA with high tacticity and the evaluation of the physical properties of PVA-H. Chapter 5 presents a summary and future prospects for this research.

## 1-8. References

1. W. Haehnel, W.O. Hermann, *German Patent 450*, 286 (1924)
2. R. Nagarkar, J. Patel, Polyvinyl Alcohol: A Comprehensive Study, *Acta Scientific Pharmaceutical Sciences, Vol.3 (4)* p.34-44 (2019)
3. W.O Hermann, W. Haehnel, *German Patent 685*, 048 (1931)
4. M.I. Baker, S.P. Walsh, Z. Schwartz, B.D. Boyan, A review of polyvinyl alcohol and its uses in cartilage and orthopedic applications, *Journal of Biomedical Materials Research – Part B Applied Biomaterials, Vol.100B (5)* p1451-1457 (2012)
5. P. J. Flory, F.S. Leutner, Occurrence of head-to-head arrangements of structural units in polyvinyl alcohol, *Journal of Polymer Science, Vol.3 (6)* p880-890 (1948)
6. K.V. Cauter, V.V. Speybroeck, M. Waroquier, Ab Initio Study of Poly(vinyl chloride) Propagation Kinetics: Head-to-Head versus Head-to-Tail Additions, *ChemPhysChem, Vol.8 (4)* p541-552 (2007)
7. S. Murahashi, Poly(vinyl alcohol) - Selected topics on its synthesis, *Pure and Applied Chemistry, Vol.15 (3-4)* p435-452 (1967)
8. C. Forder, S.P. Armes, N.C. Billingham, Synthesis of poly(vinyl alcohol)s with narrow molecular weight distribution from poly(benzyl vinyl ether) precursors, *Polymer Bulletin, Vol.35* p291-297 (1995)
9. H. Ohgi, T. Sato, H. Watanabe, F. Horii, Highly Isotactic Poly(vinyl alcohol) Derived from tert-Butyl Vinyl Ether V. Viscoelastic Behavior of Highly Isotactic Poly(vinyl alcohol) Films, *Polymer Journal, Vol.38* p1055-1060 (2006)
10. H. Ohgi, T. Sato, S. Hu, F. Horii, Highly isotactic poly(vinyl alcohol) derived from tert-butyl vinyl ether. Part IV. Some physical properties, structure and hydrogen bonding of highly isotactic poly(vinyl alcohol) films, *Polymer, Vol.47 (8)* pp1324-1332 (2006)

11. H.Wang, J. He, L. Zou, C. Wang, Y.V. Li, Preparation of high-strength, high-modulus PVA fiber by synthesis of syndiotacticity-rich high molecular weight PVA polymers with VAc and VBz via emulsifier-free emulsion polymerization, *Polymers for advanced technologies*, Vol.34 (6) p1948-1958 (2023)
12. S. Nozakura, M. Sumi, M. Uoi, T. Okamoto, S. Murahashi, Stereoregulation in the radical polymerization of vinyl esters, *Journal of Polymer Science: Polymer Chemistry Edition*, Vol. 11 (1) p279-288 (1973)
13. W.S. Lyoo, I. S. Seo, B.C. Ji, J.H. Kim, S.S. Kim, H.D. Ghim, Role of the stereosequences of poly(vinyl alcohol) in the rheological properties of syndiotacticity-rich poly(vinyl alcohol)/water solutions, *Journal of Applied Polymer Science*, Vol.88 (7) p1858-1863 (2003)
14. S. Nozakura, T. Okamoto, K. Toyora, S. Murahashi, Synthesis and polymerization of vinyl esters and vinyl ethers having bulky substituents, *Journal of Polymer Science: Polymer Chemistry Edition*, Vol.11 (5) p1043-1051 (1973)
15. M. Uchiyama, K. Satoh, M. Kamigaito, Stereospecific cationic RAFT polymerization of bulky vinyl ethers and stereoblock poly(vinyl alcohol) via mechanistic transformation to radical RAFT polymerization of vinyl acetate, *Giant*, Vol.5 100047 (2021)
16. Y. Gotoh, Y. Nagara, T. Nakano, Y. Okamoto, Y. Ohkoshi, M. Nagura, Viscoelastic behaviors and molecular motions of highly syndiotactic poly(vinyl alcohol) fibers, *Journal of Polymer Science Part B Polymer Physics*, Vol.42 (5) p800-808 (2004)
17. W.S. Lyoo, I.S. Seo, J. H. Yeum, W. S. Yoon, B.C. Ji, B.S. Kim, S.S. Lee, B.C. Kim, Effect of degree of saponification on the rheological properties of syndiotactic poly(vinyl alcohol)/water solution, *Journal of Applied Polymer Science*, Vol.86 (2) pp463-467 (2003)
18. R. Jamarani, H.C. Erythropel, J.A. Nicell, R.L. Leasl, M. Maric, How Green is Your Plasticizer? *Polymers*, Vol.10 (8) 834 (2018)

19. A. Bodaghi, An overview on the recent developments in reactive plasticizers in polymers, *Polymers for Advanced Technologies*, Vol.31 (3) p355-367 (2020)
20. V. Marturano, P. Cerruti, V. Ambrogi, Polymer additives, *Physical Science Reviews*, Vol.2 (6) (2017)
21. Y. Sato, A. Ito, S. Maeda, M. Yamaguchi, Structure and optical properties of transparent polyamide 6 containing lithium bromide, *Journal of Polymer Science Part B Polymer Physics*, Vol. 56 (22) p1513-1520 (2018)
22. A. Ito, A. Shin, K. Nitta, Additive effects of lithium halides on the tensile and rheological properties of poly(methyl methacrylate), *Polymer Journal*, Vol.54 p1279-1285 (2022)
23. O.N. Tretinnikov, S.A Zagorskaya, Effect of alkali halide salt additives on the structure of poly(vinyl alcohol) films cast from aqueous solutions, *Polymer Science Series A*, Vol.15 p463-470 (2013)
24. S.A. Zagorskaya, O.N. Tretinnikov, Infrared Spectra and Structure of Solid Polymer Electrolytes Based on Poly(vinyl alcohol) and Lithium Halides, *Polymer Science Series A*, Vol.61 p21-28 (2019)
25. N.L. Ma, F.M. Siu, C.W. Tsang, Interaction of alkali metal cations and short chain alcohols: effect of core size on theoretical affinities, *Chemical Physics Letters*, Vol.332 (1-2) p65-72 (2000)
26. R.A. Saari, R. Maeno, R. Tsuyuguchi, W. Marujiwat, P. Phulkerd, M. Yamaguchi, Impact of Lithium halides on rheological properties of aqueous solution of poly(vinyl alcohol), *Journal of Polymer Research*, Vol.27 218 (2020)
27. R.A. Saari, M.S. Nasri, W.Marujiwat, R. Maeno, M. Yamaguchi, Application of the Hofmeister series to the structure and properties of poly(vinyl alcohol) films containing metal salts, *Polymer Journal*, Vol.53 p557-564 (2021)

28. W.F. McDevit, F.A. Long, The Self-Interaction of Mandelic Acid as Determined from Solubilities in Salt Solutions, *Journal of the American Chemical Society*, Vol.74 p1090-1091 (1952)
29. Y. Zhou, C. Zhang, K. Liang, J. Li, H. Yang, X. Liu, X. Yin, D. Chen, W. Xu, Photopolymerized water-soluble maleilated chitosan/methacrylated poly (vinyl alcohol) hydrogels as potential tissue engineering scaffolds, *International Journal of Biological Macromolecules*, Vol.106 p227-233 (2018)
30. J. Kuundu, L.A.Poole-Warren, P. Martens, S.C. Kundu, Silk fibroin/poly(vinyl alcohol) photocrosslinked hydrogels for delivery of macromolecular drugs, *Acta Biomaterialia*, Vol.8 (5) p 1720-1729 (2012)
31. D. Zhou, Q. Dong, L. Liang, W. Xu, Y. Zhou, P. Xiao, Photocrosslinked methacrylated poly(vinyl alcohol)/hydroxyapatite nanocomposite hydrogels with enhanced mechanical strength and cell adhesion, *Journal of Polymer Science Part A: Polymer Chemistry*, Vol.57 (18) p1882-1889 (2019)
32. M. Mabrouk, H.H. Beherei, D.B. Das, Recent progress in the fabrication techniques of 3D scaffolds for tissue engineering, *Materials Science and Engineering: C*, Vol.110 110716 (2020)
33. E.A. Kamoum, A.M. Omer, M.M. Abu-serie, S.N. Khattab, H.M. Ahmed, A.A. Elbardan, Photopolymerized PVA-g-GMA Hydrogels for Biomedical Applications: Factors Affecting Hydrogel Formation and Bioevaluation Tests, *Arabian Journal for Science and Engineering*, Vol.43 p3565-3575 (2018)
34. X. Hong, J. He, L. Zou, Y. Wang, Y.V. Li, Preparation and characterization of high strength and high modulus PVA fiber via dry-wet spinning with cross-linking of boric acid, *Journal of Applied Polymer Science*, Vol.138 (47) 51394 (2021)

35. J. Chen, Y. Li, Y. Zhang, Y. Zhu, Preparation and characterization of graphene oxide reinforced PVA film with boric acid as crosslinker, *Journal of Applied Polymer Science*, Vol.132 (22) (2015)
36. R.A. Saari, R. Maeno, W. Marujiwat, M.S. Nasri, K. Matsumura, M. Yamaguchi, Modification of poly(vinyl alcohol) fibers with lithium bromide, *Polymer*, Vol.213 (20) 123193 (2021)
37. Y. Taoka, R.A. Saari, T. Kida, M. Yamaguchi, K. Matsumura, Enhancing the Mechanical Properties of Poly(vinyl alcohol) Fibers by Lithium Iodide Addition, *ACS omega*, Vol.8 (36) p32623-32634 (2023)
38. M.A. Karatas, H. Gökkaya, A review on machinability of carbon fiber reinforced polymer (CFRP) and glass fiber reinforced polymer (GFRP) composite materials, *Defence Technology*, Vol.14 (4) p318-326 (2018)
39. S. Pervaiz, T.A. Qureshi, G. Kashwani, S. Kannan, 3D Printing of Fiber-Reinforced Plastic Composites Using Fused Deposition Modeling: A Status Review, *Materials*, Vol.14 (16) 4520 (2021)
40. S. Prashanth, K.M. Subbaya, K. Nithin, S. Sachhidananda, Fiber Reinforced Composites - A Review, *Journal of Materials Sciences & Engineering*, Vol.6 (3) (2017)
41. H. Fang, Y. Bai, W. Liu, Y. Qi, J. Wang, Connections and structural applications of fibre reinforced polymer composites for civil infrastructure in aggressive environments, *Composites Part B: Engineering*, Vol.164 (1) p129-143 (2019)
42. H. Zheng, W. Zhang, B. Li, J. Zhu, C. Wang, G. Song, G. Wu, X. Yang, Y. Huang, L. Ma, Recent advances of interphases in carbon fiber-reinforced polymer composites: A review, *Composites Part B: Engineering*, Vol.233 (15) 109639 (2022)
43. M.N.F. Norrrahim, T.A.T. Yasim-Anuar, M.A. Jenol, N.M. Nurazzi, S.M. Sapuan, R.A. Ilyas,

- Chapter 7 - Performance evaluation of cellulose nanofiber reinforced polypropylene biocomposites for automotive applications, *Biocomposite and Synthetic Composites for Automotive Applications*, p199-215 (2021)
44. R. Nishikawa, N. Aridome, N. Ojima, M. Yamaguchi, Structure and properties of fiber-reinforced polypropylene prepared by direct incorporation of aqueous solution of poly(vinyl alcohol), *Polymer*, Vol.199 (11) 122566 (2020)
  45. H. Kurita, Y. Xie, K. Katabira, R. Honda, F. Narita, The insert effect of cellulose nanofiber layer on glass fiber-reinforced plastic laminates and their flexural properties, *Material Design & Processing Communications*, Vol.1 (13) e58 (2019)
  46. S. Tan, C. Wang, Q. Zheng, F. Chen, Y. Huang, Durability Performance of PVA Fiber Cement-Stabilized Macadam, *Sustainability*, Vol.14 (24) 16953 (2022)
  47. D. Sikarskas, V. Antonovic, J. Malaiškiene, R. Boris, R. Stonys, G. Šahmenko, Modification of the Structure and Properties of Lightweight Cement Composite with PVA Fibers, *Materials*, Vol.14 (20) 5983 (2021)
  48. Y. Zhang, Y. Zheng, C. Du, S. Hu, Z. Wang, Hybrid effects of basalt and polyvinyl alcohol fibers on the mechanical properties and macro-microscopic analysis of low-heat portland cement concrete, *Journal of Materials Research and Technology*, Vol.25 p608-632 (2023)
  49. K. Varaprasad, G.M. Raghavendra, T. Jayaramudu, M.M. Yallapu, R. Sadiku, A mini review on hydrogels classification and recent developments in miscellaneous applications, *Materials Science and Engineering: C*, Vol.79 (1) p958-971 (2017)
  50. Y. Guo, J. Bae, P. Li, F. Zhao, G. Yu, Hydrogels and Hydrogel-Derived Materials for Energy and Water Sustainability, *Chemical Reviews*, Vol.120 (15) p7642-7707 (2020)
  51. C.D. Spicer, Hydrogel scaffolds for tissue engineering: the importance of polymer choice, *Polymer Chemistry*, 2 (2020)

52. S. Jacob, A.B. Nair, J. Shah, N. Sreeharsha, S. Gupta, P. Shinu, Emerging Role of Hydrogels in Drug Delivery Systems, Tissue Engineering and Wound Management, *Pharmaceutics*, Vol.13 (3) 357 (2021)
53. A. Fatimi, O.V. Okoro, D. Podstawczyk, J.Siminska-Stanny, A. Shavandi, Natural Hydrogel-Based Bio-Inks for 3D Bioprinting in Tissue Engineering: A Review, *Gels*, Vol.8 (3) 179 (2022)
54. N. Park, J. Kim, Hydrogel-Based Artificial Muscles: Overview and Recent Progress, *Advanced Intelligent Systems*, Vol.2 (4) 1900135 (2020)
55. F. Oveissi, D.F. Fletcher, F. Dehghani, S. Naficy, Tough hydrogels for soft artificial muscles, *Materials & Design*, Vol.203 109609 (2021)
56. M. Vigata, C.D. O'Connell, S. Cometta, D.W. Hutmacher, C. Meinert, N. Bock, Gelatin Methacryloyl Hydrogels for the Localized Delivery of Cefazolin, *Polymers*, Vol.13 (22) 3960 (2021)
57. J. Pushpamalar, P. Meganathan, H.L. Tan, N.A. Dahlan, L.T. Ooi, B.N.H.M. Neerooa, R.Z. Essa, K. Shameli, S.Y. Teow, Development of a Polysaccharide-Based Hydrogel Drug Delivery System (DDS): An Update, *Gels*, Vol.7 (4) 153 (2021)
58. W. Wei, Y. Ma, X. Yao, W. Zhou, X. Wang, C. Li, J. Lin, Q. He, S. Leptihn, H. Ouyang, Advanced hydrogels for the repair of cartilage defects and regeneration, *Bioactive Materials*, Vol.6 (4) p998-1011 (2021)
59. T. Nonoyama, J.P Gong, Tough Double Network Hydrogel and Its Biomedical Applications, *Annual Review of Chemical and Biomolecular Engineering*, Vol.12 p393-410 (2021)
60. X. Zhang, Z. Lou, X. Yang, Q. Chen, K. Chen, C. Feng, J. Qi, Y. Luo, D. Zhang, Fabrication and Characterization of a Multilayer Hydrogel as a Candidate for Artificial Cartilage, *ACS Applied Polymer Materials*, Vol.3 (19) p5039-5050 (2021)

61. M. Hao, Y. Wang, L. Li, Y. Liu, Y. Bai, W. Zhou, Q. Lu, F. Sun, L. Li, S. Feng, W. Wei, T. Zhang, Tough Engineering Hydrogels Based on Swelling–Freeze–Thaw Method for Artificial Cartilage, *ACS Applied Materials & Interfaces*, Vol.14 (22) p25093-25103 (2022)
62. Y. Chen, J. Song, S. Wang, W. Liu, PVA-Based Hydrogels: Promising Candidates for Articular Cartilage Repair, *Macro-Molecular Bioscience*, Vol.21 (10) 2100147 (2021)
63. M. Frounchi, S. Dadbin, M. Tabatabaei, Poly (vinyl alcohol)/graphene oxide nanocomposite films and hydrogels prepared by gamma ray, *Macromolecular Engineering*, Vol.48 (2) p42-47 (2019)
64. S.M. Nasef, E.E. Khozemy, E.A. Kamoun, H. El-Gendi, Gamma radiation-induced crosslinked composite membranes based on polyvinyl alcohol/chitosan/AgNO<sub>3</sub>/vitamin E for biomedical applications, *International Journal of Biological Macromolecules*, Vol.137 (15) p878-885 (2019)
65. H. Adelnia, R. Ensandoost, S.S. Moonshi, J.N. Gavvani, E.I. Vasafi, H.T. Ta, Freeze/thawed polyvinyl alcohol hydrogels: Present, past and future, *European Polymer Journal*, Vol.164 (5) 110974 (2022)
66. M. Wang, J. Bai, K. Shao, W. Tang, X. Zhao, D. Lin, S. Huang, C. Chen, Z. Ding, J. Ye, Poly(vinyl alcohol) Hydrogels: The Old and New Functional Materials, *International Journal of Polymer Science*, Vol.2021 (2021)
67. S.-H. Hyon, W.-I. Cha, Y. Ikeda, Preparation of transparent poly(vinyl alcohol) hydrogel, *Polymer Bulletin* Vol.22 p119-122 (1989)
68. Y. Pan, J. Ding, Y. Chen, Q. Shen, Study on mechanical and optical properties of poly(vinyl alcohol) hydrogel used as soft contact lens, *Advanced Performance Materials*, Vol.31 (5) p266-273 (2016)
69. T. Sakaguchi, S. Nagano, M. Hara, S.-H. Hyon, M. Patel, K. Matsumura, Facile preparation

- of transparent poly(vinyl alcohol) hydrogels with uniform microcrystalline structure by hot-pressing without using organic solvents, *Polymer Journal*, Vol.49 p535-542 (2017)
70. K. Arakaki, N. Kitamura, H. Fujiki, T. Kurokawa, M. Iwamoto, M. Ueno, F. Kanaya, Y. Osada, J.P. Gong, K. Yasuda, Artificial cartilage made from a novel double-network hydrogel: In vivo effects on the normal cartilage and ex vivo evaluation of the friction property, *Journal of Biomedical Materials Research Vol.93A (3)* p1160-1168 (2010)
71. J. Chen, L. Cui, C. Yan, D. Xiong, Mechanical and Tribological Study of PVA–pMPDSA Double-Network Hydrogel Prepared by Ultraviolet Irradiation and Freeze–Thaw Methods for Bionic Articular Cartilage, *Journal of Bionic Engineering*, Vol.18 p1192-1201 (2021)
72. L. Huang, Z. Li, S. Ma, D. Ye, J. Yang, G. Qin, H. Yin, Q. Chen, Articular Cartilage-Inspired Hybrid Double-Network Hydrogels with a Layered Structure and Low Friction Properties, *ACS Applied Polymer Materials*, Vol.4 (10) p7634-7644 (2022)
73. P. E. Milner, M. Parkes, J.L. Puetzer, R. Chapman, M.M. Stevens, P. Cann, J.R.T. Jeffers, A low friction, biphasic and boundary lubricating hydrogel for cartilage replacement, *Acta Biomaterialia*, Vol.65 p102-111 (2018)
74. M. Kobayashi, S.H Hyon, Development and Evaluation of Polyvinyl Alcohol-Hydrogels as an Artificial Articular Cartilage for Orthopedic Implants, *Materials*, Vol.3 (4) p2753-2771 (2010)
75. F.D. Puccio, L. Mattei, Biotribology of artificial hip joints, *World Journal of Orthopedics*, Vol.6 (1) p77-94 (2015)
76. B.J. McGrory, G.D. Etkin, D.G. Lewallen, Comparing contemporary revision burden among hip and knee joint replacement registries, *Arthroplasty Today*, Vol.2 (2) p83-86 (2016)
77. H. Kosukegawa, K. Mamada, K. Kuroki, L. Liu, K. Inoue, T. Hayase, M. Ohta, Evaluation of mechanical properties of blood vessel biomodeling with poly(vinyl alcohol) hydrogel, *Nano-*

- Biomedical Engineering*, 2009 p63-69 (2009)
78. J.A. Hisam, M.Y. Salehudin, M.I.M. Lizah, M.I.A. Suhaimi, M.H.M. Hisham, I. Ishak, M.J.M. Mokhtarudin, *Advances in Intelligent Manufacturing and Mechatronics*, Vol.988 p163-173 (2023)
79. H. Kosukegawa, K. Mamada, K. Kuroki, L. Liu, K. Inoue, T. Hayase, M. Ohta, Measurements of Dynamic Viscoelasticity of Poly (vinyl alcohol) Hydrogel for the Development of Blood Vessel Biomodeling, *Journal of Fluid Science and Technology*, Vol.3 (4) p533-543 (2008)
80. <https://eng.bluepractice.co.jp/>, Blue Practice Co., Ltd., (2023/11/10, Accessed)

*Chapter 2: Enhancing the mechanical  
properties of Poly(vinyl alcohol) fibers by  
lithium iodide addition*

## Chapter 2: Enhancing the mechanical properties of Poly (vinyl alcohol) fibers by lithium iodide addition

### 2-1. Introduction

This paper reports on the effect of lithium iodide (LiI) on the mechanical strength and molecular orientation of poly (vinyl alcohol) (PVA) fibers. PVA is a water-soluble synthetic polymer with hydroxyl groups that exhibits chemical resistance, alkali resistance, biodegradability, and biocompatibility [1-5]. It is suitable for various applications such as clothing, food packaging films, biomaterials, and fibers, and it is widely used in our daily lives [3,5-10]. In particular, a PVA fiber is a highly effective material that can be used for infrastructure equipment that requires high reliability because it can be mass-produced at low cost and has high mechanical strength as a crystalline polymer [5,11-14]. PVA fibers are used as cement reinforcement because they have good adhesion to cement matrixes [5,13]. Research to improve adhesion by modifying their surface has been conducted frequently in recent years [15,16].

However, PVA fiber is not the only high-performance fiber that has been developed in recent years. The textile industry has developed many high-performance fibers such as carbon fiber (CF), glass fiber (GF), and aramid fiber (AF) [17-20]. A great deal of research has been conducted on fiber-reinforced plastics (FRPs) with high strength and high modulus using these materials [21,22]. These FRPs are used in many fields, including the automotive and aerospace industries, ships, and infrastructure facilities, as an alternative to metals and ceramics due to their lightweight properties [20-24]. However, CF and AF are very expensive, and GF has a weight problem. Moreover, these fibers have no established disposal method and can hardly be recycled [25-27]. In view of current environmental issues, this is a major challenge that needs to be addressed. Therefore, this study aims to develop high-performance fibers with excellent mechanical

properties, low cost, and low environmental impact by using lithium iodide (LiI) as an additive for PVA fibers.

Recently, some research has focused on the use of the PVA fiber as a reinforcing fiber in FRPs, and its low cost makes it a promising candidate [28]. In addition, the PVA fiber is extremely lightweight, making it excellent for FRPs. Nishikawa et al. mixed PVA fibers with polypropylene and molded them by injection molding [29]. They reported that this greatly improved the mechanical properties of polypropylene. This research shows promise for the application of the PVA fiber as a reinforcing fiber. Similar results have also been reported for composites of polypropylene and GF [30]. However, the use of GF increases weight. PVA fibers have lower mechanical properties than CF, however, comparable strength to GF can be achieved with perfect molecular orientation [28,29,31].

Many studies have attempted to increase the strength of PVA fibers, including syndiotactic poly (vinyl alcohol) (PVA with alternating stereochemistry) [32-34]. However, researchers have reported that orientation by advanced stretching is difficult for syndiotactic PVA because strong hydrogen bonds between PVA molecules inhibit high molecular orientation [31]. Also, with the development of gel spinning and other methods, high-strength PVA fibers are available in the market. Many studies have been conducted on these fibers [35,36]. However, these spinning methods use organic solvents and raise concerns about cost and environmental impact. Therefore, there are issues that need to be addressed. The PVA fiber was developed by Sakurada et al. using only water as a solvent. This method does not require acid or organic solvents for wet spinning and does not generate toxic gases in the production process [37].

Recently, Saari et al. added lithium bromide (LiBr), which improves the ductility of PVA fibers and increases their strength by reducing the hydrogen bonding network [28]. Similarly, they reported that adding LiI and LiBr to a PVA aqueous solution reduced hydrogen bonding in PVA

more than LiBr alone [38]. This may result in a higher ductility enhancement effect than LiBr.

In this study, I added LiI to a PVA solution and spun fibers by a wet spinning method. Wet spinning is a fiber-forming process in which the polymer solution is extruded into a chemical bath that solidifies the filaments. I chose this method because it can produce fine and uniform fibers with high molecular orientation. I then heat-stretched the fibers at different temperatures and ratios and investigated how LiI affected their molecular orientation and mechanical properties.

## **2-2. Materials and methods**

### 2-2-1. Materials

PVA was provided by Kuraray Co., Ltd (Tokyo, Japan). The degree of polymerization was 1700, and the degree of saponification was 99.8 mol %. LiI was purchased from Sigma-Aldrich (USA) and used without further purification. Sodium sulfate ( $\text{Na}_2\text{SO}_4$ ) was purchased from Kanto Chemical Co., Ltd (Tokyo, Japan). Methanol was purchased from Nacalai Tesque (Kyoto, Japan). Distilled water was used throughout the experimental system.

### 2-2-2. Sample preparation

The PVA solution was prepared by dissolving PVA in distilled water at 95 °C using a magnetic stirrer at a PVA concentration of 16 wt %. LiI was then added and stirred until the PVA was completely dissolved; the amount of LiI added was 0.1 molar ratio to the hydroxyl group of PVA. The amount of LiI added was determined according to the report by Saari et al [38].

### 2-2-3. PVA fiber spinning

Wet spinning was performed using a tabletop wet spinning machine (Nakamura Service Co., Ltd., Hokkaido, Japan). Figure 2-1 shows the schematic diagram of the spinning apparatus. A

PVA/LiI solution was discharged from a solution tank kept at 90 °C into a coagulation bath filled with a saturated sodium sulfate solution. The diameter of the discharge nozzle was 0.2 mm. Primary stretching was performed at this stage, with a draw ratio (DR) of 4 for the fiber. After spinning, the fibers were washed with methanol, which does not dissolve PVA, to remove sodium sulfate and LiI. The fibers with nothing added were designated as pure PVA fibers, while the fibers with LiI added were designated as LiI-PVA fibers.

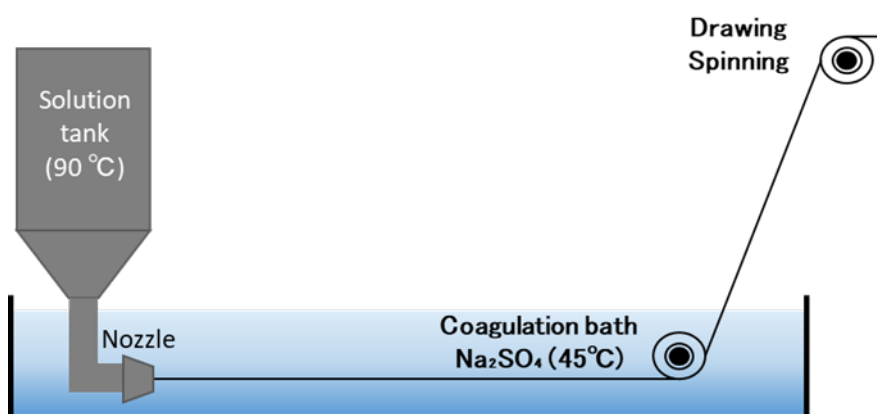


Figure 2-1 Schematic diagram of wet spinning machine.

#### 2-2-4. Secondary stretching and heat-treatment

Secondary stretching was performed by heat-stretching to improve the orientation and mechanical properties of PVA fibers using a tensile tester with a thermostatic chamber (Shimadzu Corporation Co., Ltd., Kyoto, Japan). After reaching the specified fiber temperature, the fiber was left to stand still for 2 min before stretching. The distance between the chucks was 10 mm. When stretching, the fibers were bundled and secured at both ends with polyimide tape. After stretching, the fiber was quenched by spraying it with ethanol and left in place for 1 min. The secondary extension multipliers were 4×, 5×, 6×, and 7×. The final drawing ratio was the combined ratio with the primary drawing ratio, which was 16×, 20×, 24×, and 28×. Heat treatment was then performed in order to induce crystallization. The respective conditions and sample names are

summarized in Table 2-1. In the sample names, P4 indicates the pure PVA fiber with a primary stretch only; PL4 indicates the LiI-PVA fiber; P16 indicates the pure PVA fiber stretched 16 $\times$ , and PL16 indicates the LiI-PVA fiber stretched 16 $\times$ . For fibers stretched 20 $\times$  or more, all fibers were spun with the addition of LiI. P20 indicates the draw ratio, 120-1.0 indicates the temperature and speed during heating and stretching, and the temperature of heat treatment is shown in parentheses. If the heat treatment is performed at 150 °C, there are two heat treatment time points indicated by -1 and -6 after the temperature in parentheses. To avoid the effects of moisture, the samples were stored in a vacuum desiccator because PVA is hygroscopic.

Table 2-1 Sample name and preparation conditions.

Sample name	Primary draw ratio	Secondary draw ratio	Draw ratio	Drawing speed (mm/s)	Drawing temperature (°C)	Heat treatment
P4	4	-	4	-	-	90 °C One night
PL4		-	4	-	-	90 °C One night
PL16		4	16	0.5	120	90 °C One night
P20-120-1.0(120), P20-120-1.0(150)		4	16	0.5	120	90 °C One night
P24-120-1.0(120), P24-120-1.0(150)		5	20	1.0	120	120 °C One night, 150 °C 1h
P28-120-1.0(120), P28-120-1.0(150)		6	24			
P20-180-1.0(120), P20-180-1.0(150)		7	28			
P24-180-1.0(120), P24-180-1.0(150)		5	20			
P28-180-1.0(120), P28-180-1.0(150)		6	24	1.0	180	120 °C One night, 150 °C 1h
P20-180-1.5(120), P20-180-1.5(150-1)		7	28			
P24-180-1.5(120), P24-180-1.5(150-1)		5	20			
P28-180-1.5(120), P28-180-1.5(150-1)		6	24	1.5	180	120 °C One night, 150 °C 1h
P20-180-1.5(150-6), P20-180-1.5(190)	7	28				
P24-180-1.5(150-6), P24-180-1.5(190)	5	20				
P28-180-1.5(150-6), P28-180-1.5(190)	6	24	1.5	180	150 °C 6h, 190 °C 5min	

## 2-2-5. Measurements

### 2-2-5-1. Differential scanning calorimetry (DSC)

Thermal analysis was performed by differential scanning calorimetry (DSC) to investigate the thermal transitions and crystallization behavior of PVA fibers (DSC6200, Seiko Instruments, Tokyo, Japan). About 10 mg of each sample was placed in an aluminum pan, sealed with a sealer, and measured under a nitrogen atmosphere at a temperature increase rate of 10 °C/min. An empty pan was used as the reference material. Samples were heated from 25 to 350 °C. Crystallinity  $X_C$  was calculated from the value of heat of fusion  $\Delta H$  determined from the DSC heating curve using the following eq. (2-1), where  $\Delta H_f$  is the heat of fusion (152 J/g) in a perfect crystal of pure PVA [28,39].

$$X_C = \frac{\Delta H}{\Delta H_f} \times 100 (\%) \quad (2 - 1)$$

### 2-2-5-2. Scanning electron microscope (SEM)

The surface and shape of the spun PVA fibers were observed with a scanning electron microscope (SEM) (TM3030plus, Hitachi, Tokyo, Japan).

### 2-2-5-3. Tensile test

Tensile tests were performed at room temperature using a tensile testing machine (Series 3360, Instron, USA) connected to a 5 N load cell. Each fiber was tested individually and fixed between chucks by fixing both ends to a sandpaper. The distance between chucks was 12 mm, and the tensile speed was set at 0.2 mm/min. Three measurements were taken for each sample, and the average value was calculated.

#### 2-2-5-4. Wide-angle X-ray diffraction (WAXD)

Two-dimensional wide-angle X-ray diffraction (2D-WAXD) was measured using an X-ray diffractometer (XRD) (Smart Lab, Rigaku Corp., Tokyo, Japan) equipped with an imaging plate. 45 kV, 200 mA Cu K $\alpha$  radiation was applied to the fiber samples. The exposure time for each sample was 2700 seconds. The crystalline orientation of the PVA fiber was calculated and quantitatively evaluated by using the azimuthal distribution in the [101] plane. The orientation degree  $A$  was calculated by the half-width method using the following eq. (2-2) [28].

$$A = \frac{360 - \Sigma W_{half}}{360} \times 100 \quad (2 - 2)$$

where  $W_{half}$  is the half of the maximum value of the peak, i.e., the half-width.

#### 2-2-5-5. Measurement of lithium concentration

Residual lithium concentrations were measured using the Metalloassay Lithium LS Kit (Metallogenics, Chiba, Japan), a lithium assay kit for measuring lithium concentrations in serum and plasma. (40) For the measurement, LiI-PVA solution was diluted to the specified value, PVA fiber solution, dissolved in hot water, and chromogenic solution were added to a 96-well plate. The absorbance was measured at 550 nm main wavelength and 600 nm secondary wavelength using a microplate reader (Infinito 200pro M Nano Plus, Tecan Japan, Kanagawa, Japan).

## 2-3. Results and Discussion

### 2-3-1. Fiber surface observation and fiber diameter measurement by SEM

As shown in Figure 2, SEM images of PVA fibers revealed that there were white substances around the fiber, which were dried sodium sulfate used in the spinning process to coagulate the polymer solution into solid fibers. The sodium sulfate solution did not affect the physical properties of the fiber. The surface of the fiber was very smooth, indicating that no problem occurred during spinning. However, I observed that none of the PVA fibers were perfectly cylindrical in shape, which is a common phenomenon in wet spinning (Figure 2-3). In solution spinning methods such as wet spinning, the fiber shape depends on the solidification rate, which can vary depending on various factors such as temperature, concentration, and viscosity. Ideally, circularly shaped fibers have higher strength than non-circular ones because they have less stress concentration and more uniform load distribution. Therefore, this shape irregularity was a problem not only for this study but also for other studies involving solution spinning of PVA and acrylic fibers [41,42]. I calculated fiber diameters from SEM images and obtained average fiber diameters for each drawing ratio, DR16 [24.0  $\mu\text{m}$ ], DR20 [20.0  $\mu\text{m}$ ], DR24 [16.0  $\mu\text{m}$ ], and DR28 [13.0  $\mu\text{m}$ ] with small variation (Table 2-2).

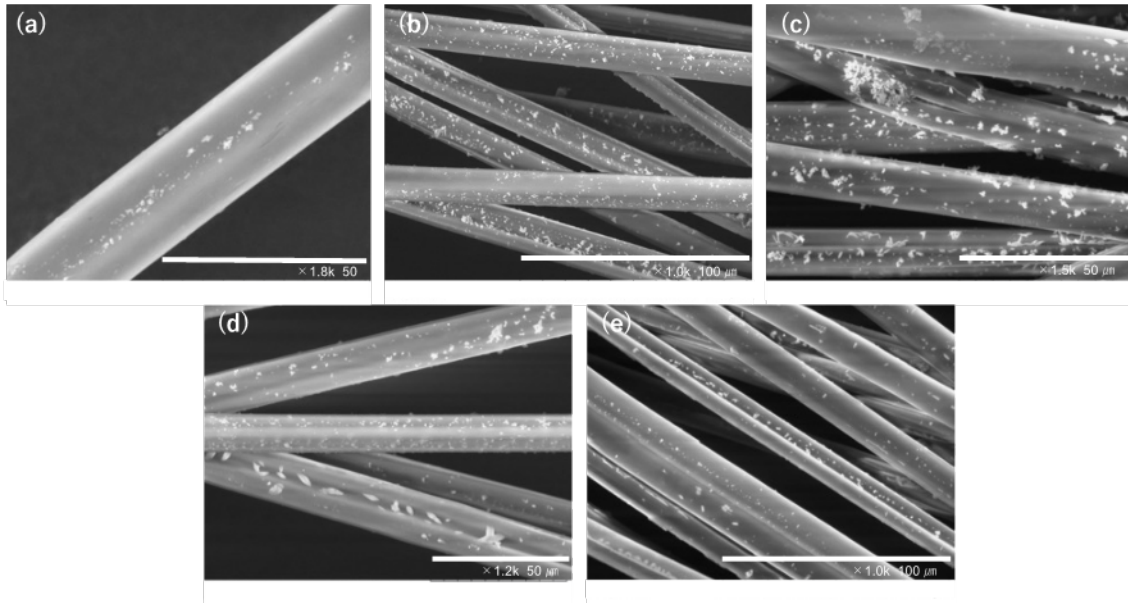


Figure 2-2 SEM images of PVA fibers. (a) Pure PVA DR16, (b) LiI-PVA DR16, (c) LiI-PVA DR20, (d) LiI-PVA DR24, (e) LiI-PVA DR28

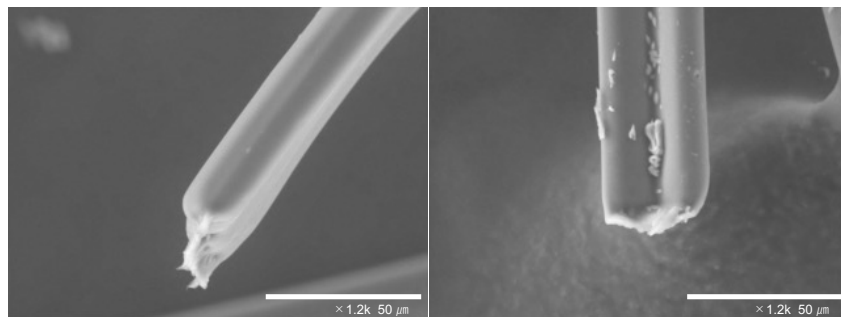


Figure 2-3 SEM images of PVA fiber shape observed at different angles.

Table 2-2 Fiber diameter at some points and average.

	1	2	3	4	5	6	7	8	9	10	Average [ $\mu\text{m}$ ]
DR4(P4,PL4)	35.0	35.3	35.5	40.7	39.6	40.0	28.0	27.2	45.5	39.3	$36.6 \pm 1.63$
DR16(P16)	22.7	23.1	23.2	23.7	24.4	23.5	23.2	29.1	22.3	21.4	$23.6 \pm 0.42$
DR16(PL16)	26.4	25.8	25.7	29.0	28.8	26.1	22.2	15.9	23.7	17.4	$24.1 \pm 1.40$
DR20	14.7	19.4	14.4	19.8	21.4	20.3	20.4	20.3	23.1	19.2	$19.3 \pm 0.87$
DR24	16.8	19.2	18.3	14.0	13.8	16.1	19.1	13.4	13.8	15.8	$16.0 \pm 0.72$
DR28	13.0	13.6	12.6	13.3	15.0	10.1	12.5	13.9	12.9	13.5	$13.0 \pm 0.41$

### 2-3-2. Thermal analysis of PVA fiber

As shown in Figure 2-4, the DSC heating curve of the PVA fiber reveals different melting peaks depending on the composition and stretching process. In P4, the melting peak appears at 236 °C, which is a characteristic peak of PVA due to its high degree of crystallization [43]. However, in PL4, the melting peak was reduced to 227 °C because LiI acts as a plasticizer that lowers the crystallization temperature and disrupts the hydrogen bonding network of PVA [28]. Figure 2-4(b) shows a PVA fiber after secondary stretching that had a higher melting point than that after only primary stretching. This indicates that secondary stretching increased the crystallinity and orientation of PVA fibers. The melting point measured from the DSC heating curve and the crystallinity  $X_C$  calculated using eq 1 are shown in Table 2-3.

This result is as expected and is caused by the fact that adding Li salts to PVA reduces crystallinity: Tretinnikov et al. reported that the addition of alkali metal salts to PVA changes crystallinity [44]. It has also been reported by Saari et al. that among alkali metal salts, lithium salts specifically decrease crystallinity [38]. It is known that the affinity between Li ions and hydroxyl groups (-OH) is high [45]. Therefore, the interaction of Li ions with the hydroxyl groups of PVA inhibits the hydrogen bonding between them, reducing its strength.

The effect of the Hofmeister series on PVA fibers was also investigated, as it has been reported to break hydrogen bonds and reduce crystallinity. Iodine ions, in particular, have a high hydrogen bond-breaking capacity [46], which improves the crystallinity of the stretched fibers due to the stretching and heat generated during the process. The aim of the LiI addition is to suppress the hydrogen bonding during heating and dissolving, which results in defect-free orientation during spinning, and the subsequent removal of LiI, resulting in high-strength fibers. To induce crystallization, heat treatment was performed after secondary drawing, as it was found to be more effective than simultaneous heat treatment and drawing.

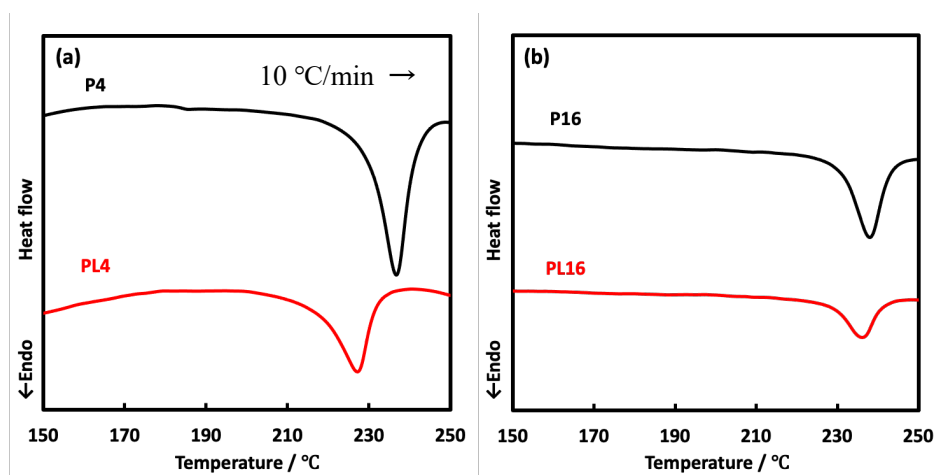


Figure 2-4 DSC heating curves of PVA fibers. (a) DR4, (b) DR16

Table 2-3 Melting point and crystallinity of stretched PVA fibers. ( $\pm$  standard error)

	Melting point ( $^{\circ}\text{C}$ )	Crystallinity (%)
P4	$236 \pm 0.2$	$36.2 \pm 0.3$
PL4	$227 \pm 0.1$	$28.3 \pm 0.2$
P16	$236 \pm 1.4$	$38.7 \pm 1.9$
PL16	$233 \pm 2.5$	$35.7 \pm 0.9$

### 2-3-3. Secondary stretching with LiI addition

Figure 2-5 shows the drawn fibers at different draw ratios. In pure PVA, the number of broken fibers increased as the drawing ratio was increased, but in LiI-PVA, no fiber breakage was observed as the drawing ratio was increased. This indicates that the addition of LiI suppresses hydrogen bonding in PVA and reduces crystallinity, thereby improving the ductility of the PVA fiber. This phenomenon is a major discovery in the process of increasing the strength of PVA fibers during drawing. Previously, Saari et al. reported that the addition of LiBr to PVA and thermal drawing increased strength [28], However, its drawing ratio was not very high. In this research, I have confirmed that heat-stretching can be performed up to 8 $\times$ .

One characteristic of heat-stretching is its temperature dependence. At low temperatures, the material may break even at a low drawing ratio when the stretching speed was increased. However, at high temperatures, the material could be stretched without a rupture even at a high drawing ratio. This behavior is likely due to the state of the molecular chains of PVA. For example, at lower temperatures, the molecular chains are less mobile, and the molecular chains slide, causing cleavage during stretching and orientation [47,48]. In other words, higher temperatures increase the mobility of the molecular chains, thus preventing breakage during stretching. It has also been found that the temperature and speed during stretching affect the tensile strength and Young's modulus of PVA fibers [44].

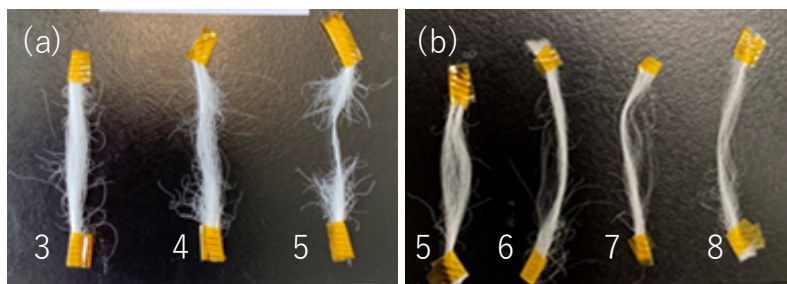


Figure 2-5 Heat-stretched of PVA fivers. (a) Pure PVA, (b) LiI PVA  
The numbers alongside the fibers represent the drawing ratio for heat-stretching.

#### 2-3-4. Tensile test

The results of tensile testing of the fibers are shown. Stress–strain curves for each drawing and heat treatment condition are summarized. The values of the axes of stress in all graphs are unified. Nominal stress (in MPa) and nominal strain are also shown in these results.

Figure 2-6 shows the tensile test results for the fiber with only primary stretch (PL4), where PL4 donates the ratio of final to initial length during drawing. The tensile strength was found to 139 MPa, and its Young's modulus was 3.2 GPa, which is expected since no advanced stretching, involving additional heating and cooling cycles, was performed on the fiber. These results are

being used as a reference point for comparison to results obtained from fibers that have undergone stretching.

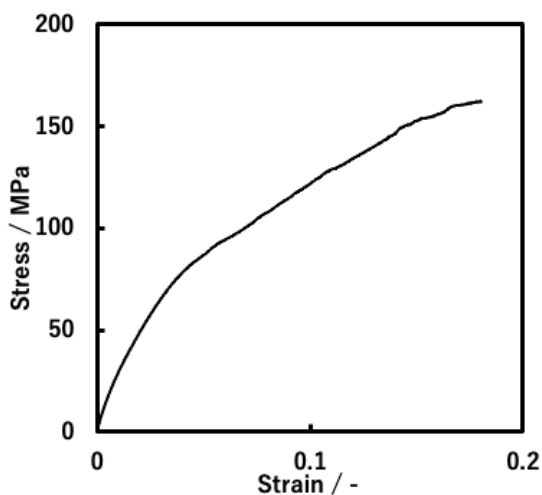


Figure 2-6 Stress-Strain curve of non-drawing fiber (PL4).

Figure 2-7 shows the stress-strain curves for P16 and PL16. As can be seen, there is almost no difference between P16 and PL16 at 16 $\times$ . The addition of LiI by itself does not indicate that it improves strength. However, by adding LiI, it is possible to achieve more than 16 $\times$  stretched, which was not possible without lithium addition, as shown in Figure 5.

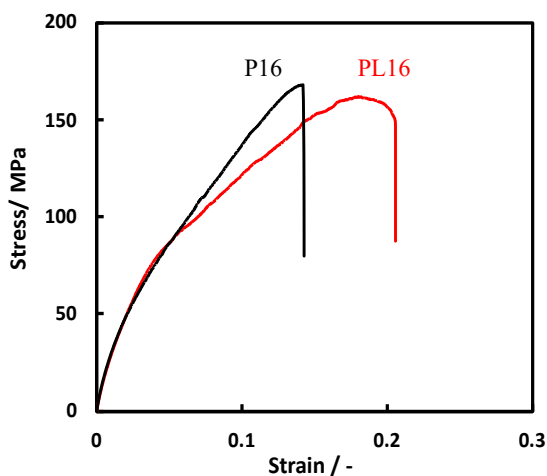


Figure 2-7 Stress-strain curves for P16 and P16 fibers.

Figure 2-8 shows a representative nominal stress–nominal strain curve for a fiber drawn at 120 °C, 1.0 mm/s. Table 2-4 shows the average values and error ranges for tensile strength and Young’s modulus. It is noteworthy that the differences in mechanical strength with a draw ratio (DR), which is the ratio of final to initial length during drawing, were substantial. Particularly for DR28, both the tensile strength and Young’s modulus showed improvement compared to DR20. Furthermore, the fiber labeled as P28-120-1.0(120), which was stretched at 120 °C with DR28 and heat-treated at 120 °C, displayed the highest value of 775 MPa, serving as the champion data with an average value of 639 MPa. This indicates that secondary stretching, involving additional heating and cooling cycles after primary stretching, can enhance the strength of the fiber. It is worth noting that the effect of secondary stretching on fiber strength is likely influenced by the conditions of heat-treatment.

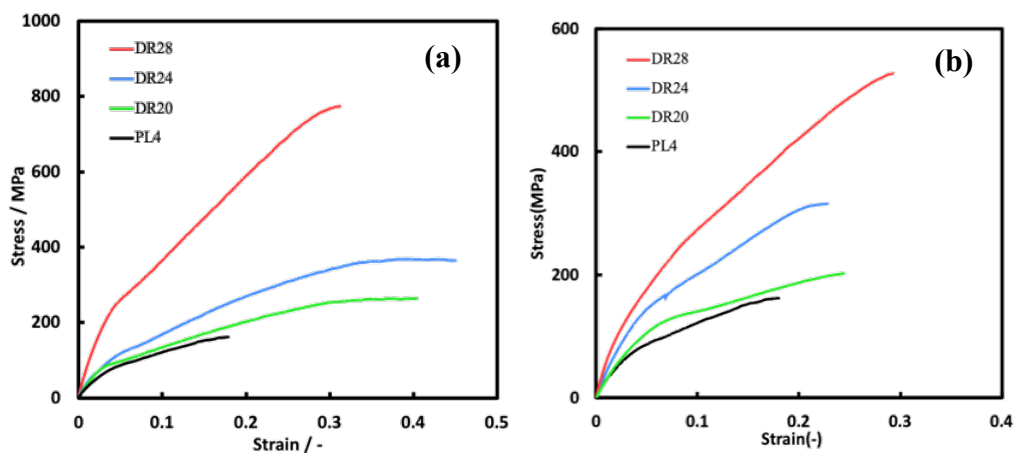


Figure 2-8 Stress-Strain curves of PVA fibers stretched at 120 °C, 1.0 mm/s. (a) Heat-treatment at 120 °C for one night, and (b) Heat-treatment at 150 °C 1 hour

Table 2-4 Tensile strength and Young's modulus of fibers stretched at 120 °C, 1.0 mm/s. ( $\pm$  standard error)

	Tensile strength / MPa	Young's modulus / GPa
P20-120-1.0(120)	251 $\pm$ 13.4	3.5 $\pm$ 0.40

P24-120-1.0(120)	$308 \pm 38.4$	$4.1 \pm 0.55$
P28-120-1.0(120)	$639 \pm 67.9$	$9.7 \pm 0.60$
P20-120-1.0(150)	$180 \pm 21.6$	$3.0 \pm 0.070$
P24-120-1.0(150)	$424 \pm 62.0$	$5.9 \pm 0.76$
P28-120-1.0(150)	$509 \pm 44.5$	$5.4 \pm 0.60$

Figure 2-9 shows the results of the tensile test conducted on fibers stretched at 180 °C and 1.0 mm/s. Table 2-5 shows the average values and error ranges for the tensile strength and Young's modulus. The mechanical strength of these fibers was found to be lower than that of fibers stretched at 120 °C, 1.0 mm/s. Notably, when the heat-treatment condition was 120 °C for one night (24 h) (P28-180-1.0(120)), the average value was 370 MPa for DR28 and 524 MPa as champion data, which was lower than those obtained at other conditions. This may be due to the effect of higher temperature during stretching on the crystals of PVA, which are affected by heat exposure [5,49,50]. Additionally, the decomposition of PVA can generate volatile products such as water, carboxyl acid, unsaturated aldehydes, and other unsaturated compounds [51].

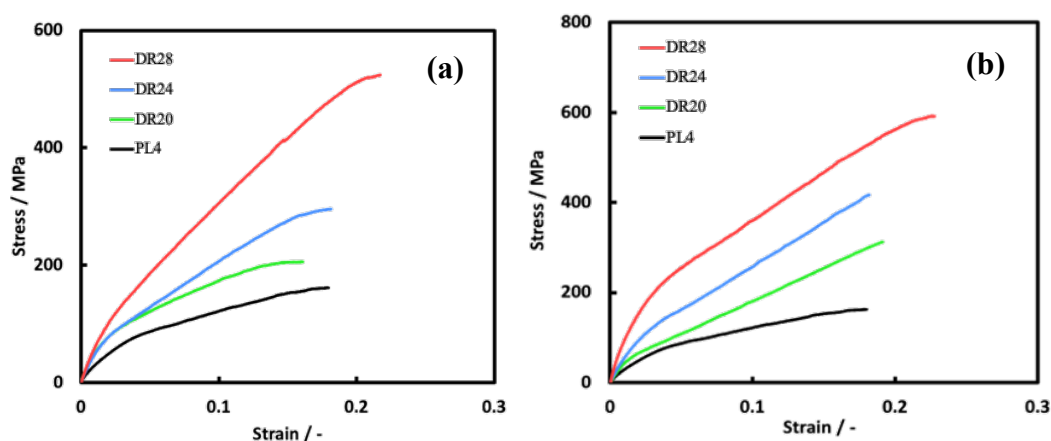


Figure 2-9 Stress-Strain curves of PVA fibers stretched at 180 °C, 1.0 mm/s. (a) Heat-treatment at 120 °C for one night, and (b) Heat-treatment at 150 °C 1 hour

Table 2-5 Tensile strength and Young's modulus of fibers stretched at 180 °C, 1.0 mm/s. ( $\pm$  standard error)

	Tensile strength / MPa	Young's modulus / GPa
P20-180-1.0(120)	176 $\pm$ 16.5	4.0 $\pm$ 0.4
P24-180-1.0(120)	246 $\pm$ 31.1	5.9 $\pm$ 0.39
P28-180-1.0(120)	370 $\pm$ 88.0	6.9 $\pm$ 0.90
P20-180-1.0(150)	242 $\pm$ 38.8	4.8 $\pm$ 0.43
P24-180-1.0(150)	309 $\pm$ 60.5	6.3 $\pm$ 0.10
P28-180-1.0(150)	460 $\pm$ 76.2	7.6 $\pm$ 2.0

Figure 2-10 shows the results of tensile tests conducted on fibers stretched at 180 °C and 1.5 mm/s. Table 2-6 shows the average values and error ranges of the tensile strength and Young's modulus. The mechanical strength of fibers was found to be significantly improved by increasing the drawing speed while maintaining the stretching temperature at 180 °C. This improvement can be attributed to two factors. First, increasing the drawing speed reduced the exposure time of the fibers to high temperatures, preventing thermal decomposition. Second, high temperature and high drawing speed can suppress the relaxation of orientation during stretching, which is a common issue with stretched fibers. When fibers are stretched at high temperatures, the polymer molecular chain becomes more mobile and can easily be stretched in the direction of stress [47]. However, at high temperatures, the stretched molecular chains also become more mobile, and some degree of shrinkage occurs when the relaxation time of the molecular chains is long. This results in orientation relaxation, which reduces the fiber orientation, thereby decreasing strength and crystallinity [47]. As mentioned above, stretching speed is known to affect the mechanical strength of fibers, and it has been shown that fibers can attain very high mechanical strength at

certain speeds [47]. In this study found that the highest value was obtained when the fibers were stretched at a relatively fast speed of 1.5 mm/s.

In addition to the differences observed in the mechanical strength of fibers under different drawing conditions, the study found that the heat-treatment conditions also have a significant impact on the fiber strength. For instance, the fiber heat-treated at 150 °C for 1 h (P28-180-1.5(150)) exhibited a tensile strength of 1436 MPa and Young's modulus of 18.9 GPa as champion data, which was about 1.5 times higher than the highest value obtained for other conditions. This finding is particularly interesting because heat-treatment is a crucial process used in many polymer products to improve their crystallinity, toughness, and water resistance [52,53]. Thus, the results suggest that achieving high fiber strength requires optimizing not only the drawing conditions but also the heat-treatment conditions. Furthermore, the addition of LiI to suppress defects in molecular orientation during spinning alone may not be sufficient to achieve high fiber strength. Saari et al. reported that the drawing ratio of the LiBr-doped PVA fiber in their wet spinning method was about 10×, and its elastic modulus and tensile strength were 17.5 GPa and 177 MPa, respectively [28]. In this study, I was able to increase the drawing ratio by a factor of 28×, resulting in a significant increase in elastic modulus and tensile strength. This is attributed to the fact that LiI is more effective than LiBr in inhibiting hydrogen bonding, thereby reducing orientation defects during stretching.

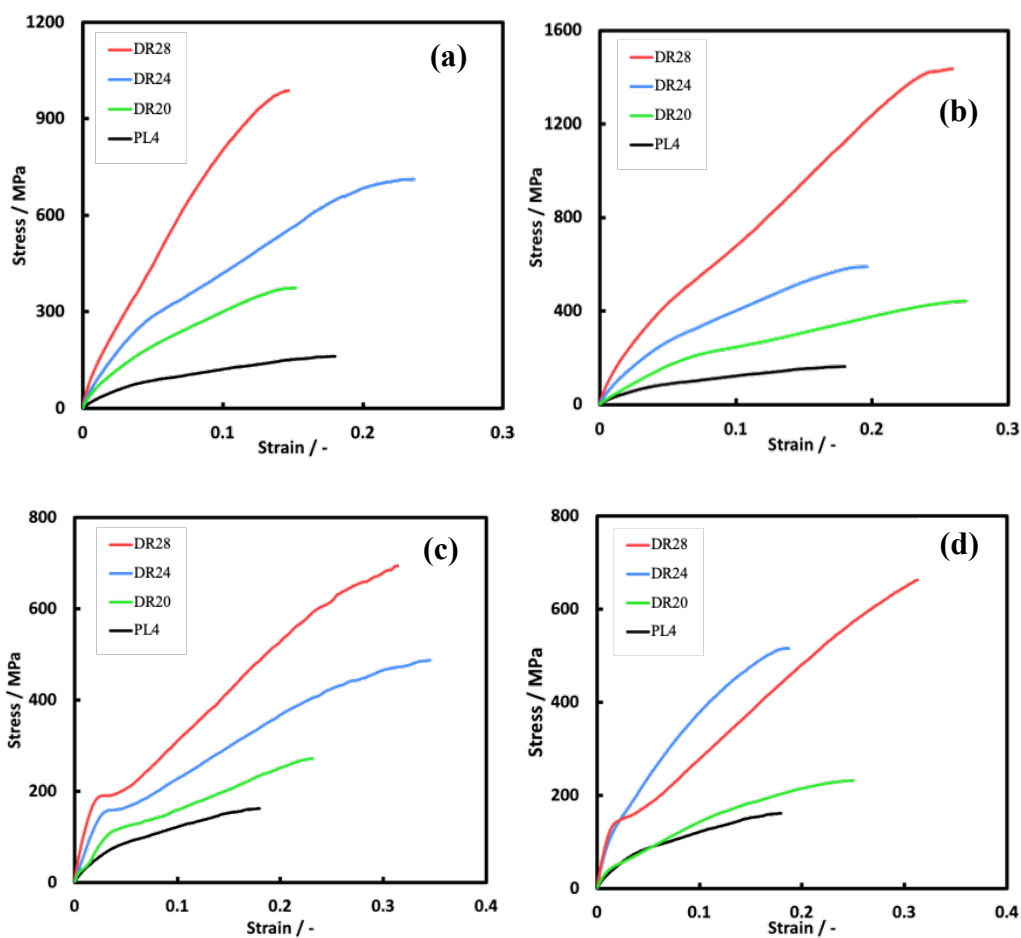


Figure 2-10 Stress-Strain curves of PVA fibers stretched at 180 °C, 1.5 mm/s. (a) Heat-treatment at 120 °C for one night, (b) Heat-treatment at 150 °C for 1 hour, (c) Heat-treatment at 150 °C for 6 hours, and (d) Heat-treatment at 190 °C for 5 minutes

Table 2-6 Tensile strength and Young's modulus of fibers stretched at 180 °C, 1.5 mm/s. ( $\pm$  standard error)

	Tensile strength / MPa	Young's modulus / GPa
P20-180-1.5(120)	$316 \pm 53.1$	$7.4 \pm 0.50$
P24-180-1.5(120)	$588 \pm 72.0$	$9.9 \pm 0.41$
P28-180-1.5(120)	$842 \pm 76.1$	$16 \pm 0.39$
P20-180-1.5(150)	$352 \pm 45.5$	$5.1 \pm 0.36$
P24-180-1.5(150)	$519 \pm 59.1$	$9.0 \pm 0.76$

P28-180-1.5(150)	1078 ± 232	16 ± 2.20
P20-180-1.5(150-6)	250 ± 12.8	5.1 ± 0.70
P24-180-1.5(150-6)	434 ± 18.4	6.2 ± 1.06
P28-180-1.5(150-6)	710 ± 27.3	11 ± 0.81
P20-180-1.5(190)	196 ± 36.0	3.2 ± 0.60
P24-180-1.5(190)	388 ± 68.3	6.7 ± 1.50
P28-180-1.5(190)	668 ± 18.4	9.6 ± 1.20

Figures 2-11 and 2-12 present a comparison of the tensile strength and Young's modulus of fibers subjected to different drawing conditions. The fibers were stretched and heat-treated at either 1.0 or 1.5 mm/s at 180 °C. There is a large difference between the two drawing conditions. The numbers on the horizontal axis represent different samples. 'None' denotes fibers that were only subjected to primary stretching without any subsequent heat treatment. "1" denotes fibers that were stretched at 180 °C, 1.0 mm/s and heat-treated at 120 °C for one night. "2" denotes fibers that were stretched at 150 °C for 1 h. "3" denotes fibers that were stretched at 180 °C, 1.5 mm/s and heat-treated at 120 °C for one night. "4" denotes fibers that were heat-treated at 150 °C for 1 h. "5" denotes fibers that were heat-treated at 150 °C for 6 h. "6" denotes fibers that were heat-treated at 190 °C for 5 min.

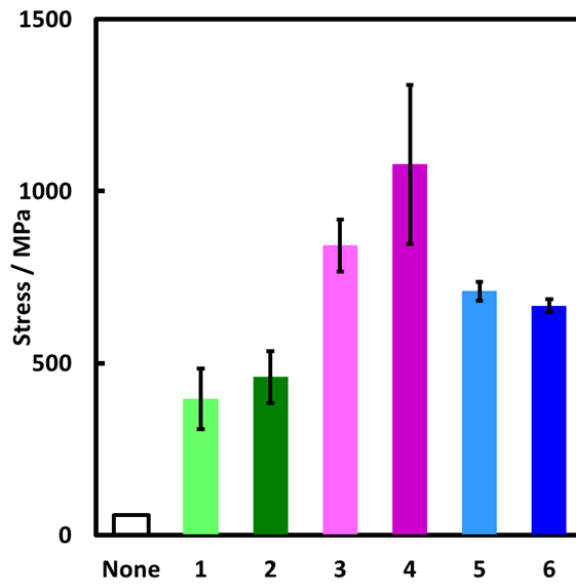


Figure 2-11 Comparison of tensile strength of fibers stretched at 180 °C, 1.0 mm/s and 1.5 mm/s.

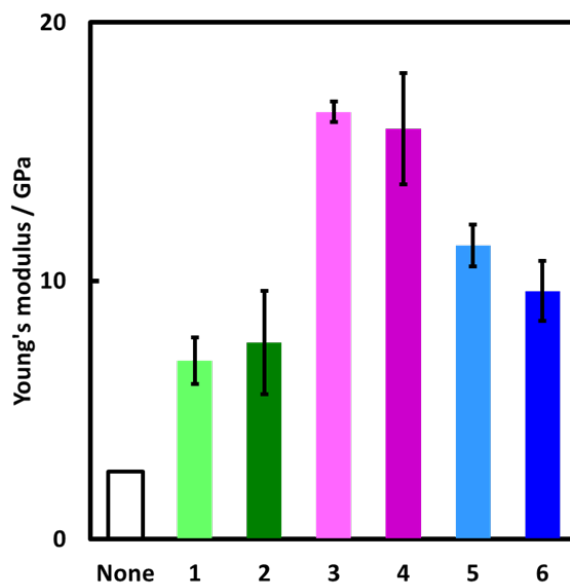


Figure 2-12 Comparison of young's modulus of fibers stretched at 180 °C, 1.0 mm/s and 1.5 mm/s.

### 2-3-5. Orientation analysis by 2D-WAXD

The crystalline orientation of the fibers subjected to the drawing and heat-treatment conditions that resulted in the highest strength was investigated using 2D-WAXD. Figure 2-13 displays 2D-WAXD images of unstretched and stretched fibers at 180 °C and 1.5 mm/s. In the X-ray diffraction images, the perpendicular direction is along the fiber axis. The stretched fiber exhibits strong diffraction spots at the equator, indicating that the molecular chains of PVA are oriented.

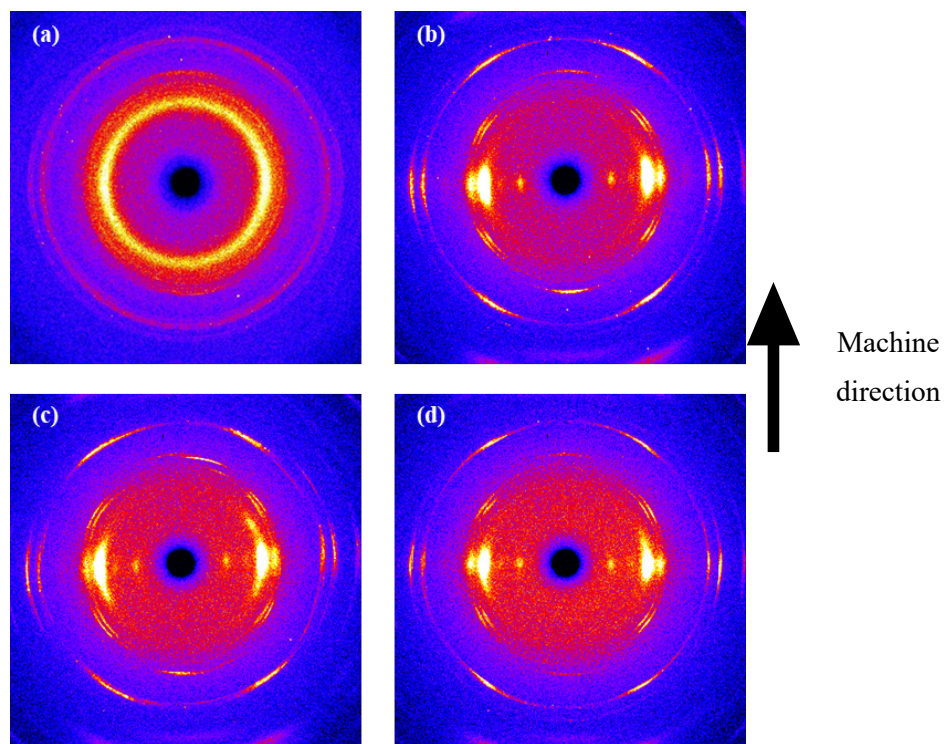


Figure 2-13 2D-WAXD images of PVA fiber stretched at 180 °C, 1.5mm/s (The machine direction is in the direction of the arrow).  
(a) DR4, (b) DR20, (c) DR24, and (d) DR28

Figure 2-14 shows the  $2\theta$  profile at the equator. The profile exhibits  $\alpha$ -monoclinic peaks in the (001), (101), and (200) crystal planes, which can be attributed to PVA. These peaks are easily identified since they have been previously reported in various studies [54]. The peak around 32–35° corresponds to sodium sulfate adhered to the fiber during spinning (Figure 2-15). This residue

is left over from the washing process. As shown in Figure 13, the crystalline orientation of the PVA fiber is greatly enhanced by heat-stretching, and the (001), (101), and (200) equatorial spots, which are due to PVA crystals, are stronger than in the DR4 fiber. In particular, the equatorial spots are smaller for the DR28 fiber, indicating that the crystalline orientation becomes stronger as the fiber is stretched and the draw ratio is increased.

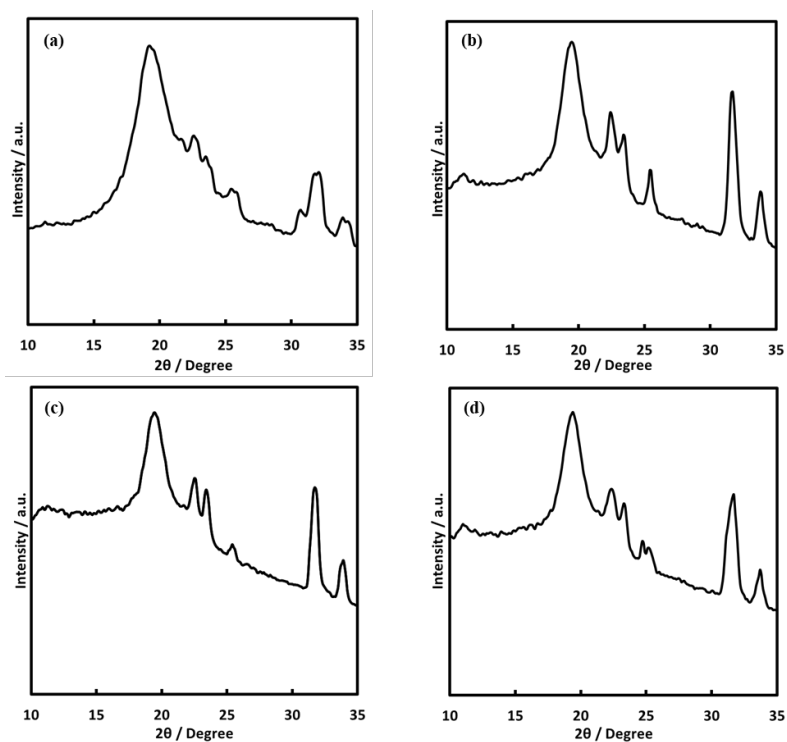


Figure 2-14  $2\theta$  profiles of PVA fibers stretched at 180 °C, 1.5mm/s.  
(a) DR4, (b) DR20, (c) DR24, and (d) DR28

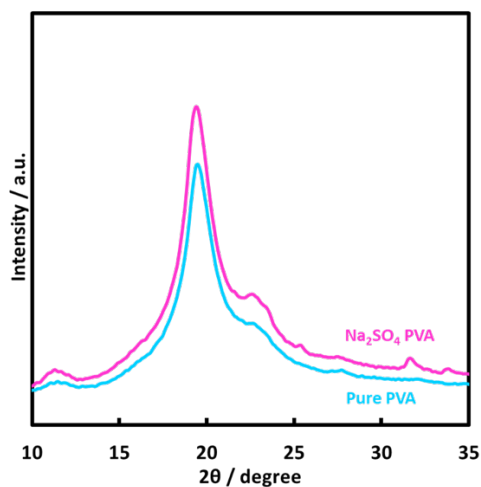


Figure 2-15  $2\theta$  profiles of Pure PVA film and PVA film with sodium sulfate.  $\text{Na}_2\text{SO}_4$  PVA film shows a characteristic peak between  $32^\circ$  and  $35^\circ$ , which is not seen in Pure PVA.

Figure 2-16 illustrates the azimuthal distribution in the (101) crystal plane. The azimuthal distribution is used to determine the orientation of the molecular chains of PVA fibers [28,55]. The widths of the peaks at values of  $\beta$  at  $90^\circ$  and  $270^\circ$  on the equator were evaluated. The diffraction patterns reveal a stronger orientation for fibers that have undergone secondary stretching, indicating that secondary stretching has enhanced the molecular orientation of PVA. Compared to DR4, the difference is significant, with an orientation value of 73.0%, which has now increased to over 90.0%. In particular, the highest value of 93.7% was achieved for DR28. This indicates that it is possible to increase the orientation of the PVA fiber spun with LiI by stretching while applying heat. However, DR20 and DR24 did not show much difference in the degree of orientation. With DR28, the range of improvement became somewhat larger, and more advanced secondary stretching is required to increase the degree of orientation further. Although this study only evaluated PVA fibers stretched to a maximum of  $28\times$ , it was confirmed that it is possible to stretch PVA fibers to even higher stretch magnifications, which would improve the degree of orientation.

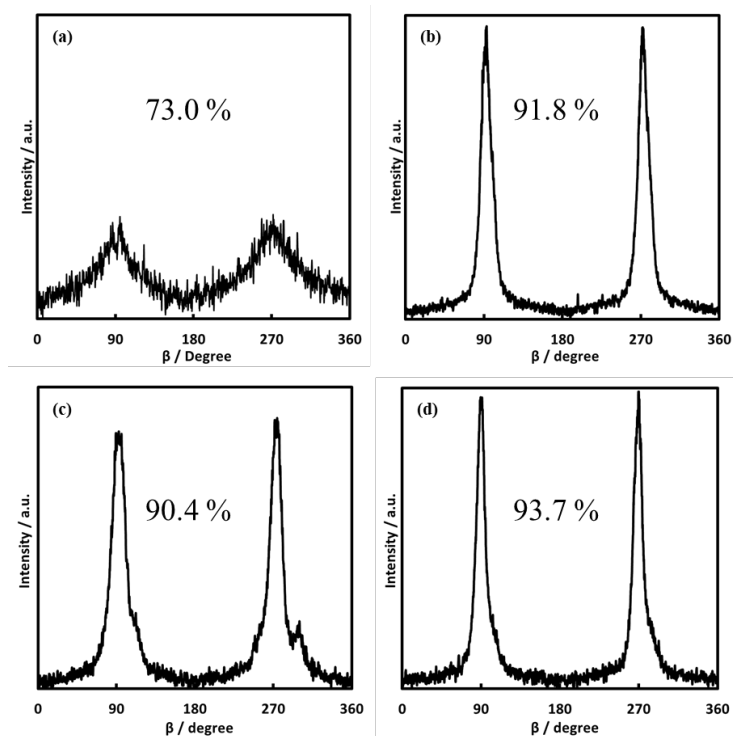


Figure 2-16 Azimuthal distribution in the (101) plane of PVA fibers stretched at 180 °C, 1.5mm/s.  
 (a) DR4, (b) DR20, (c) DR24, and (d) DR28

### 2-3-6. Measurement of lithium concentration

Residual LiI in the fiber can cause certain disadvantages for the industrial use of PVA fibers. The runoff of high concentrations of I, Br, and other halogens into the environment can harm ecosystems and nature [56,57]. Additionally, several studies have been conducted on the risks of plasticizers in polymer products [58-60]. This means that care should be taken regarding additives and plasticizers in polymer products. Therefore, I investigated the residual Li concentration.

Table 2-7 displays the Li concentration in the LiI-PVA solution before spinning, the fiber after spinning, and the fiber after washing. The Li concentration in the final PVA fiber was 0.01 mg/mg. The Li ion concentration of the LiI-added PVA solution used for spinning was 0.30 mg/mg. In other words, it was found that about 97% of the lithium was removed compared to the amount of

lithium in the solution state. This indicates that most of the LiI can be removed by wet spinning and washing. Therefore, PVA fibers produced by this method can be used in many fields without any issues.

Table 2-7 Measurements of lithium concentration. ( $\pm$  standard error)

	Lithium concentration (mg/mg)
LiI PVA solution	0.30
Fiber after spinning	$0.05 \pm 0.01$
Fibers after washing	$0.01 \pm 0.001$

### 2-3-7. Summary of this study

In this study, I focused on increasing strength by improving ductility and orientation. Although a significant improvement in mechanical strength was confirmed, there were limitations with the current method, such as the variability caused by manual wet spinning. However, I found that stretching of 28 $\times$  or more was possible, and the improvement in stretchability due to the addition of LiI was tremendous. It was not possible to obtain the mechanical strength of high-performance fibers such as CF and GF. However, my proposed wet spinning of the LiI-based PVA fiber can be easily mass-produced using current equipment. This can minimize the cost increase in industrial applications to the greatest extent possible. In addition, wet spinning of the PVA fiber is an organic solvent-free method with a low environmental impact, which is one of the solutions to our current environmental problems.

In the future, I believe that further improvement of mechanical strength and molecular orientation can be achieved by using mechanically spinnable equipment to enable uniform stretching. Furthermore, the interfacial strength of PVA fibers with a matrix resin as FRP reinforcing fibers should be evaluated.

## **2-4. Conclusion**

In this study, I proposed a new method for producing high-strength PVA fibers for composite applications by adding LiI to reduce hydrogen bonds in the PVA molecular chain and improve the spinnability of the PVA fibers. I enhanced the mechanical strength of the PVA fibers by improving their heat stretchability and increasing their level of molecular orientation. I was able to remove almost all of the LiI added to PVA through the spinning and washing processes. This simple and effective method of increasing the strength of PVA fibers can be achieved by simply adding LiI to the PVA solution, which is the raw material for spinning. This technology has the potential to provide inexpensive, lightweight, and mechanically strong PVA fibers that can contribute to the development of high sustainability.

## 2-5. References

- [1] M.I. Baker, S.P. Walsh, Z. Schwartz, B.D. Boyan, A review of polyvinyl alcohol and its uses in cartilage and orthopedic applications, *Journal of Biomedical Materials Research Part B Applied Biomaterials*, Vol.100B (5) p1451-1457 (2012)
- [2] F. Kawai, X. Hu, Biochemistry of microbial polyvinyl alcohol degradation, *Applied Microbiology and Biotechnology*, Vol.84 (2) p227-237 (2009)
- [3] C.C. Demerlis, D.R. Schoneker, Review of the oral toxicity of polyvinyl alcohol (PVA), *Food and Chemical Toxicology*, Vol.41 (3) p319-326 (2003)
- [4] M. Shimano, Biodegradation of plastics, *Current Opinion in Biotechnology*, Vol.12 (3) p242-247 (2003)
- [5] M. Aslam, M.A. Kalyar, Z.A. Raza, Polyvinyl alcohol: A review of research status and use of polyvinyl alcohol based nanocomposites, *Polymer Engineering and Science*, Vol.58 (12) p2119-2132 (2018)
- [6] K.K. Gaikwad, J.Y. Lee, Y.S. Lee, Development of polyvinyl alcohol and apple pomace bio-composite film with antioxidant properties for active food packaging application, *Journal of Food Science and Technology*, Vol.53 (3) p1608-1619 (2016)
- [7] S.R. Kanatt, M.S. Rao, S.P. Chawla, A. Sharma, Active chitosan-polyvinyl alcohol films with natural extracts, *Food Hydrocolloids*, Vol.29 (2) p290-297 (2012)
- [8] K. Matsumura, Special issue: Nanocomposite hydrogels for biomedical applications, *Applied Sciences*, Vol.10 (1) 389 (2020)
- [9] T. Sakaguchi, S. Nagano, M. Hara, S.H. Hyon, M. Patel, K. Matsumura, Facile preparation of transparent poly (vinyl alcohol) hydrogels with uniform microcrystalline structure by hot-pressing without using organic solvents, *Polymer Journal*, Vol.49 (7) p535-542 (2017)
- [10] Y. Zhao, W. Terai, Y. Hoshijima, K. Gotoh, K. Matsuura, K. Matsumura, Development and

characterization of a poly (Vinyl Alcohol)/graphene oxide composite hydrogel as an artificial cartilage material, *Applied Science*, Vol.8 (11) 2272 (2018)

[11] W. Si, M. Cao, L. Li, Establishment of fiber factor for rheological and mechanical performance of polyvinyl alcohol (PVA) fiber reinforced mortar, *Construction and Building Materials*, Vol.265 (30) 120347 (2020)

[12] J. Nam, G. Kim, B. Lee, R. Hasegawa, Y. Hama, Frost resistance of polyvinyl alcohol fiber and polypropylene fiber reinforced cementitious composites under freeze thaw cycling, *Composites Part B: Engineering*, Vol.90 (1) p241-250 (2016)

[13] C.C. Thong, D.C.L. Teo, C.K. Ng, Application of polyvinyl alcohol (PVA) in cement-based composite materials: A review of its engineering properties and microstructure behavior, *Construction and Building Materials*, Vol.107 (15) p172-180 (2016)

[14] J. Jang, D.K. Lee, Plasticizer effect on the melting and crystallization behavior of polyvinyl alcohol, *Polymer*, Vol.44 (26) p8139-8146 (2003)

[15] W. Zhang, X. Zou, F. Wei, H. Wang, G. Zhang, Y. Huang, Y. Zhang, Grafting SiO<sub>2</sub> nanoparticles on polyvinyl alcohol fibers to enhance the interfacial bonding strength with cement, *Composites Part B: Engineering*, Vol.162 (1) p500-507 (2019)

[16] I. Curosu, M. Liebscher, G. Alsous, E. Muja, H. Li, A. Drechsler, R. Frenzel, A. Synytska, V. Mechtcherine, Tailoring the crack-bridging behavior of strain-hardening cement-based composites (SHCC) by chemical surface modification of poly(vinyl alcohol) (PVA) fibers, *Cement and Concrete Composites*, Vol.114 103722 (2020)

[17] X. Huang, Fabrication and properties of carbon fibers, *Materials*, Vol.2 (4) p2369-2403 (2009)

[18] J. Chen, D. Zhao, X. Jin, C. Wang, D. Wang, H. Ge, Modifying glass fibers with graphene oxide: Towards high-performance polymer composites, *Composites Science and Technology*, Vol.97 (16) p41-45 (2014)

- [19] P.M. Gore, B. Kandasubramanian, Functionalized Aramid Fibers and Composites for Protective Applications: A Review, *Industrial & Engineering Chemistry Research*, Vol.57 (49) p16537-16563 (2018)
- [20] B. Zhang, L. Jia, M. Tian, N. Ning, L. Zhang, W. Wang, Surface and interface modification of aramid fiber and its reinforcement for polymer composites: A review, *European Polymer Journal*, Vol.147 (15) 110352 (2021)
- [21] S. Prashanth, K.M. Subbaya, K. Nithin, S. Sachhidananda, Fiber Reinforced Composites - A Review, *Journal of Materials Science & Engineering*, Vol.6 (3) 1000341 (2017)
- [22] F. Rubino, A. Nisticò, F. Tucci, P. Carlone, Marine application of fiber reinforced composites: A review, *Journal of Marine Science and Engineering* Vol.8 (1) 26 (2019)
- [23] S. Hegde, B.S. Shenoy, K.N. Chethan, Review on carbon fiber reinforced polymer (CFRP) and their mechanical performance, *Materials Today: Proceedings*, Vol.19 (2) p658-662 (2019)
- [24] H. Ahmad, A.A. Markina, M.V. Porotnikov, F. Ahmad, A review of carbon fiber materials in automotive industry. *IOP Conference Series: Materials Science and Engineering*, Vol.71 (3) 032011 (2020)
- [25] A. Jacob, Composites can be recycled, *Reinforced Plastics*, Vol.55 (3) p45-46 (2011)
- [26] D.S. Cousins, Y. Suzuki, R.E. Murray, J.R. Samaniuk, A.P. Stebner, Recycling glass fiber thermoplastic composites from wind turbine blades, *Journal of Cleaner Production*, Vol.209 (1) p1252-1263 (2019)
- [27] S.R. Naqvi, H.M. Prabhakara, E.A. Bramer, W. Dierkes, R. Akkerman, G. Brem, A critical review on recycling of end-of-life carbon fibre/glass fibre reinforced composites waste using pyrolysis towards a circular economy, *Resources, Conservation and Recycling*, Vol.136 p118-129 (2018)
- [28] R.A. Saari, R. Maeno, W. Marujiwat, M.S. Nasri, K. Matsumura, M. Yamaguchi, Modification of poly(vinyl alcohol) fibers with lithium bromide. *Polymer*, Vol.213 123193 (2021)

- [29] R. Nishikawa, N. Aridome, N. Ojima, M. Yamaguchi, Structure and properties of fiber-reinforced polypropylene prepared by direct incorporation of aqueous solution of poly(vinyl alcohol). *Polymer, Vol.199* 122566 (2020)
- [30] M. Guo, H. Yang, H. Tan, C. Wang, Q. Zhang, R. Du, Q. Fu, Shear enhanced fiber orientation and adhesion in PP/glass fiber composites, *Macromolecular Materials and Engineering, Vol.291 (3)* p239-246 (2006)
- [31] D. Lai, Y. Wei, L. Zou, Y. Xu, H. Lu, Wet spinning of PVA composite fibers with a large fraction of multi-walled carbon nanotubes, *Progress in Natural Science: Materials International, Vol.25 (5)* p445-452 (2015)
- [32] N. Nagashima, S. Matsuzawa, M. Okazaki, Syndiotacticity-rich poly(vinyl alcohol) fibers spun from N-methylmorpholine-N-oxide/water mixture, *Journal of Applied Polymer Science, Vol.62 (10)* p1551-1559 (1996)
- [33] H. Wang, J. He, L. Zou, C. Wang, Y. Wang, Synthesis of syndiotacticity-rich high polymerization degree PVA polymers with VAc and VPa, fabrication of PVA fibers with superior mechanical properties by wet spinning, *Journal of Polymer Research , Vol.28 (10)* 386 (2021)
- [34] L. Dai, L. Ying, Infrared Spectroscopic Investigation of Hydrogen Bonding in EVOH Containing PVA Fibers, *Macromolecular Materials and Engineering, Vol.287 (8)* p509-514 (2002)
- [35] X. Hong, Y. Xu, L. Zou, Y.V. Li, J. He, J. Zhao, The Effect of Degree of Polymerization on the Structure and Properties of Polyvinyl Alcohol Fibers with High Strength and High Modulus, *Journal of Applied Polymer Science, Vol.138 (10)* 49971 (2021)
- [36] X. Hong, J. He, L. Zou, Y. Wang, Y.V. Li, Preparation and Characterization of High Strength and High Modulus PVA Fiber via Dry-wet Spinning with Cross-linking of Boric Acid, *Journal of Applied Polymer Science, Vol.138 (47)* 51394 (2021)
- [37] I. Sakurada, Wet Spinning I: Use of a Sodium Bath. In Polyvinyl Alcohol Fibers. Sakurada I. Ed.;

Maecel Dekker. Inc.; New York and Basel, p63-186 (1985)

[38] R.A. Saari, R. Maeno, R. Tsuyuguchi, W. Marujiwat, O. Phulkard, M. Yamaguchi, Impact of Lithium halides on rheological properties of aqueous solution of poly (vinyl alcohol), *Journal of Polymer Research*, Vol.27 218 (2020)

[39] X. Wang, S.Y. Park, K.H. Yoon, W.S. Lyoo, B.G. Min, The effect of multi-walled carbon nanotubes on the molecular orientation of poly(vinyl alcohol) in drawn composite films, *Fibers and Polymers*, Vol.7 (4) p323-327 (2006)

[40] M. Iwai, F. Kondo, T. Suzuki, T. Ogawa, H. Seno, Application of Lithium Assay kit LS for quantification of lithium in whole blood and urine, *Legal Medicine*, Vol.49 101834 (2021)

[41] J.S. Tsai, W.C. Su, Control of cross-section shape for polyacrylonitrile fibre during wet-spinning, *Journal of Materials Science Letters*, Vol.10 p1253-1256 (1991)

[42] Y.X. Wang, C.G. Wang, M.J. Yu, Effects of different coagulation conditions on polyacrylonitrile fibers wet spun in a system of dimethylsulphoxide and water, *Journal of Applied Polymer Science*, Vol.104 (6) p3723-3729 (2007)

[43] D. Thomas, P. Cebe, Self-nucleation and crystallization of polyvinyl alcohol, *Journal of Thermal Analysis and Calorimetry*, Vol.127 p885-894 (2017)

[44] O.N. Tretinnikov, S.A. Zagorskaya, Effect of alkali halide salt additives on the structure of poly(vinyl alcohol) films cast from aqueous solutions, *Polymer Science Series A*, Vol.55 (8) p463-470 (2013)

[45] N.L. Ma, F.M. Siu, C.W. Tsang, Interaction of alkali metal cations and short chain alcohols: effect of core size on theoretical affinities, *Chemical Physics Letters*, Vol.322 (1-2) p65-72 (2000)

[46] R.A. Saari, M.S. Nasri, W. Marujiwat, R. Maeno, M. Yamaguchi, Application of the Hofmeister series to the structure and properties of poly(vinyl alcohol) films containing metal salts, *Polymer Journal*, Vol.53 (4) p557-564 (2021)

- [47] Q. Wu, N. Chen, Q. Wang, Crystallization behavior of melt-spun poly(vinyl alcohol) fibers during drawing process, *Journal of Polymer Research*, Vol.17 (6) p903-909 (2010)
- [48] D.R. Salem, Crystallization kinetics during hot-drawing of poly (ethylene terephthalate) film: strain-rate/draw-time superposition. *Polymer*, Vol.33 (15) p3189-3192 (1992)
- [49] M.I. Voronova, Q.V. Surov, S.S. Guseinov, V.P. Barannikov, A.G. Zakharov, Thermal stability of polyvinyl alcohol/nanocrystalline cellulose composites, *Carbohydrate Polymers*, Vol.130 (5) p440-447 (2015)
- [50] W. Wu, H. Tian, A. Xiang, Influence of polyol plasticizers on the properties of polyvinyl alcohol Films Fabricated by Melt Processing, *Journal of Polymers and the Environment*, Vol.20 p53-69 (2012)
- [51] R. Lu, E. Ma, Z. Xu, Application of pyrolysis process to remove and recover liquid crystal and films from waste liquid crystal display glass, *Journal of Hazardous Materials*, Vol.243 p311-318 (2012)
- [52] H. Simmons, P. Tiwary, J.E. Colwell, M. Kontopoulou, Improvements in the crystallinity and mechanical properties of PLA by nucleation and annealing, *Polymer Degradation and Stability*, Vol.166 pp248-257 (2019)
- [53] B.A.G. Schrauwen, R.P.M. Janssen, L.E. Govaert, H.E.H Meijer, Intrinsic deformation behavior of semicrystalline polymers. *Macromolecules*, Vol.37 (16) p6069-6078 (2004)
- [54] M.L. Minus, H.G. Chae, S. Kumar, Single wall carbon nanotube templated oriented crystallization of poly(vinyl alcohol). *Polymer*, Vol.47 (11) p3705-3710 (2006)
- [55] X. Hong, Y. Xu, L. Zou, Y.V. Li, J. He, J. Zhao, The effect of degree of polymerization on the structure and properties of polyvinyl alcohol fibers with high strength and high modulus, *Journal of Applied Polymer Science*, Vol.138 (10) 49971 (2021)
- [56] J.S. Harkness, G.S. Dwyer, N.R. Warner, K.M. Parker, W.A. Mitch, A. Vengosh, Iodide, bromide, and ammonium in hydraulic fracturing and oil and gas wastewaters: Environmental implications,

*Environmental Science & Technology*, Vol.49 (3) p1955-1963 (2015)

[57] K. Watson, M.J Farré, N. Knight, Strategies for the removal of halides from drinking water sources, and their applicability in disinfection by-product minimisation: A critical review, *Journal of Environmental Management*, Vol.110 p276-298 (2012)

[58] R.U. Halden, Plastics and health risks, *Annual Review of Public Health*, Vol.31 p179-194 (2010)

[59] E. Gustafsson, T.M. Bowden, A.R. Rennie, Interactions of amphiphiles with plasticisers used in polymers: Understanding the basis of health and environmental challenges, *Advances in Colloid and Interface Science*, Vol.277 102109 (2020)

[60] M. Mukhopadhyay, M. Jalal, G. Vignesh, M. Ziauddin, S. Sampath, G.K. Bharat, L. Nizzetto, P. Chakraborty, Migration of Plasticizers from Polyethylene Terephthalate and Low-Density Polyethylene Casing into Bottled Water: A Case Study From India, *Bulletin of Environmental Contamination and Toxicology*, Vol.109 (6) p949-955 (2022)

*Chapter 3: Effect of Lithium Halide on  
Mechanical Properties and  
Thermoplasticity of Poly(vinyl alcohol)  
Molded by Hot Press*

## Chapter 3: Effect of lithium halide on mechanical properties and thermoplasticity of Poly(vinyl alcohol) molded by hot press

### 3-1. Introduction

Poly(vinyl alcohol) (PVA) is a water-soluble synthetic polymer with hydroxyl groups. PVA is well known as a low-cost resin with properties such as chemical resistance, alkali resistance, biodegradability, and biocompatibility [1-3]. It is used in a wide variety of applications, including clothing, food packaging film, textiles, and polarizing plates [4-6]. It is well known that PVA forms a physical cross-linked gel by forming hydrogen bonds between hydroxyl groups, and its hydrogel has been studied for biomaterial applications such as artificial cartilage [7, 8]. PVA hydrogels (PVA-H) are mostly produced by the low-temperature crystallization (LTC) method. The LTC method using a mixture of dimethyl sulfoxide (DMSO) and water reported by Hyon et al was revolutionary and remains the main method for PVA-H preparation [9]. However, the use of DMSO, with its strong oxidizing power and high skin permeability, is certainly not desirable [10]. In particular, skin permeability requires exceptional care in handling because of the possibility of carrying toxic substances into the body. Therefore, it is inappropriate as a biomaterial.

Recently, Sakaguchi et al. reported the hot press method (HP) method for gelation of PVA using only water as a solvent [11]. The HP method melts a mixture of PVA and water by applying a certain pressure under heating conditions. This method is characterized by the fact that it does not require the use of organic solvents such as DMSO. In addition, PVA-H can now be made at concentrations as high as 50 wt% because PVA does not need to be dissolved in water, whereas previously the limit was 20~30 wt% PVA concentration. Because of its high concentration, this material has high mechanical strength and is expected to be used in applications such as artificial

joint cartilage. However, gelation by the HP method has a problem in that it is not easy to fabricate the gel in an arbitrary shape. In addition, PVA has almost no thermoplasticity due to the close proximity of its melting and decomposition points, so it cannot be molded or otherwise processed by heat after gelation.

Many studies have reported that the addition of salts, such as metal salts, to polymers can affect the glass transition temperature, melting point, and optical properties [12-15]. This is also true for PVA; it is well known that the addition of alkali metal salts to PVA can affect crystallinity and other properties. Zagorskaya et al. investigated the effect of adding alkali metal salts on the crystallinity of PVA using Fourier transform infrared spectroscopy (FT-IR) and reported that the maximum value of the stretching vibration of the hydroxyl group shifted in PVA containing lithium salt, resulting in a significant decrease in crystallinity [15]. Saari et al. also reported that the addition of lithium salts to a PVA solution reduced the plateau modulus in the low-frequency range by suppressing hydrogen bonding [16]. Hydrogen bond suppression between hydroxyl groups is a very effective means of PVA modification, and several studies have shown that it is highly effective. For example, Saari et al. reduced hydrogen bonding in PVA by adding lithium bromide (LiBr), which improved the ductility of PVA fibers [17]. In chapter 2, I succeeded in spinning high-strength PVA fiber with high orientation by reducing orientation defects by spinning and drawing PVA with lithium iodide (LiI) added to suppress hydrogen bonds in PVA [18]. This resulted in a higher increase in ductility than the PVA fiber with LiBr.

Therefore, in this chapter, lithium halide was added to PVA to form hydrogel by the HP method, and its properties were evaluated in terms of crystalline, thermophysical, and mechanical properties. The results obtained were compared with PVA without salt addition and discussed. In addition, the presence or absence of thermoplasticity at the lower melting point that occurs with the addition of salt was investigated through actual thermoforming, and the mechanical properties

before and after were also evaluated in a simplified manner. The addition of thermoplasticity to PVA may improve the processability of PVA-H.

## **3-2. Materials and methods**

### 3-2-1. Materials

PVA was supplied by Japan VAM & POVAL Co. (Osaka, Japan) The grade was VF-17 with a degree of polymerization of 1700 and a degree of saponification of 98.0-99.0 mol%. Lithium chloride (LiCl) was purchased from Fujifilm Wako Pure Chemicals Corporation (Osaka, Japan), lithium bromide (LiBr) and lithium iodide (LiI) from Tokyo Chemical Industry Co., Ltd, (Tokyo, Japan). Distilled water was used throughout the experimental system.

### 3-2-2. Preparation of PVA-H

PVA-H was prepared by the hot press method. The gel preparation procedure is briefly described below. Salt was dissolved in distilled water to make a salt solution. PVA is added to the salt solution and stirred well with a spatula. The PVA was then allowed to stand for 15 minutes to swell. A mold with a thickness of 1 mm was used. The swollen PVA was placed in the mold and pressed in a hot press machine (ASONE, Osaka, Japan) set at 95 °C for 5 min at 2 MPa, 10 min at 10 MPa, and finally 15 min at 20 MPa. The product was placed in a polyethylene bag and allowed to gel for 2 days. Then, they were vacuum dried for 3 days. Finally, they were dried in a vacuum oven at 50 °C for at least 1 day to allow the water to evaporate completely. The thickness of the gel produced was  $1 \pm 0.2$  mm. The prepared PVA-H was stored in a vacuum desiccator to avoid moisture effects until measurement. In this study, the dried state was used for all measurements. Therefore, the prepared samples are denoted as PVA, not PVA-H.

### 3-2-3. Washing of salts

Some of the salt-added PVA was washed to compare to PVA without removing salt. Washing was performed by soaking the PVA in distilled water and stirring constantly with a magnetic stirrer for 5 days. The distilled water was changed daily. After desalting, PVA was completely dried by vacuum drying for at 3 days.

### 3-2-4. Thermal melt forming

Thermoplasticity was confirmed by melting and reforming the gel at high temperatures. As a method, salt added PVA was cut into small pieces. A suitable amount of the cut PVA was placed in a mold placed on a steel plate covered with a Teflon sheet with a 1 mm thick mold frame and hot pressed at 180 °C. The hot press conditions were as follows: preheating at 180 °C for 1 minute at 2 MPa, then pressing at 10 MPa for 3 minutes. After completion, the press was left under pressure for 1 hour to lower the temperature.

### 3-2-5. Measurement

#### 3-2-5-1. Measurement of light transmittance

The light transmittance of PVA gels was measured using a UV-vis spectrophotometer (Lambda 25, Perkin Elmer, USA) at 25 °C in the wavelength range 400~800 nm.

#### 3-2-5-2. Fourier transform infrared spectroscopy (FT-IR) (ATR method)

Fourier transform infrared spectroscopy was measured by attenuated total reflection (ATR) method using FT/IR 4X (JASCO, Tokyo, Japan). Spectra were obtained by scanning 16 times with a resolution of 4 cm<sup>-1</sup>. The measurement range was 4000~400 cm<sup>-1</sup>. The crystallinity  $X_C$  (%) of PVA was calculated using eq. (3-1) reported by Tretinnikov et al [19].

$$X_C(\%) = -13.1 + 89.5(A_{1144}/A_{1094}) \quad (3 - 1)$$

where  $A_{1144}$  is the absorbance at  $1144 \text{ cm}^{-1}$  and  $A_{1094}$  is the absorbance at  $1094 \text{ cm}^{-1}$ .

### 3-2-5-3. Tensile test

Tensile testing of dry PVA and lithium salt-added PVA was performed using an Autograph AGS-J (Shimadzu Corporation, Kyoto, Japan) equipped with a 100 N load cell. The test specimens were cut into dumbbell shapes with a dumbbell cutter of Japanese Industrial Standard (JIS) No. 7, JIS K 6152 standard, and elongated to failure at a rate of 1 mm/min to obtain Young's modulus and maximum tensile stress. Three measurements were taken for each sample, and the average values of maximum stress and Young's modulus were calculated. Young's modulus was calculated from between 0.1~1.5 mm based on Hooke's law.

The specimens after thermoforming were also measured 3 times for each of the samples cut into dumbbell shapes in the same way. The test conditions and Young's modulus calculation conditions were the same.

### 3-2-5-4. Dynamic mechanical analysis (DMA)

Dynamic viscoelasticity was measured using a Rheogel-E4000 (UBM Co., Ltd., Kyoto, Japan), and the temperature dependence of the tensile storage modulus  $E'$  and loss modulus  $E''$  was measured from  $-20 \text{ }^\circ\text{C}$  to  $160 \text{ }^\circ\text{C}$ . Measurements were taken at a frequency of 10 Hz and a heating rate of  $2 \text{ }^\circ\text{C}/\text{min}$ . The cut dry PVA sample was 10 mm long and 5 mm wide. Samples were stored in a vacuum desiccator until just prior to measurement to avoid the effects of moisture.

### 3-2-5-5. Measurement of water content

Water content was calculated from the weight of PVA before and after water adsorption. The

water content was completely evaporated by vacuum drying at 60 °C for 1 day before measuring the weight when dry. After swelling at room temperature for 3 days, the weight was measured. Water content  $W_c$  was calculated using Eq. (3-2).

$$W_c (\%) = \frac{W_{wet} - W_{dry}}{W_{wet}} \times 100 \quad (3 - 2)$$

where  $W_{wet}$  is the weight of PVA-H in the hydrated state and  $W_{dry}$  is the weight of PVA hydrogel in the dry state.

#### 3-2-5-6. Differential Scanning Calorimetry (DSC)

Thermal analysis was performed by DSC, and the melting point ( $T_m$ ) and crystallization behavior of PVA in the dry state were investigated using DSC 6200 (Seiko Instruments, Tokyo, Japan). Approximately 15 mg of each sample was placed in an aluminum pan and sealed with a sealer. The samples were heated from -10 °C to 350 °C at a rate of 5 °C/min under a nitrogen atmosphere. An empty aluminum pan was used as the reference material. In DSC, the melting point appears as an endothermic peak in the DSC heating curve.

#### 3-2-5-7. Measurement of residual lithium concentration

The residual lithium concentration of the washed PVA was determined by dissolving a 1 g PVA specimen in 10 mL of boiling distilled water to prepare a sample for measurement. The measurements were made with a lithium-selective dichroic probe using the Lithium Assay Kit (MAK358) (Sigma-Aldrich, USA). Aqueous solution dissolving PVA and assay buffer were added to a 96-well plate and absorbance was measured at two wavelengths, 540 nm and 630 nm, using a microplate reader (Infinito 200pro M Nano Plus, Tecan Japan, Kanagawa, Japan).

### 3-3. Results and discussion

#### 3-3-1. Appearance of PVA with lithium salt added

Figure 3-1 shows the appearance of PVA-H prepared by the HP method; PVA with LiCl and LiBr was almost transparent. No change in appearance was observed when the amount of LiCl or LiBr added increased from 4% to 8%. In PVA with LiI, the gel was slightly yellowish due to iodine. The color was even darker when the amount of LiI added increased from 4% to 8%. In other words, the color darkens as the amount of LiI added increases and the amount of iodine present in the gel increases. The results of light transmittance, a quantitative evaluation of transparency, are shown in Figures 3-2. Almost all samples showed transmittance of about 60%. This can be attributed to light scattering by the crystals of PVA. In particular, LiCl and LiBr loaded PVA showed higher transmittance than No salt PVA.

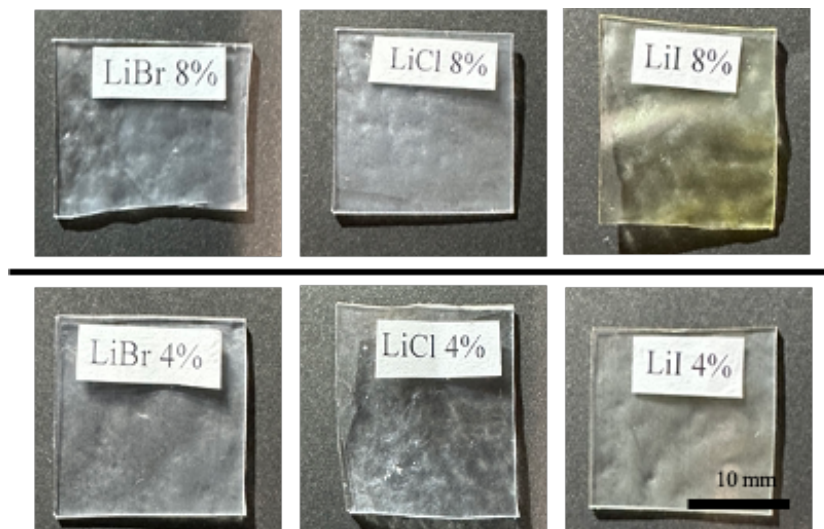


Figure 3-1 Appearance of PVA prepared by HP method with addition of salt.

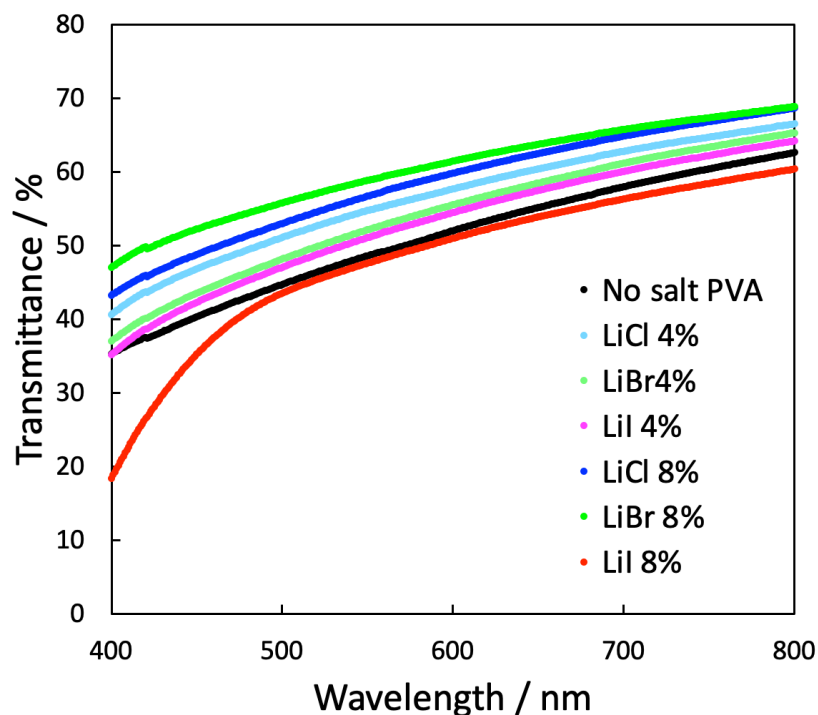


Figure 3-2 Light transmittance of PVAs.

### 3-3-2. FT-IR

The structure of crystalline polymers containing hydroxyl groups, such as PVA, can be characterized by the amount of crystals and the system of hydrogen bonds. Absorption bands in the range of  $930\sim 1180\text{ cm}^{-1}$  are important for the evaluation of the crystallinity of PVA. In this range, an absorption band with a maximum at  $1094\text{ cm}^{-1}$  formed by overlapping bands of C-O stretching vibrations of COH groups and a band with a maximum at  $1144\text{ cm}^{-1}$  due to crystallization of PVA appear. In particular, the band intensity at  $1144\text{ cm}^{-1}$  increases as the amount of crystals in PVA increases [20, 21]. Tretinnikov et al. reported that the above effect allows the IR spectrum to be used to calculate the crystallinity of PVA [19]. Therefore, in this chapter, the spectra at  $3000\sim 3600\text{ cm}^{-1}$  and  $1000\sim 1200\text{ cm}^{-1}$  are presented in detail and investigated. The crystallinity was also calculated from the spectra.

Figure 3-3a shows the IR spectra of each PVA with 4% salt added; absorption bands corresponding to stretching vibrations of the hydroxyl groups of PVA are observed in the range 3100~3600  $\text{cm}^{-1}$  [20]. Almost no peak shift in the absorption band was observed, indicating that it is almost the same as that of PVA without salt. Since the amount of salt added is not large, it can be assumed that the effect on the hydroxyl group is small. There is also a band at 1144  $\text{cm}^{-1}$  due to crystallization of PVA. However, only LiCl shows a decrease in band intensity, suggesting that LiCl affects the crystallinity of PVA more than the other lithium salts and reduces the crystallinity.

Figure 3-3b shows the case of 8% salt addition; only LiBr and LiI show a shift of the absorption band maximum of the hydroxyl group to the high frequency region. The peak in the crystallization band at 1144  $\text{cm}^{-1}$  almost disappeared in LiCl. The peak intensities of LiBr and LiI also decreased compared to the 4% case, indicating that the effect of the salt on the crystals of PVA increases as the amount of salt added increases.

Figure 3-4a and 4b show the IR spectra of PVA prepared with 4% and 8% salt after desalting by washing. The maximum value of the hydroxyl band, which had shifted to the high frequency region at 8%, returned to the same place as in No salt. The peak appeared in LiCl, where the crystallization band at 1144  $\text{cm}^{-1}$  had almost disappeared; an increase in the peak was also observed in LiBr and LiI. This suggests that the lithium salt present inside the PVA can be almost completely removed by desalting with water. It can also be inferred that once the lithium salt is removed, the PVA can crystallize again.

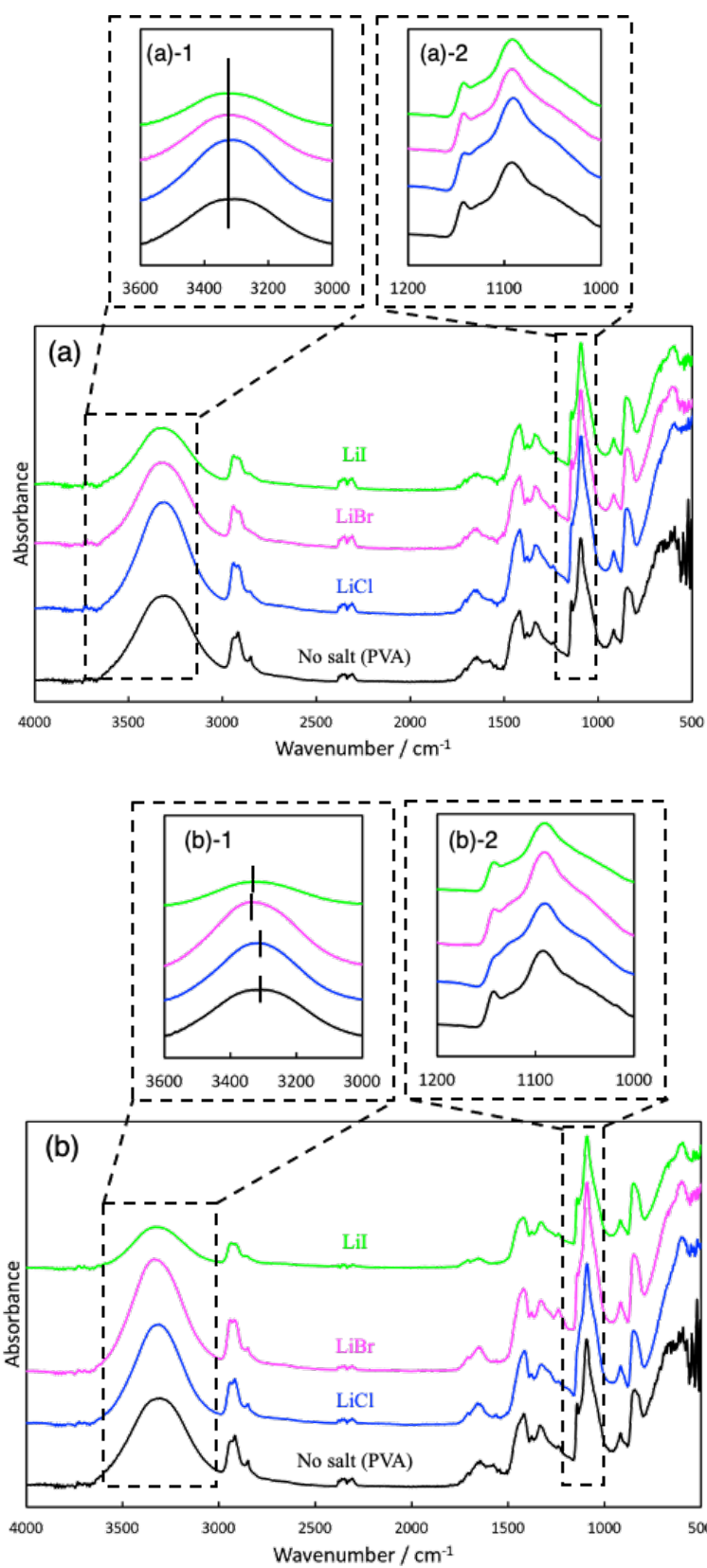


Figure 3-3 IR spectra of PVA prepared by adding salt. (a) 4%, (b) 8%

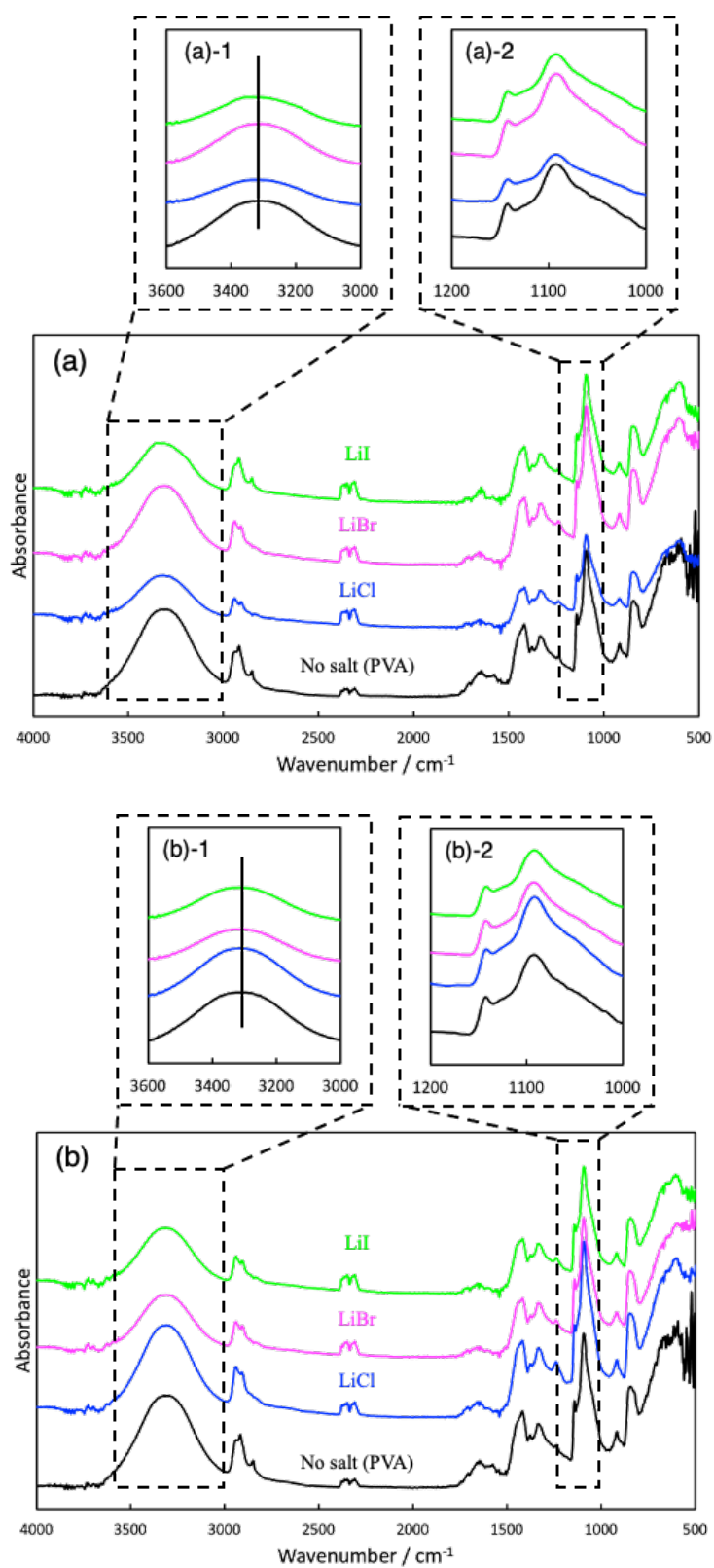


Figure 3-4 IR spectra of PVA prepared by adding salt after washing and desalting. (a) 4%, (b) 8%

Table 3-1 shows the crystallinity of PVA-H calculated from the IR spectra. Crystallinity  $X_C$  was calculated from the IR spectra according to the formula described in Methods section. The crystallinity of No salt was 40.7%. The addition of lithium salt decreased the crystallinity. The percentage decrease in crystallinity was greater when 8% lithium salt was added than that when 4% was added. The decrease was particularly pronounced in 8% LiCl, where the decrease was up to 30.3%. The crystallinity of PVA with lithium salts after washing and desalting was found to increase compared to that in the presence of the salts. The lowest crystallinity was observed in 8%LiCl. However, it recovered to 36.6 % after washing and desalting. This means that the crystallinity can be almost restored to its original state by removing the salt, as mentioned in the IR spectrum. The decrease in crystallinity was as expected. Normally, PVA crystallizes by hydrogen bonding between hydroxyl groups. However, in the presence of lithium salt, the hydrogen bonding is reduced as the hydroxyl group and lithium ion form a  $\text{Li}^+\cdots\text{OH}$  bond [16, 20]. It is well known that lithium ions have a high affinity for alcohols (-OH), such as hydroxyl groups, and that many lithium ions can be dissolved [20, 22]. Several PVA modifications have been carried out by applying this effect [17, 18]. However, the crystallinity data indicate that the influence of anions must also be taken into account. Saari et al. found that in aqueous PVA solutions and PVA films (200  $\mu\text{m}$  thickness), the Hofmeister series (HS) can account for the strength of the ability of cations and anions, such as lithium ions, to inhibit hydrogen bonds in PVA [23]. In the case of anions, we reported that iodine ion ( $\text{I}^-$ ) and perchlorate ion ( $\text{ClO}_4^-$ ) are particularly effective in inhibiting hydrogen bonding. However, in this study, the gel containing  $\text{I}^-$  resulted in a high degree of crystallinity and the gel containing  $\text{Cl}^-$  resulted in a low degree of crystallinity. Sorting the anions in order of their effectiveness in inhibiting hydrogen bonding,  $\text{Cl}^- > \text{Br}^- > \text{I}^-$ , indicating that  $\text{Cl}^-$  is higher and does not follow HS. In other words, for PVA prepared by the HP method, the crystallinity increased as the size of the salt anion increased. The high

hydration capacity of halide ions should also be considered as a cause of this [24, 25].

Table 3-1 Crystallinity of PVA prepared by the HP method calculated from IR spectra.

4%		8%	
Salt	Crystallinity / %	Salt	Crystallinity / %
No salt	40.7	No salt	40.7
LiCl	35.4	LiCl	30.3
LiBr	38.0	LiBr	35.8
LiI	38.8	LiI	38.5

4% wash		8% wash	
Salt	Crystallinity / %	Salt	Crystallinity / %
No salt	40.7	No salt	40.7
LiCl	43.3	LiCl	36.6
LiBr	37.8	LiBr	39.4
LiI	39.0	LiI	41.0

### 3-3-3. DSC

Figure 3-5a and 5b show the DSC heating curves of No salt PVA and PVA containing lithium salt heated at a rate of 5 °C/min. The endothermic peak at 228.9 °C in No salt is attributed to the melting point of PVA crystals. This is appropriate because it is close to the previously reported values for the melting point of PVA [26]. First, I would like to discuss the heating curve of PVA with 4% salt added. In this case, the peaks of LiCl, LiBr, and LiI are weakly present around 195~200 °C, indicating a lower melting point compared to No salt. Next, I would like to discuss PVA with 8% salt added. The melting point is further reduced compared to the 4% addition. In particular, LiCl gives a much lower melting point of 163.2 °C. Similarly, melting point of PVA with LiBr and LiI also decreased when compared with that with 4% addition. In other words, increasing the amount of lithium salt added can significantly lower the melting point of PVA. The effect is particularly strong when LiCl is added. These results also suggest that the melting point temperature can be varied to some extent arbitrarily by controlling the amount of salt added.

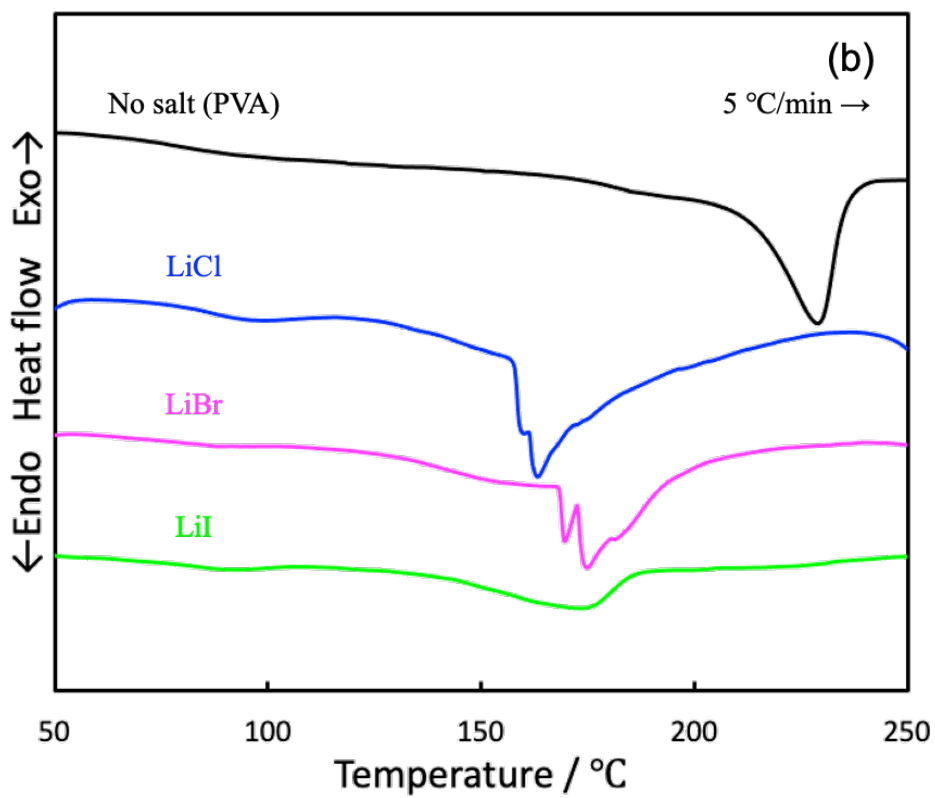
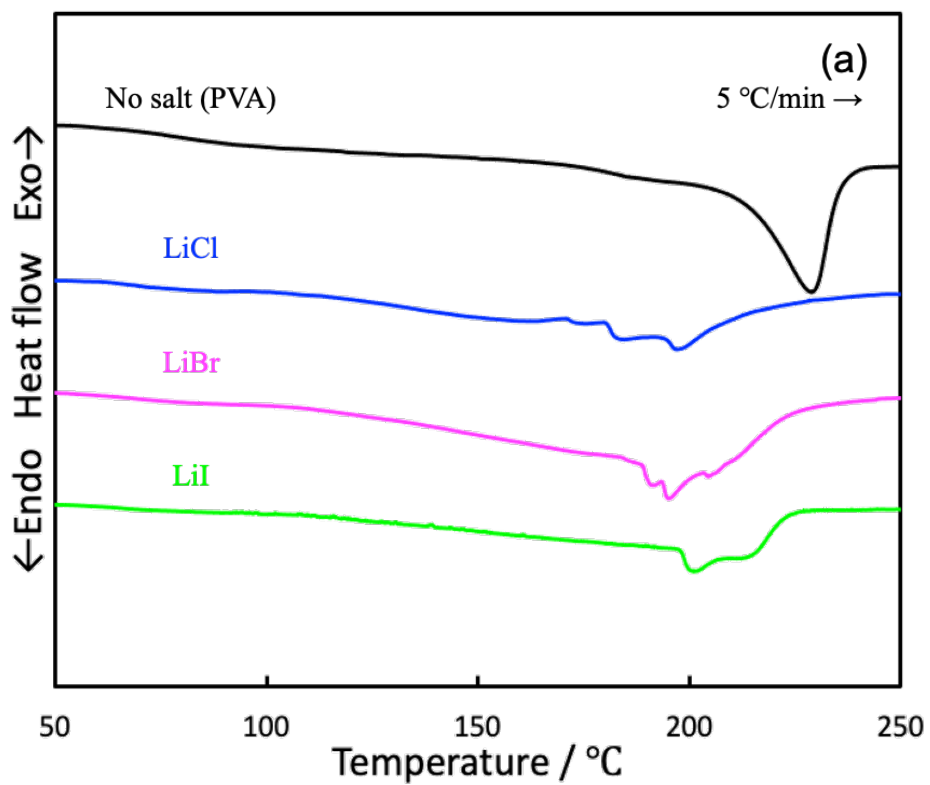


Figure 3-5 DSC heating curve of PVA prepared by HP method. (a) 4%, (b) 8%

Figure 3-6 shows the DSC heating curve of PVA prepared with 8% lithium salt after washing and desalting. The melting point of PVA with lithium salts was recovered to the same level of PVA without salt. In other words, the addition of salt temporarily lowers the melting point, making PVA capable of melting at temperatures lower than the decomposition temperature. This may improve the processability of PVA. The fact that the melting point has returned to normal also suggests that most of the salt has been removed.

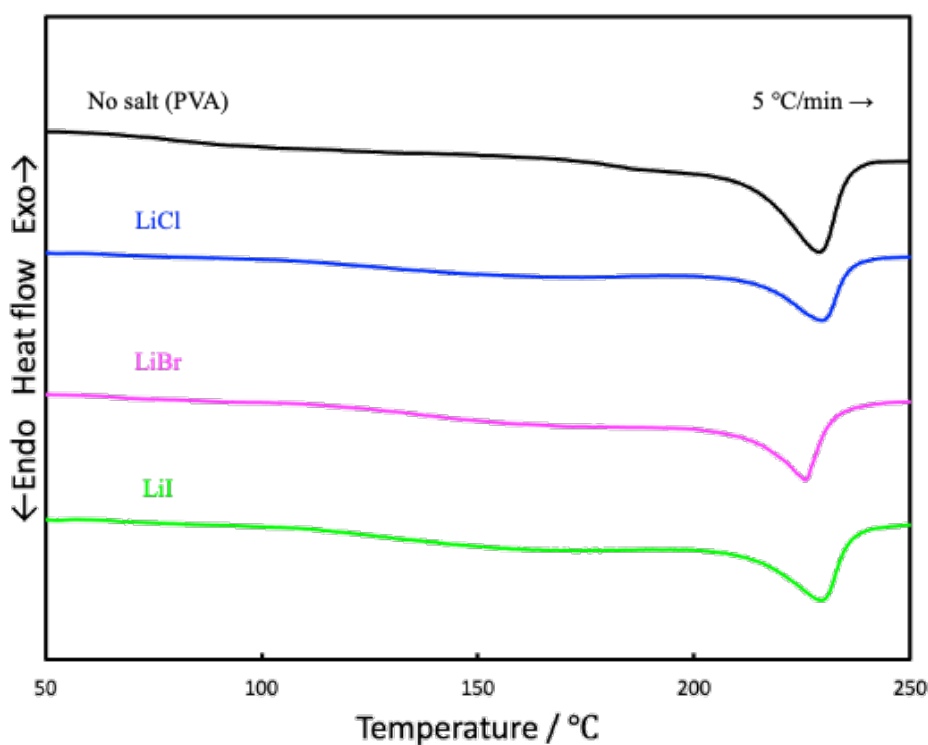


Figure 3-6 DSC heating curves of PVA after washing and desalting.

#### 3-3-4. Tensile test

Figure 3-7a and 7b show some of the stress-strain curves obtained from tensile tests of PVA with 4% and 8% lithium salt addition. The average values of Young's modulus and maximum tensile stress are shown in Figure 3-8 and 3-9 and Table 3-2. From these data for each, the average values for No salt PVA were Young's modulus of 660.9 MPa and maximum stress of 44.4 MPa. In particular, at 4%, LiCl showed the greatest decrease, with a Young's modulus of 145.1 MPa and a maximum stress of 29.3 MPa. When the magnitude of the decrease in mechanical strength was sorted by the added salt,  $\text{LiCl} > \text{LiBr} > \text{LiI}$ . Regarding the strain, PVA with LiCl, whose mechanical strength is much lower, is significantly higher than the other PVAs.

Young's modulus and maximum stress are lowest for LiCl at 8% lithium salt addition, as well as at 4%. It should be noted here that the range of decrease is unusually large, with Young's modulus and maximum stress of 35.2 MPa and 17.4 MPa, respectively. Compared to 4%, there is a decrease with LiBr and LiI, but not as much as with LiCl. In other words, the increase in LiCl addition can significantly reduce the mechanical strength of PVA, such as Young's modulus and maximum stress. This result can also be corroborated with the lower crystallinity. The strain was also higher for the PVA with 8% LiCl than that with 4%. In other words, the PVA in 8% LiCl is more flexible.

The decrease in mechanical strength provides evidence to support that the lithium salt added to PVA inhibits crystallization. It indicates that not only  $\text{Li}^+$  has an effect, but anions have a strong influence. In particular,  $\text{Cl}^-$  is suggested to have a strong influence on the physical properties of PVA with lithium salt added by the HP method.

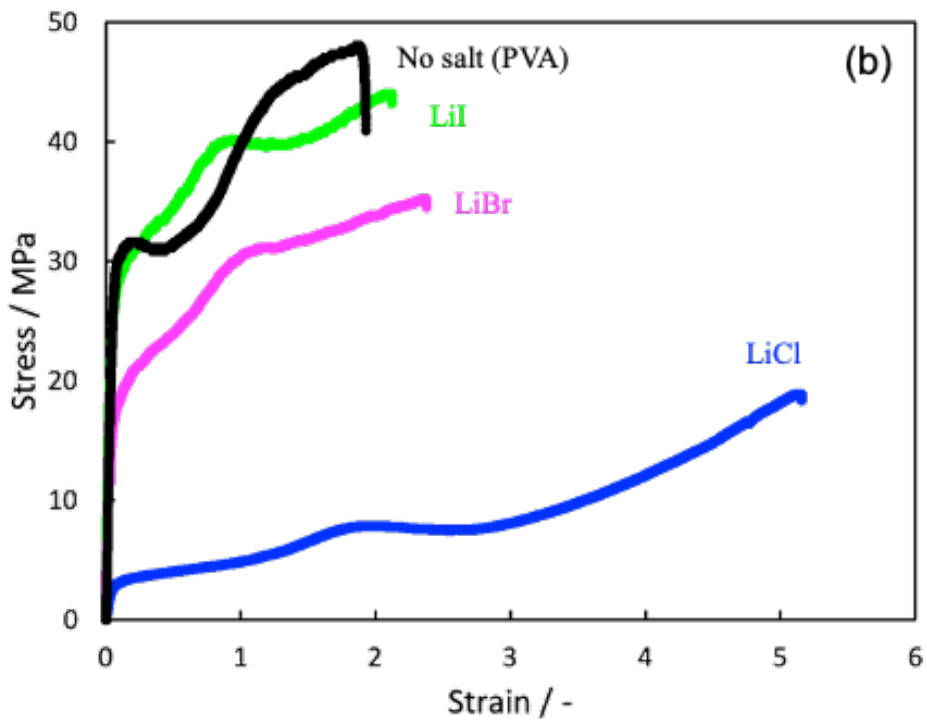
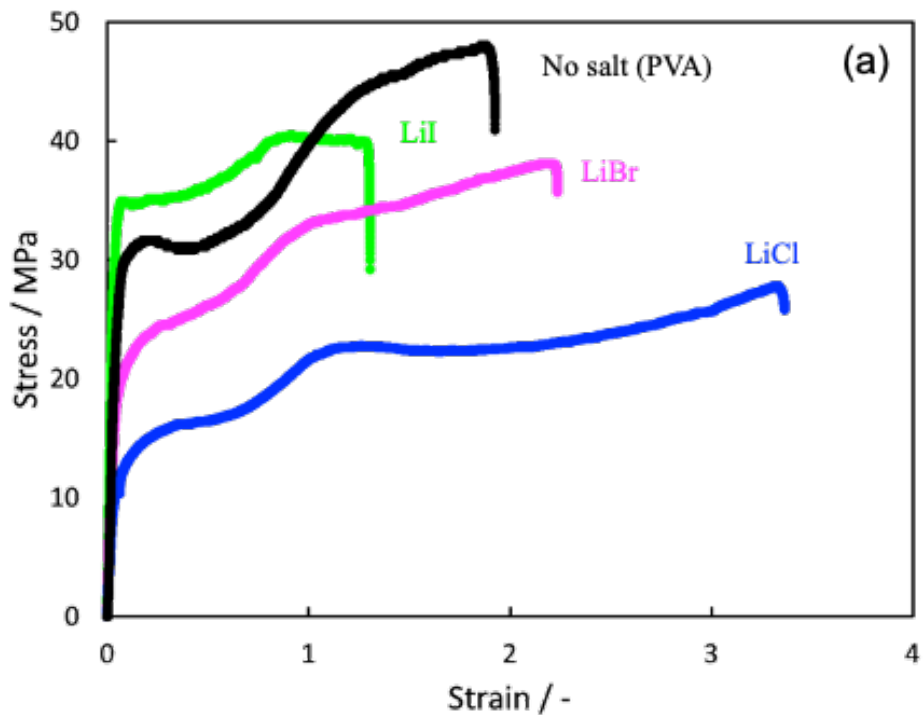


Figure 3-7 Stress-strain curves of PVA prepared by HP method with lithium salt.  
 (a) 4%, and (b) 8%

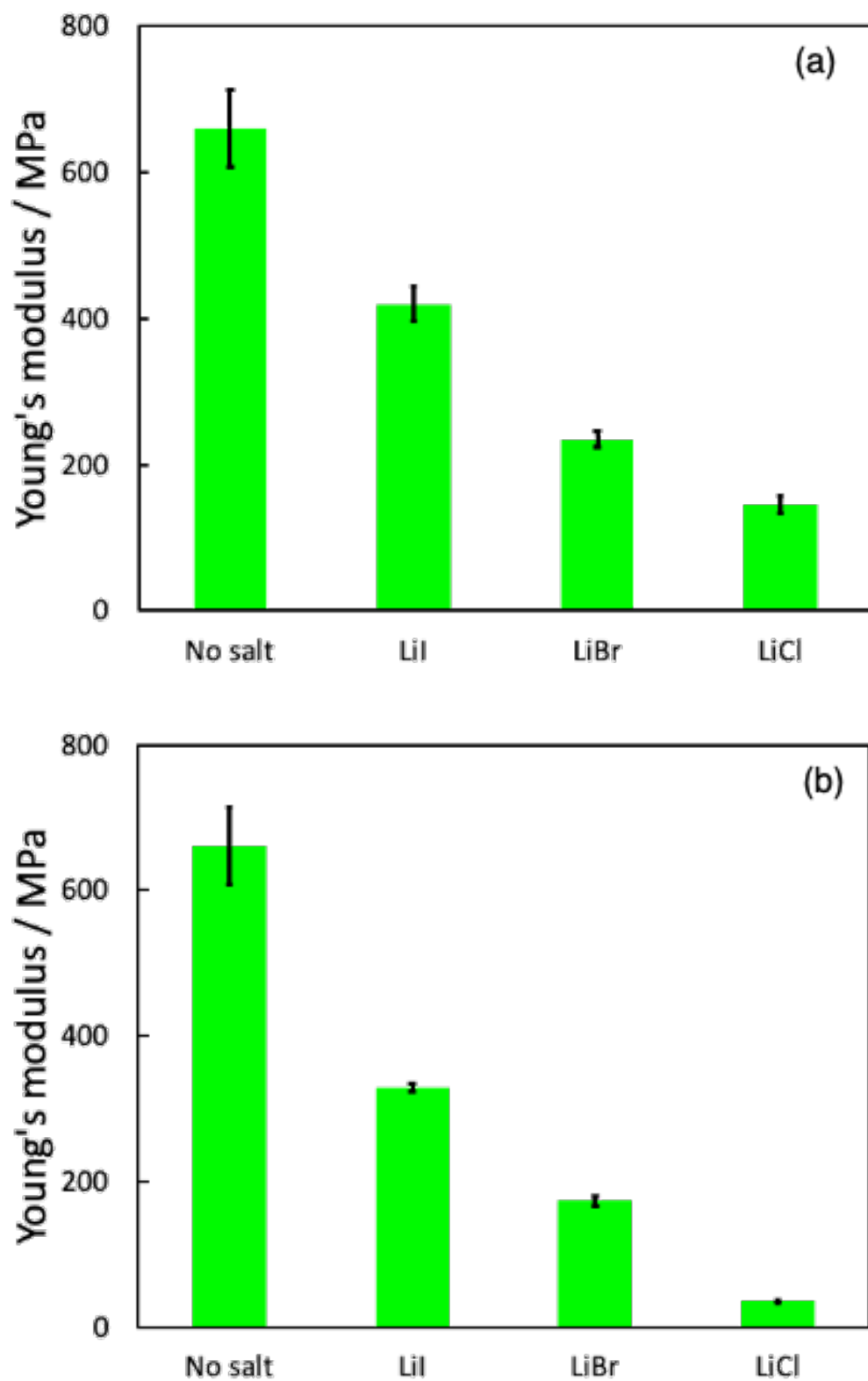


Figure 3-8 Young's modulus of PVA prepared by HP method with lithium salt.  
 (a) 4%, and (b) 8%

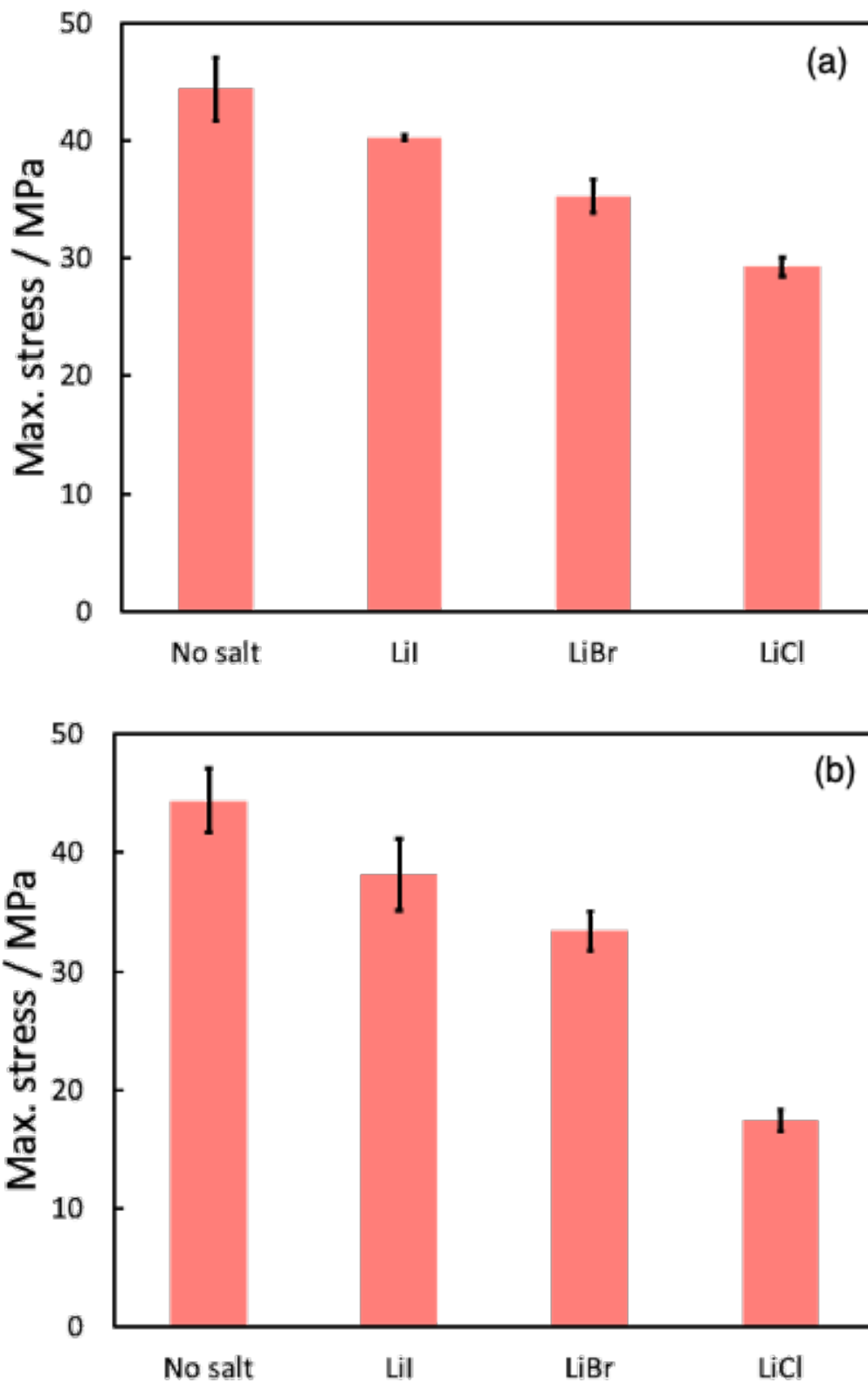


Figure 3-9 Maximum tensile stress of PVA prepared by HP method with lithium salt.  
 (a) 4%, and (b) 8%

Table 3-2 Average values of Young's modulus and maximum tensile stress of PVA prepared by HP method with lithium salt. ( $\pm$  Standard deviation)

	Young's modulus / MPa	Max. stress / MPa
No salt	660.9 $\pm$ 53.2	44.4 $\pm$ 2.7
<b>4% salts</b>		
LiCl	145.1 $\pm$ 12.5	29.3 $\pm$ 0.8
LiBr	234.8 $\pm$ 10.3	35.3 $\pm$ 1.4
Lil	419.5 $\pm$ 23.6	40.3 $\pm$ 0.2
<b>8% salts</b>		
LiCl	35.2 $\pm$ 2.9	17.4 $\pm$ 0.8
LiBr	173.1 $\pm$ 5.6	33.4 $\pm$ 1.6
Lil	328.3 $\pm$ 5.5	38.2 $\pm$ 3.0

### 3-3-5. Dynamic mechanical analysis (DMA)

Figures 3-10 to 3-12 show the results of the temperature dependence of dynamic mechanical analysis at 10 Hz. The addition of lithium salt was found to lower the glass transition temperature of hot-pressed PVA. This indicates that the lithium salts present between the PVA molecular chains affect the hydrogen bonding. Figure 3-7 shows the results for PVA with 4% salt added. Compared to No salt PVA, a decrease in  $E'$  was observed at lower temperatures.

Figure 3-10 shows the results for PVA with 4% salt added. Compared to No salt PVA, a decrease in  $E'$  was observed at lower temperatures. In particular, there was a larger shift in LiCl compared to the other salts. The glass transition temperatures ( $T_g$ ) were as shown below. No salt PVA: 30.8 °C, LiCl: 10.8 °C, LiBr: 16.8 °C, LiI: 16.9 °C.

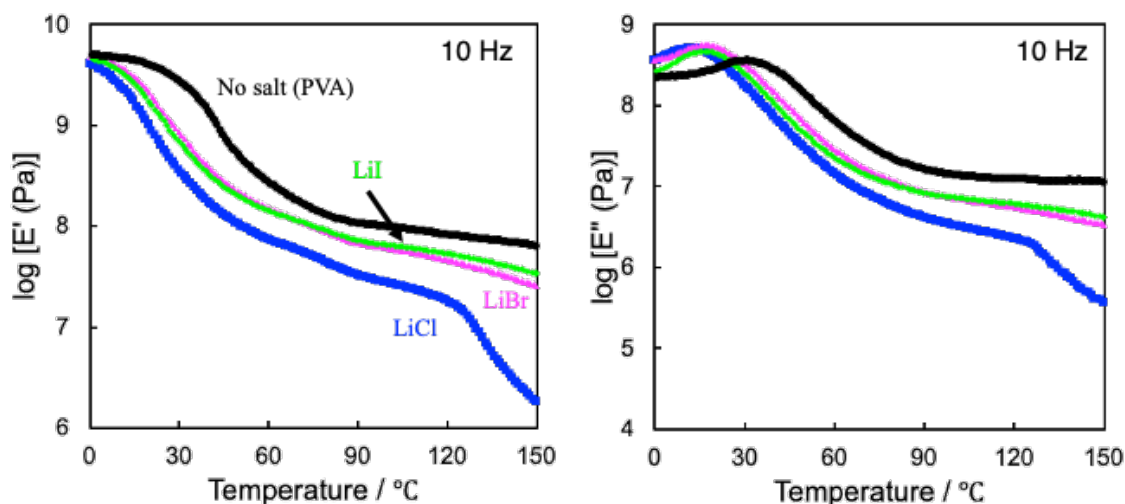


Figure 3-10 Temperature dependence of storage modulus  $E'$  and loss modulus  $E''$  of No salt PVA and PVA with 4% lithium salt at 10 Hz.

Figure 3-11 shows DMA results for PVA with 8% lithium salt.  $E'$  and  $E''$  were reduced compared to No salt PVA as well as with the addition of 4% lithium salt. In particular, there was a large decrease in the rubbery region for LiCl. However, as shown next,  $T_g$  was higher than in the 4% case. LiCl: 20.9 °C, LiBr: 21.9 °C, LiI: 24.8 °C.

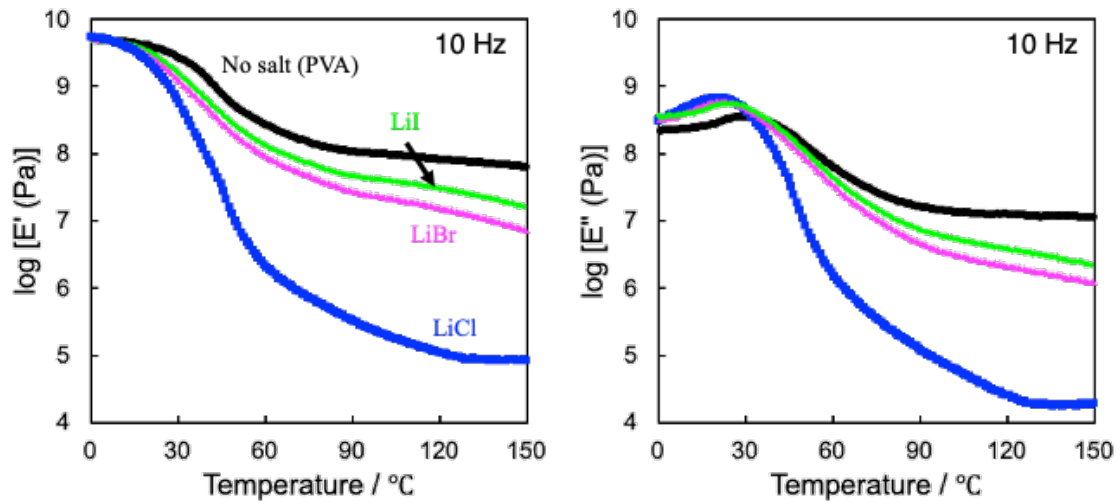


Figure 3-11 Temperature dependence of storage modulus  $E'$  and loss modulus  $E''$  of No salt PVA and PVA with 8% lithium salt at 10 Hz.

Figure 3-12 shows the DMA results of PVA after washing and removal of lithium salts. No salt PVA shows almost the same  $E'$  and  $E''$  as compared to PVA. This suggests that most of the lithium salt present inside the PVA has been removed.  $T_g$  was shown next. LiCl: 22.9  $^{\circ}\text{C}$ , LiBr: 19.9  $^{\circ}\text{C}$ , LiI: 23.8  $^{\circ}\text{C}$ .

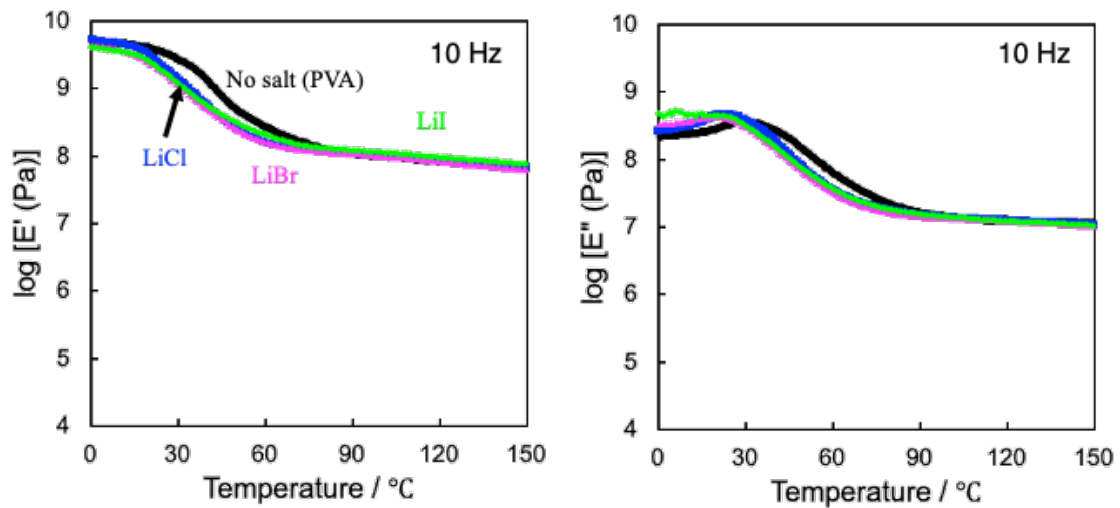


Figure 3-12 Temperature dependence of storage modulus  $E'$  and loss modulus  $E''$  of No salt PVA and PVA with lithium salt after washing at 10 Hz.

### 3-3-6. Measurement of water content

The water content was measured to corroborate the crystallinity and tensile test results. Water content is closely related to mechanical properties such as the modulus of elasticity of the hydrogel, which decreases with higher water content [27, 28]. Therefore, examining the water content allows for a more detailed consideration of the mechanical properties. It is also expected that the water content will be affected by hydration of lithium halide and other factors. Figure 3-13(a) and 13(b) show the water content results for PVA with 4% and 8% lithium salts added and No salt PVA. Although addition of LiCl showed somewhat higher in terms of water content when 4% lithium salt was added, there was little difference. However, at 8%, a large difference was observed: 68.2 % for LiCl, compared to 57.0 % for LiBr and 58.9 % for LiI, with LiCl being about 10 % higher. This can be assumed to be part of the reason for the low crystallinity and mechanical strength of LiCl. For halide ions, the hydration coefficient increases as the ionic potential (charge-to-radius ratio) increases. In other words, ions with high ionic potential, such as Cl<sup>-</sup>, have high hydration coefficients and can hydrate more water molecules than I<sup>-</sup> [25]. Therefore, it can be assumed that the water content is higher because more water molecules can be retained. In other words, since a certain amount of water remains after the drying process, I speculate that the residual water significantly reduces the crystallinity and tensile strength of PVA.

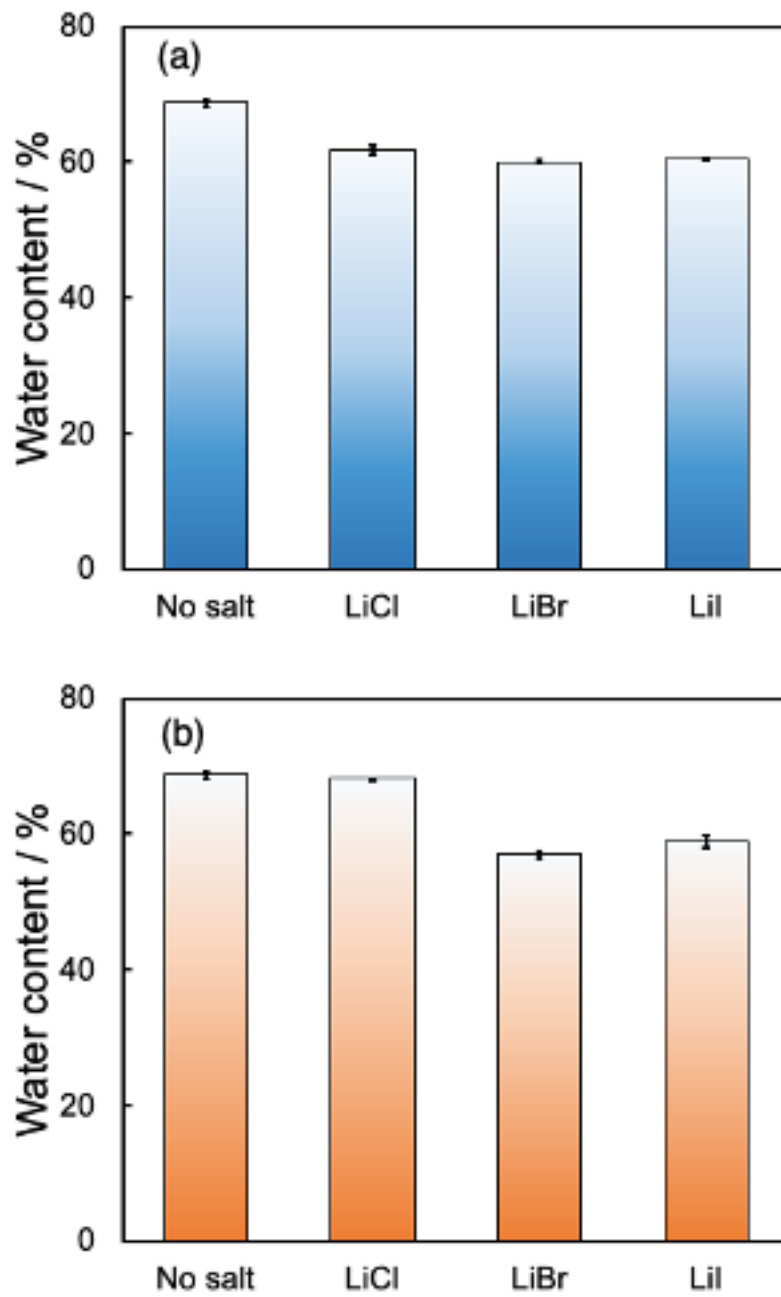


Figure 3-13 Water content of PVA prepared by the HP method with the addition of lithium salt.  
(a) 4%, (b) 8%

### 3-3-7. Testing thermoplasticity by hot press

PVA has little thermoplasticity due to the close proximity of its melting point and decomposition temperature. Although the addition of glycerin and other methods have been proposed to impart thermoplasticity, there are many limitations because they are effective only with low molecular weight and partially saponified PVA [29]. However, the addition of lithium halide is characterized by its effectiveness even in fully saponified PVA. In addition, the melting point is greatly reduced, allowing the PVA to be easily melted below the decomposition temperature. Another advantage is that the lithium salt can eventually be removed by washing.

Figure 3-14 shows PVA before and after heat molding. LiI PVA was cut into small pieces and hot-pressed at 180 °C to form a sheet again. Normally, the melting point of PVA is about 230 °C, so a higher temperature is necessary. However, this is impossible because the melting point and decomposition temperature of PVA are almost the same [30]. In this case, it was possible because the melting point was lowered by adding salt. It is also assumed that the addition of salt suppressed the hydrogen bonding of PVA, which reduced the amount of crystals and the thickness of the lamellar crystals, as a factor that contributed to the thermoplasticity of the product. Similarly, thermoplasticity was confirmed for all lithium halides used in this study.

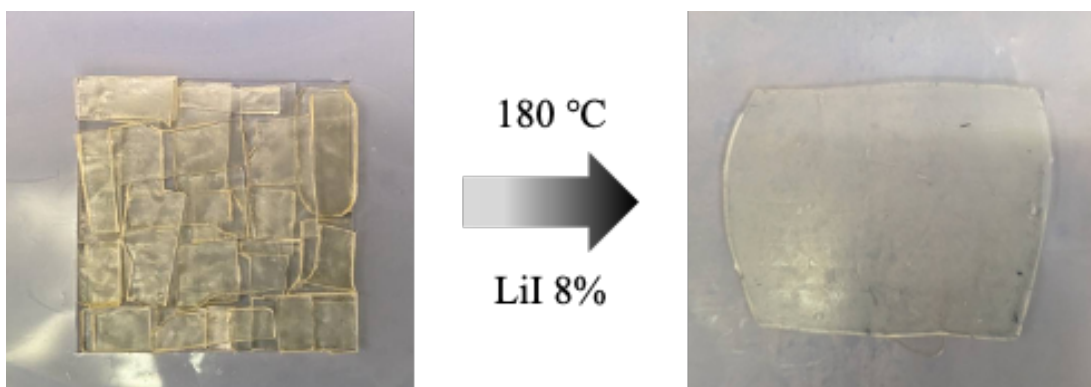


Figure 3-14 Comparison of LiI PVA before and after thermoforming.

Figure 3-15 shows the stress-strain curves of LiI PVA before and after thermoforming. The average values of Young's modulus and maximum tensile stress are shown in Table 3-3. There

was a slight decrease in elastic modulus, but the maximum stress was higher than before thermoforming. Since the maximum strain was also smaller, it can be inferred that crystallization of PVA progressed due to the high temperature during thermoforming at 180 °C. Although PVA after thermoforming may have some impact on mechanical properties, it can be considered a major benefit in terms of improved processability.

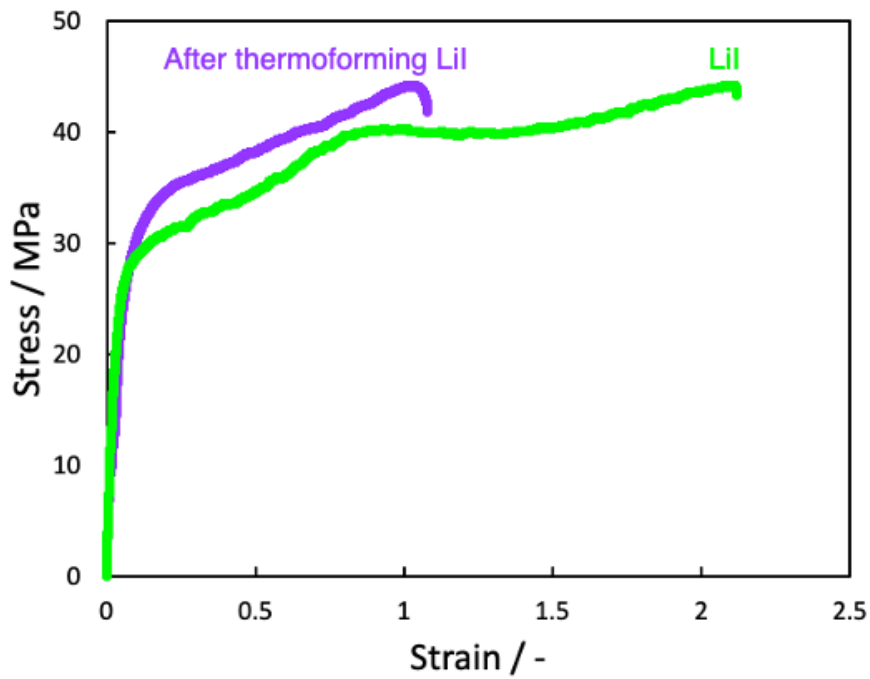


Figure 3-15 Stress-strain curve of LiI PVA before and after thermoforming.

Table 3-3 Average values of Young's modulus and maximum tensile stress of LiI PVA before and after thermoforming. ( $\pm$  Standard deviation)

	Young's modulus / MPa	Max. stress /MPa
LiI 8%	328.3 $\pm$ 5.5	38.2 $\pm$ 3.0
After thermoforming LiI 8%	265.2 $\pm$ 29.6	47.0 $\pm$ 1.5

### 3-3-8. Measurement of lithium concentration

The ability to remove lithium salts from PVA by washing is very important because the mechanical properties are restored by removing the lithium salts. In addition, high concentrations of residual lithium and halogens can be harmful to the human body and the natural environment [31]. Additives and plasticizers are commonly used in the processing of polymer materials. However, since elution of plasticizers pollutes the human body and the environment, there are many restrictions on the amount of plasticizers used, which has become a problem [32-34]. Therefore, I investigated the extent to which the lithium salt added to PVA in this study was removed by washing. Table 3-4 shows the measured lithium concentrations. Most of the lithium salts could be removed by washing, and some were below the detection limit of measurement. In other words, it was shown that almost all lithium salts can be removed by washing PVA in water for 5 days. Therefore, there is no problem in adding lithium halide for the purpose of improving the processability of PVA.

Table 3-4 Lithium concentration in PVA before and after washing and desalting.  
( $\pm$  Standard deviation)

	Sample	Li concentration (mg/L)
No salt	PVA	-
	4%	$27.8 \pm 0.01$
LiCl	4% after washing	N.D
	8	$31.2 \pm 0.05$
	8% after washing	$0.5 \pm 0.16$
	4%	$26.7 \pm 0.37$
LiBr	4% after washing	$0.2 \pm 0.27$
	8	$30.5 \pm 0.16$
	8% after washing	N.D
	4%	$22.9 \pm 0.19$
LiI	4% after washing	$0.6 \pm 0.04$
	8	$25.3 \pm 0.16$
	8% after washing	$1.4 \pm 0.35$

### 3-3-9. Summary of this study

This study focused on the property changes and thermoplasticization of PVA with lithium halide. The addition of lithium salt enabled melting at temperatures lower than the decomposition temperature, confirming thermoplasticity. However, the behavior was different from the characteristics reported by previous studies on the effect of lithium halide. One possible reason for this may be that the high hydration power of  $\text{Cl}^-$  makes it easy to contain water, but the relationship between PVA prepared by hot-pressing and lithium halide needs to be investigated in detail.

### 3-4. Conclusion

The addition of lithium halide decreased the crystallinity of PVA. The resulting decrease in melting point and crystallinity resulted in reduced mechanical properties. This study shows that the addition of lithium salts can alter the properties of PVA; LiCl has a particular impact on the properties of PVA, significantly reducing Young's modulus and maximum tensile stress. It decreased with LiBr and LiI, but was not as strong as LiCl. The effect on mechanical properties may also be influenced by the hydration power of the halide ions of the added lithium salts. Shredded PVA could be re-molded by hot pressing, and thermoplasticity could be imparted by adding lithium salt. Thermo-plasticization by adding lithium salts, which can be removed by washing, is an effective means of improving the processability of PVA. Although there was little effect on the physical properties of PVA after thermoforming compared to before thermoforming, further detailed studies are needed.

### 3-5. References

1. N.B. Halima, Poly(vinyl alcohol): review of its promising applications and insights into biodegradation, *RSC Advances*, 6 p39823-39832 (2016)
2. M. Shimano, Biodegradation of plastics, *Current Opinion in Biotechnology*, Vol.12 (3) p242-247 (2001)
3. D. Feldman, Poly(Vinyl Alcohol) Recent Contributions to Engineering and Medicine, *Journal of Composites Science*, Vol.4 (4) 175 (2020)
4. K.K. Gaikwad, J.Y. Lee, Y.S. Lee, Development of polyvinyl alcohol and apple pomace bio-composite film with antioxidant properties for active food packaging application, *Journal of Food Science and Technology*, Vol.53 p1608-1619 (2016)
5. M. Aslam, M.A. Kalyar, Z.A. Raza, Polyvinyl alcohol: A review of research status and use of polyvinyl alcohol based nanocomposites, *Polymer Engineering and Science*, Vol.58 (12) p2119-2132 (2018)
6. E.J. Shin, W.S. Lyoo, Y.H. Lee, Polarizer effect and structure of iodinated before and after casting poly(vinyl alcohol) film, *Journal of Applied Polymer Science*, Vol.120 (1) p397-405 (2011)
7. K. Matsumura, Special Issue: Nanocomposite Hydrogels for Biomedical Applications, *Applied Science*, Vol.10 (1) 389 (2020)
8. M.I. Baker, S.P. Walsh, Z. Schwartz, B.D. Boyan, A review of polyvinyl alcohol and its uses in cartilage and orthopedic applications, *Journal of Biomedical Materials Research Part B Applied Biomaterials*, Vol.100B (5) p1451-1457 (2012)
9. S.-H. Hyon, W.-I. Cha, Y. Ikeda, Preparation of transparent poly(vinyl alcohol) hydrogel, *Polymer Bulletin*, Vol.22 p119-122 (1989)
10. C. Ursin, C.M. Hansen, J.W.V. Dyk, P.O. Jensen, I.J. Christensen, J. Ebbehøj, Permeability

- of Commercial Solvents Through Living Human Skin, *American Industrial Hygiene Association Journal*, Vol.56 (7) p651-660 (1995)
11. T. Sakaguchi, S. Nagano, M. Hara, S.-H. Hyon, M. Patel, K. Matsumura, Facile preparation of transparent poly(vinyl alcohol) hydrogels with uniform microcrystalline structure by hot-pressing without using organic solvents, *Polymer Journal*, Vol.49 p535-542 (2017)
  12. Y. Sato, A. Ito, S. Maeda, M. Yamaguchi, Structure and optical properties of transparent polyamide 6 containing lithium bromide, *Journal of Polymer Science Part B Polymer Physics*, Vol. 56 (22) p1513-1520 (2018)
  13. T. Sako, A. Miyagawa, M. Yamaguchi, Modulus enhancement of polycarbonate by addition of lithium perchlorate, *Journal of Applied Polymer Science*, Vol.134 (22) 44882 (2017)
  14. N. Tsugawa, A. Ito, M. Yamaguchi, Effect of lithium salt addition on the structure and optical properties of PMMA/PVB blends, *Polymer*, Vol.146 (20) p242-248 (2018)
  15. S.A. Zagorskaya, O.N. Tretinnikov, Infrared Spectra and Structure of Solid Polymer Electrolytes Based on Poly(vinyl alcohol) and Lithium Halides, *Polymer Science Series A*, Vol.61 p21-28 (2019)
  16. R.A. Saari, R. Maeno, R. Tsuyuguchi, W. Marujiwat, P. Phulkerd, M. Yamaguchi, Impact of Lithium halides on rheological properties of aqueous solution of poly(vinyl alcohol), *Journal of Polymer Research*, Vol.27 218 (2020)
  17. R.A. Saari, R. Maeno, W. Marujiwat, M.S. Nasri, K. Matsumura, M. Yamaguchi, Modification of poly(vinyl alcohol) fibers with lithium bromide, *Polymer*, Vol.213 (20) 123193 (2021)
  18. Y. Taoka, R.A. Saari, T. Kida, M. Yamaguchi, K. Matsumura, Enhancing the Mechanical Properties of Poly(vinyl alcohol) Fibers by Lithium Iodide Addition, *ACS omega*, Vol.8 (36) p32623-32634 (2023)

19. O.N. Tretinnikov, S.A. Zagorskaya, Determination of the degree of crystallinity of poly(vinyl alcohol) by FTIR spectroscopy, *Journal of Applied Spectroscopy*, Vol.79 (4) p521-526 (2021)
20. S.A. Zagorskaya, O.N. Tretinnikov, Infrared Spectra and Structure of Solid Polymer Electrolytes Based on Poly(vinyl alcohol) and Lithium Halides, *Polymer Science, Series A*, Vol.61 p21-28 (2019)
21. H. Tadokoro, S. Seki, I. Nitta, The Crystallinity of Solid High Polymers. I. The Crystallinity of Polyvinyl alcohol Film, *Bulletin of the Chemical Society of Japan*, Vol.28 (8) p559-564 (1955)
22. N.L. Ma, F.M. Siu, C.W. Tsang, Interaction of alkali metal cations and short chain alcohols: effect of core size on theoretical affinities, *Chemical Physics Letters*, Vol.322 (1-2) p65-72 (2000)
23. R.A. Saari, M.S. Nasri, W. Marujiwat, R. Maeno, M. Yamaguchi, Application of the Hofmeister series to the structure and properties of poly(vinyl alcohol) films containing metal salts, *Polymer Journal*, Vol.53 p557-564 (2021)
24. A. Likholyot, J.K. Hovey, T.M. Seward, Experimental and theoretical study of hydration of halide ions, *Geochimica et Cosmochimica Acta*, Vol.69 (12) p2949-2958 (2005)
25. Z. Jing, Y. Zhou, T. Yamaguchi, K. Yoshida, K. Ikeda, K. Ohara, G. Wang, Hydration of Alkali Metal and Halide Ions from Static and Dynamic Viewpoints, *The Journal of Physical Chemistry Letters*, Vol.14 (27) p6270-6277 (2023)
26. R.K. Tubbs, Melting point and heat of fusion of poly(vinyl alcohol), *Journal of Polymer Science Part A*, Vol.3 (12) p4181-4189 (1965)
27. D. Pasqui, M.D. Cagna, R. Barbucci, Polysaccharide-Based Hydrogels: The Key Role of Water in Affecting Mechanical Properties, *Polymers*, Vol.4 (3) p1517-1534 (2012)
28. F. Urushizaki, H. Yamaguchi, K. Nakamura, S. Numajiri, K. Sugibayashi, Y. Morimoto,

- Swelling and mechanical properties of poly(vinyl alcohol) hydrogels, *International Journal of Pharmaceutics*, Vol.58 p135-142 (1990)
29. C.A. Lin, H.C. Tsai, T.H. Ku, Manufacturing Process and Application of Pseudo-thermoplastic Polyvinyl Alcohol, *Polymer-Plastics Technology and Engineering*, Vol.46 (7) p689-693 (2007)
30. N. Chen, L. Li, Q. Wang, New technology for thermal processing of poly(vinyl alcohol), *Plastics, Rubber and Composites*, Vol.36 (7-8) p283-290 (2007)
31. J.S. Harkness, G.S. Dwyer, N.R. Warner, K.M. Parker, W.A. Mitch, A. Vengosh, Iodide, Bromide, and Ammonium in Hydraulic Fracturing and Oil and Gas Wastewaters: Environmental Implications, *Environmental Science & Technology*, Vol.49 (3) p1955-1963 (2015)
32. R. Jamarani, H.C. Erythropel, J.A. Nicell, R.L. Leask, How Green is Your Plasticizer?, *Polymers*, Vol.10 (8) 834 (2018)
33. A. Qadeer, K.L. Kirsten, Z. Ajmal, X. Jiamg, X. Zhao, Alternative Plasticizers As Emerging Global Environmental and Health Threat: Another Regrettable Substitution?, *Environmental Science & Technology*, Vol.56 (3) p1482-1488 (2022)
34. T.T. Bui, G. Giovanoulis, A.P. Cousins, J. Magner, I.T. Cousins, C.A. Dewit, Human exposure, hazard and risk of alternative plasticizers to phthalate esters, *Science of Total Environment*, Vol.541 (15) p451-467 (2016)

*Chapter 4: Effect of Gelation and Heat-treatment of Syndiotactic-rich Poly(vinyl alcohol) on Mechanical Properties*

## Chapter 4: Effect of gelation and heat-treatment of syndiotactic-rich Poly(vinyl alcohol) on mechanical properties

### 4-1. Introduction

Poly(vinyl alcohol) (PVA) is a synthetic polymer with hydroxyl groups. It is used in a wide variety of applications, including the textile industry, polarizing plates, food packaging films, and tissue engineering [1-5]. PVA has characteristics such as water solubility, alkali resistance, chemical resistance, and biodegradability [6-9]. In addition, its low toxicity to organisms and high biocompatibility have led to much research into its use as a biomaterial [10, 11]. In particular, PVA hydrogel (PVA-H), which is gelling by physical cross-linking, is suitable as a biomaterial because, unlike chemical crosslinking, it does not require toxic crosslinking agents [12]. For example, it is used as a contact lens because of its high transparency and high water content [13]. It is also used as a cell scaffold material in tissue engineering [5].

PVA-H with physical crosslinking exhibits very high mechanical strength due to the formation of microcrystals by hydrogen bonds resulting. Bray et al. first reported on the application of PVA-H to artificial cartilage, its application has been extensively studied [14]. This is because PVA-H exhibits mechanical and frictional properties comparable to those of biological articular cartilage and is highly biocompatible. However, most PVA-H is prepared using the freeze-thaw (FT) method [15]. PVA-H produced by the FT method is opaque, cloudy, and has low mechanical strength due to phase separation between the concentrated and diluted layers during ice crystallization. In addition, problems such as melting of crystallites and over-crystallization after a long period of time exist [16]. These are problems that must be considered for long-term use such as artificial cartilage.

Hyon et al. prepared clear, high mechanical strength PVA-H by low temperature

crystallization (LTC) method at -20 °C in a mixture of water and dimethyl sulfoxide (DMSO) [17]. However, the use of DMSO, an organic solvent, for PVA-H as a biomaterial is problematic. Recently, Sakaguchi et al. reported that PVA-H, which is transparent and has very high mechanical strength, can be prepared by hot pressing with only water and PVA [18]. In addition, this technique does not require PVA to be dissolved in water, making it possible to prepare PVA-H at concentrations as high as 50 wt%. This is a material that holds promise for applications such as artificial cartilage. However, joints and cartilage are known to be subjected to very strong loads, and it is unknown to what extent PVA-H will be resistant to such loads.

Many high strength PVA-H have been developed by various methods, including chemical crosslinking such as double network (DN) gels [19, 20]. However, the most commonly used PVA is atactic PVA (aPVA). aPVA exhibits a random arrangement of side chains with hydroxyl groups relative to the main chain and has limited crystallinity. Therefore, the mechanical strength obtained is also limited. Syndiotactic PVA (sPVA) is a PVA with higher crystallinity than aPVA. sPVA has a structure in which the side chains, hydroxyl groups, are arranged alternately and regularly with respect to the main chain. Although sPVA exhibits superior mechanical strength and crystallinity compared to aPVA, it is generally rarely used. This is because sPVA is almost insoluble in water and DMSO, making it difficult to handle and impractical.

The synthesis method of sPVA is almost identical to that of aPVA, but the starting monomer is different. Several studies have reported methods to improve the syndiotacticity of PVA. Yamada et al. and Nagara et al. reported that PVA with high syndiotacticity can be synthesized by free radical polymerization of vinyl acetate (VAc) in fluoroalcohol as a solvent [21, 22]. Free radical polymerization of vinyl esters with bulky substituents as shown in Figure 4-1 is generally widely used. This is due to the steric hindrance caused by the neighboring substituents. In particular, vinyl pivalate (VPi) is often used because sPVA with a high degree of polymerization can be

prepared. The sPVA used in this study is also produced by free radical polymerization of VPi as a monomer and saponification.

In this study, sPVA hydrogel (sPVA-H) were prepared using sPVA (in this study, syndiotactic rich PVA that also has atactic in its structure) by a hot press method that does not require dissolution in water for application to materials requiring high strength and high elastic modulus such as artificial joint cartilage. The products were then heat-treated at several temperatures and evaluated in comparison with aPVA hydrogel (aPVA-H) in terms of water content, mechanical strength, and thermophysical properties.

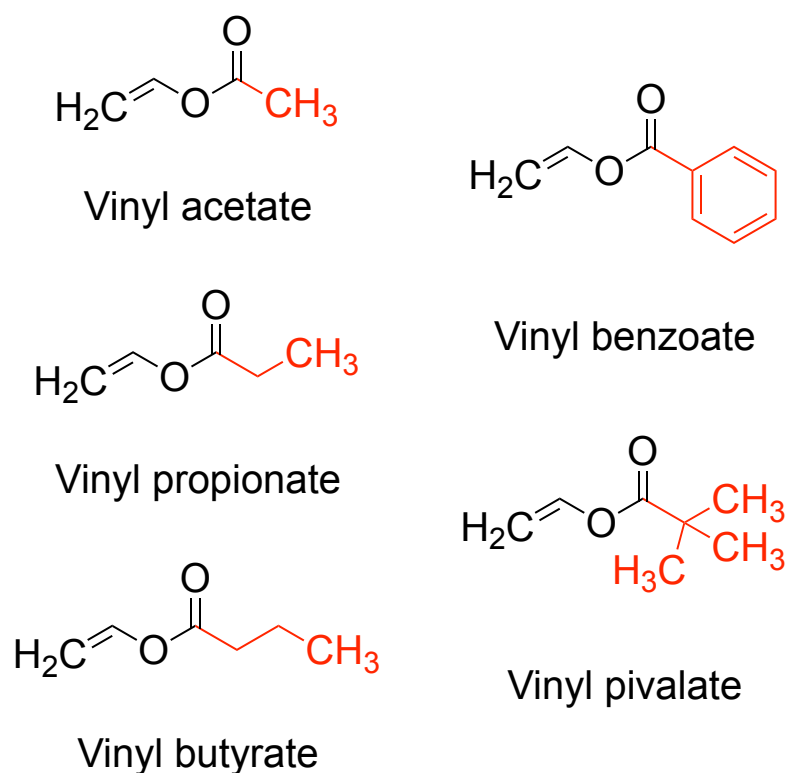


Figure 4-1 Vinyl monomers commonly used in the synthesis of sPVA.

## 4-2. Materials and methods

### 4-2-1. Materials

sPVA and aPVA were provided by Japan VAM & POVAL (Osaka, Japan). sPVA had a degree of polymerization of 1700 and 99.0 mol% saponification. aPVA had a degree of polymerization of 1700 and 99.8 mol% saponification. DMSO-d<sub>6</sub> was purchased from Kanto Chemical CO., INC. (Tokyo, Japan). Distilled water was used throughout the experimental system.

### 4-2-2. Gelation of PVA

PVA-H was formed by the hot press method. aPVA/water = 50/50 by weight in the case of aPVA was stirred well and PVA was allowed to swell for 15 minutes. The mixture was spread uniformly on a 2 mm thick mold and hot pressed in a hot press machine (ASONE, Osaka, Japan) set at 95 °C. Hot pressing was performed at 2 MPa for 5 minutes, then at 10 MPa for 10 minutes, and finally at 20 MPa for 15 minutes. After removal from the hot press, the product was allowed to gel at room temperature for 2 days while held in the mold. Finally, vacuum drying was performed for at 2 days. For gelation of sPVA, sPVA/water = 40/60 by weight is stirred well and PVA is allowed to swell for 15 minutes. The mixture was spread uniformly in a 2 mm thick mold and hot pressed in a hot press machine set at 130 °C. The hot press conditions and gelation were the same as for aPVA. The hydrogels prepared were aPVA-H and sPVA-H. Gelation by the hot press method and prepared PVA-H are shown in Figure 4-2. Figure 4-3 shows sPVA that was attempted to dissolve in a mixture of DMSO and water, but was barely soluble.

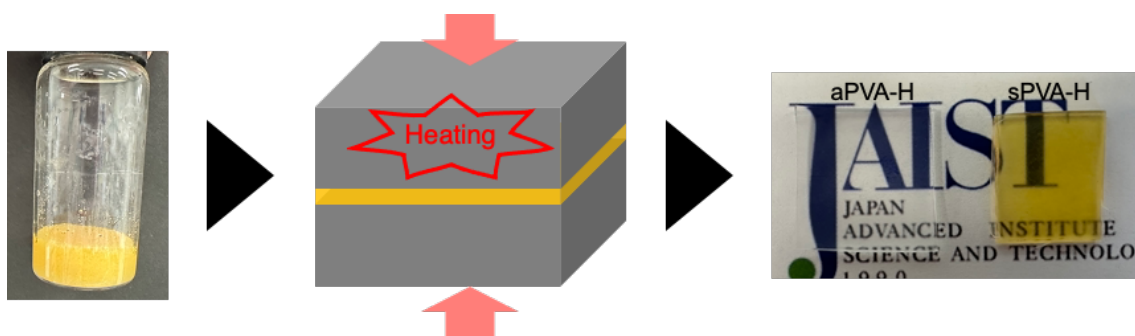


Figure 4-2 Gelation of PVA by hot press method.



Figure 4-3 sPVA not dissolved in a mixture of DMSO and water.

#### 4-2-3. Heat-treatment and swelling

Heat-treatment was performed in vacuum state on both aPVA-H and sPVA-H. A vacuum oven set to the specified temperature was used and the following conditions were used: 100 °C, 1 hour; 150 °C, 1 hour; 180 °C, 1 hour. Samples heat-treated at 100 °C were designated aPVA100 and sPVA100, samples heat-treated at 150 °C were designated aPVA150 and sPVA150, and samples heat-treated at 180 °C were designated aPVA180 and sPVA180. After completion of the heat treatment, the samples were hydrated in distilled water for 3 days, except for those used in the measurement in the dry state.

#### 4-2-4. Measurement

##### 4-2-4-1. Nuclear magnetic resonance (NMR)

<sup>1</sup>H-NMR was used to calculate the tacticity [*S*]-*triad* of PVA. DMSO-d<sub>6</sub> was used as solvent. [*S*]-*triad* (%) is an indicator of the syndiotacticity of PVA. <sup>1</sup>H-NMR of PVA shows three characteristic hydroxyl proton peaks, [*H*], [*I*], and [*S*]. Here, the peak appearing at the lowest field indicates isotactic [*I*]. The peak appearing in the middle indicates atactic (heterotactic) [*H*], and the peak appearing at the highest magnetic field is syndiotactic [*S*]. The [*S*]-*triad* (%) was calculated using the following eq. (4-1) for the integral ratio of each hydroxyl proton.

$$[S] - triad (\%) = \frac{[S]}{[I] + [H] + [S]} \times 100 \quad (4 - 1)$$

##### 4-2-4-2. Water content

The water content of aPVA-H and sPVA-H was measured by allowing PVA-H in a dry state to become hydrated for 3 days at room temperature. Water content  $W_c$  (%) was calculated using eq. (4-2).

$$W_c (\%) = \frac{W_{wet} - W_{dry}}{W_{wet}} \times 100 \quad (4 - 2)$$

where  $W_{wet}$  is the weight of PVA-H in the hydrated state and  $W_{dry}$  is the weight of PVA-H in the dry state.

##### 4-2-4-3. Fourier transform infrared spectroscopy (FT-IR)

Fourier transform infrared spectroscopy (FT-IR) was measured by attenuated total reflection (ATR) method using FT/IR 4X (JASCO, Tokyo, Japan). Spectra were obtained by scanning 16 times with a resolution of 4 cm<sup>-1</sup>. The measurement range was 4000~400 cm<sup>-1</sup>. The crystallinity  $X_c$  (%) of PVA-H was calculated using eq. (4-3) reported by Tretinnikov et al [23].

$$X_c (\%) = -13.1 + 89.5 \left( \frac{A_{1144}}{A_{1094}} \right) \quad (4 - 3)$$

Where  $A_{1144}$  is the absorbance at  $1144\text{ cm}^{-1}$  and  $A_{1094}$  is the absorbance at  $1094\text{ cm}^{-1}$

#### 4-2-4-4. Differential scanning calorimetry (DSC)

The melting points of aPVA-H and sPVA-H in the dry state were determined by differential scanning calorimetry (DSC) (DSC6200, Seiko Instruments, Tokyo, Japan). 10~20 mg of dried PVA-H was placed in an aluminum pan and sealed with a sealer. An empty aluminum pan was used as the reference material and the temperature was measured at a rate of  $10\text{ }^{\circ}\text{C}/\text{min}$  from 0 to  $300\text{ }^{\circ}\text{C}$  under a nitrogen atmosphere.

#### 4-2-4-5. Tensile test

Tensile tests of aPVA-H and sPVA-H in the water-containing state were performed in water using an Autograph AGS-J (Shimadzu Corporation, Kyoto, Japan) fitted with a 100 N load cell with a water tank. Specimen sizes were as shown in Figure 4-4. The material was elongated to failure at a rate of  $5\text{ mm}/\text{min}$ . Young's modulus was calculated based on Hooke's law from a crinkle between 0.1 and 0.5 mm. Three measurements were taken for each sample, and the average value was calculated.

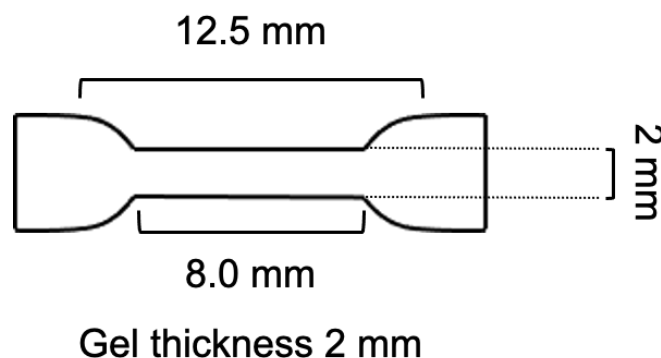


Figure 4-4 Shape of dumbbell-shaped specimen.

#### 4-2-4-6. Wide-angle X-ray diffraction (WAXD)

Wide-angle X-ray diffraction measurements were performed to analyze the amount of crystals in the dried state of PVA-H. CuK $\alpha$  rays were generated at a voltage of 45 kV and a current of 200 mA, and the irradiation time was 5 minutes. The camera length was 27 mm and the X-ray transmission width was 2 mm for all samples, irradiated in the cross-sectional direction of the hydrogel.

#### 4-2-4-7. Small-angle X-ray scattering (SAXS)

Small-angle X-ray scattering measurements were performed to analyze the crystalline state of dried PVA-H. CuK $\alpha$  rays were generated at a voltage of 45 kV and a current of 200 mA, and the irradiation time was 3 hours. The camera length was 300 mm and the sample thickness was 2 mm.

### 4-3. Results and discussion

#### 4-3-1. Syndiotacticity

Figure 4-5 shows the  $^1\text{H}$ -NMR spectra of aPVA and sPVA. It is necessary to note here the three peaks of hydroxyl protons of PVA that appear around 4 to 5 ppm. Three peaks of hydroxyl group protons appear, which differ according to the tacticity of PVA. [*S*]-*triad* is one of the indicators of the syndiotacticity of PVA. The [*S*]-*triad* of aPVA and sPVA calculated from NMR spectra was 28.8 % and 36.8 %, respectively.

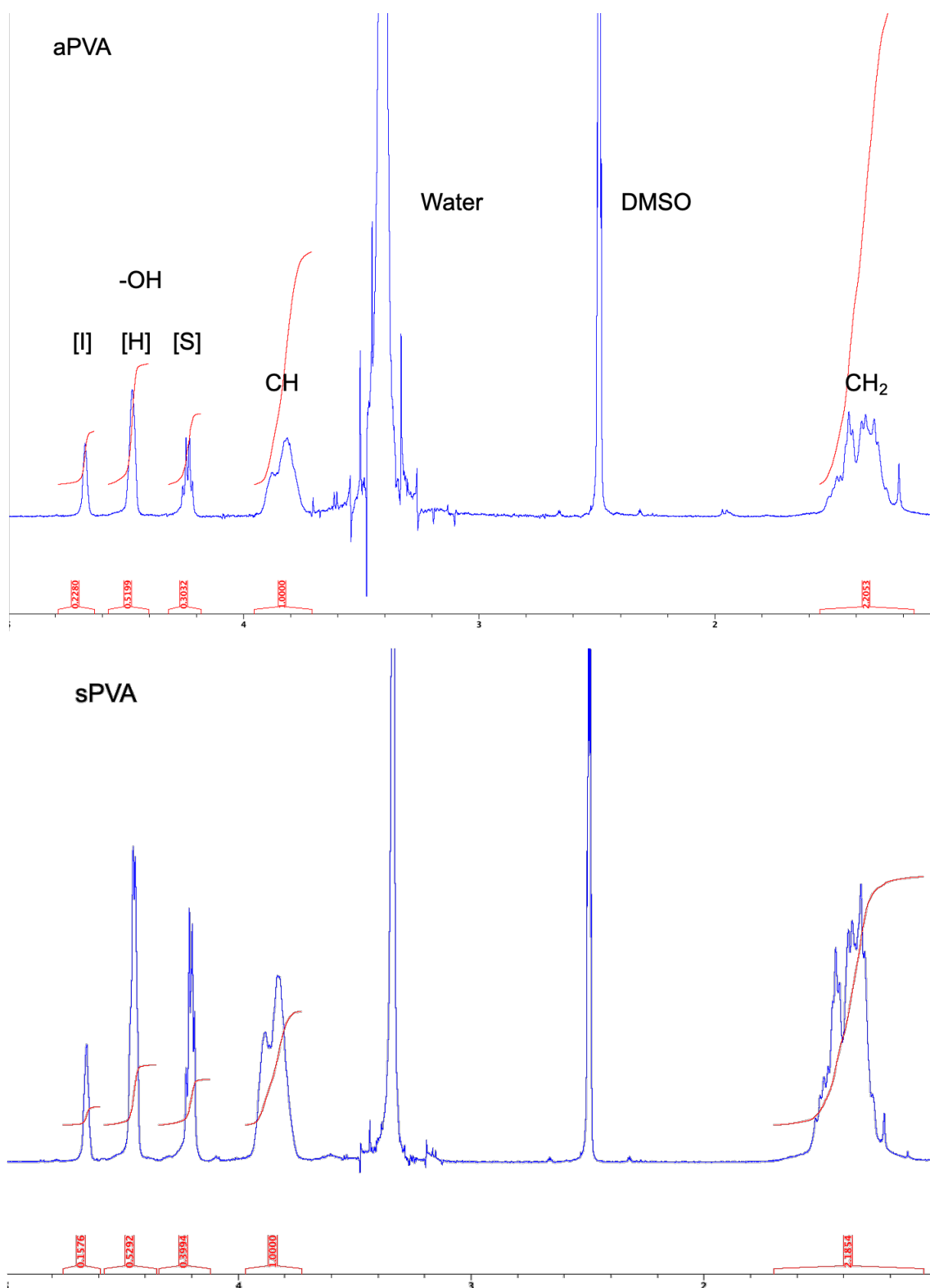


Figure 4-5 <sup>1</sup>H-NMR spectra of aPVA and sPVA.

#### 4-3-2. Water content

Figure 4-6 shows the results of water content measurements. In all heat treatment conditions, sPVA-H had lower water content than aPVA-H. When heat-treated at 100 °C, the water content of aPVA-H was 60.0 %, while that of sPVA-H was 36.5 %, showing a nearly twice difference even at the same heat treatment temperature. Overall, the water content of aPVA-H decreases with increasing heat treatment temperature. However, in the case of sPVA-H, the water content decreases from 36.5 % to 29.6 % when the temperature goes from 100 °C to 150 °C, but little change is seen thereafter, around 25 %. This suggests that the water content of sPVA-H can be controlled by heat treatment at lower temperature or shorter time than that of aPVA-H. The reason for the low water content of sPVA-H is thought to be its high tacticity, which makes it easy to crystallize. Regularly arranged hydroxyl groups easily form hydrogen bonds and easily crystallize [24]. Highly crystallized PVA then has lower water content due to lower interaction with water. Another factor contributing to the lower water content is that PVA-H made by the hot press method has a higher initial concentration of PVA than PVA-H made by the LTC method, resulting in a higher molecular density and easier crystallization [18].

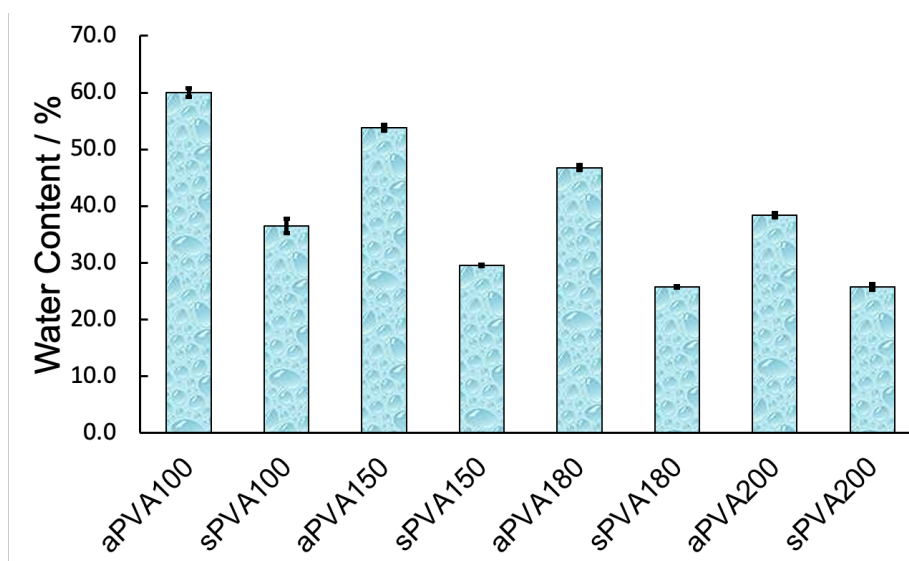


Figure 4-6 Water content of heat-treated aPVA-H and sPVA-H.

### 4-3-3. FT-IR

The structure of crystalline polymers containing hydroxyl groups, such as PVA, can be characterized by the amount of crystallization and the hydrogen bonding system. Within this range, there is an absorption band with a maximum at  $1094\text{ cm}^{-1}$  formed by the overlap of the bands of C-O stretching vibrations of the COH groups, and a band with a maximum at  $1144\text{ cm}^{-1}$  due to crystallization of the PVA. In particular, the intensity of the band at  $1144\text{ cm}^{-1}$  increases with increasing crystallinity of PVA [25, 26]. Tretinnikov et al. reported that the above effects allow the IR spectra to be used to calculate the crystallinity of PVA [23]. In this chapter, as in Chapter 3, the spectra at  $3000\sim 3600\text{ cm}^{-1}$  and  $1000\sim 1200\text{ cm}^{-1}$  were presented in detail and investigated. The crystallinity was also calculated from the spectra.

Figure 4-7(a) shows the IR spectra of aPVA-H and sPVA-H. (b) and (c) are enlarged. Looking at the bands corresponding to the stretching vibration of the hydroxyl group of PVA, the maximum of sPVA-H was shifted to a higher frequency region than that of aPVA-H. In addition, the peak intensity of sPVA-H is higher in the crystallization band at  $1144\text{ cm}^{-1}$ . This indicates that the crystalline amount of sPVA-H is clearly higher than that of aPVA-H.

The obtained IR spectra calculated crystallinity results are shown in Figure 4-8 and Table 4-1. Compared to aPVA-H, the crystallinity of sPVA-H is generally higher. It is also characteristic that the crystallinity increases as the heat treatment temperature increases. Heat-treatment is often used to increase the crystallinity of polymers including PVA and other materials. However, it is noteworthy here that even when heat-treated at the same temperature, a higher degree of crystallinity is observed for the sPVA-H. This indicates that sPVA crystallizes more easily than aPVA. It is also interesting to note that the crystallinity of aPVA180 is almost the same as that of sPVA100. In other words, sPVA can achieve a high degree of crystallinity even when heat-treated at low temperatures. In particular, heat treatment of sPVA-H at  $150\text{ }^{\circ}\text{C}$  or higher is the best means

to produce PVA-H with a crystallinity of 50 % or higher. As can be seen from the results, sPVA-H has a larger amount of microcrystals than aPVA-H, and it can be inferred that a stronger crosslinked structure is formed.

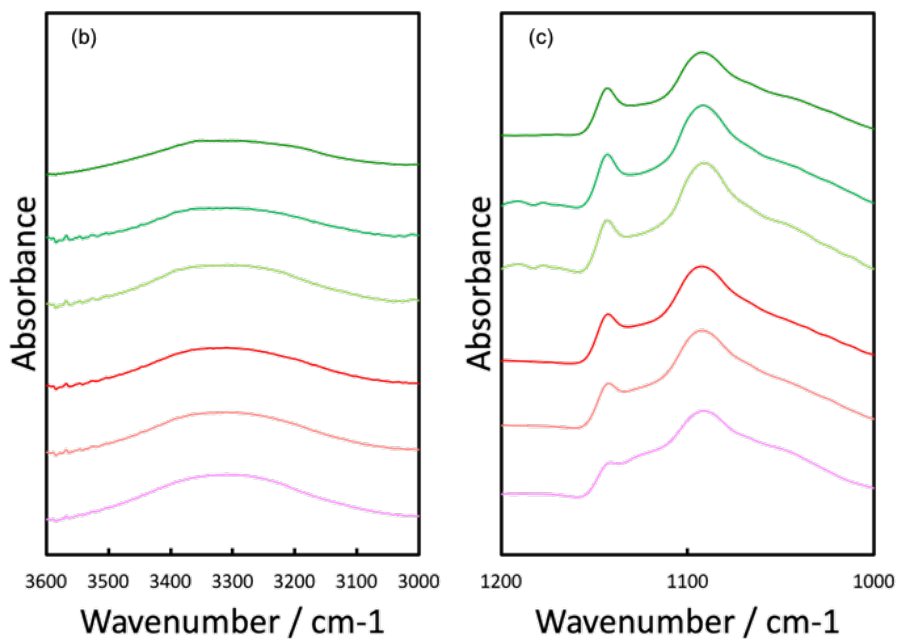
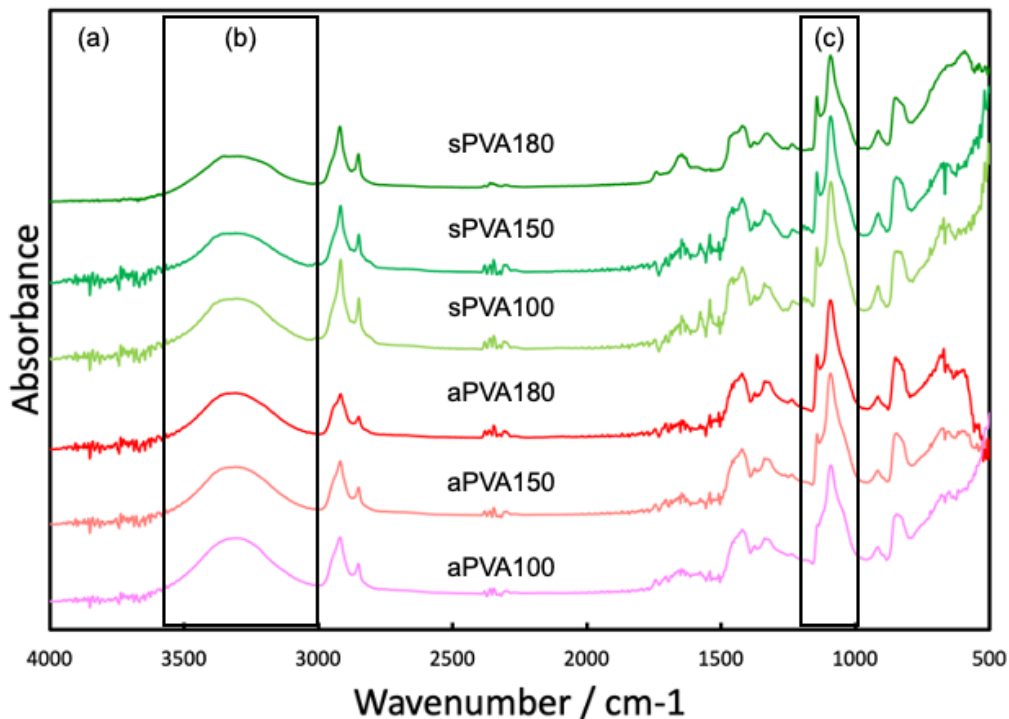


Figure 4-7 IR spectra of aPVA-H and sPVA-H.

(a) All, (b) 3000~3600  $\text{cm}^{-1}$ , and (c) 1000~1200  $\text{cm}^{-1}$

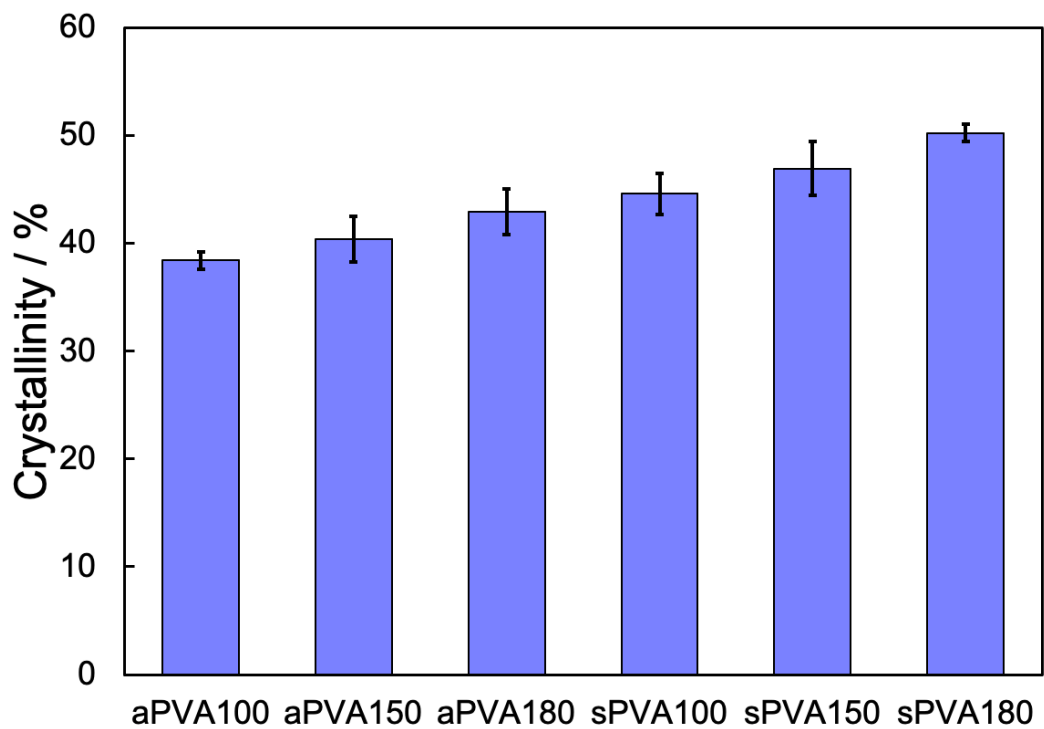


Figure 4-8 Comparison of crystallinity calculated from IR spectra.

Table 4-1 Crystallinity values calculated from IR spectra. ( $\pm$  Standard deviation)

Sample	Crystallinity / %
aPVA100	38.4 $\pm$ 0.8
aPVA150	40.4 $\pm$ 2.1
aPVA180	42.9 $\pm$ 2.1
sPVA100	44.6 $\pm$ 1.9
sPVA150	46.9 $\pm$ 2.5
sPVA180	50.2 $\pm$ 0.8

#### 4-3-4. DSC

Figure 4-9(a) and (b) are DSC heating curves of aPVA-H and sPVA-H in the dry state heated at a rate of 10 °C/min. The melting point of sPVA-H is more than 10 °C higher than that of aPVA-H. In other words, it is assumed that the crystal structure has been changed and the thickness of the lamellar crystals has increased. Since the melting point of aPVA100 is close to the value reported as the melting point of PVA, it is considered that in the case of aPVA, no change in the crystal structure occurs after heat treatment at 100 °C. However, in the case of sPVA100, the temperature is as high as 248.8 °C. In other words, it can be inferred that sPVA is easily crystallized. The melting point of aPVA-H also improved as the heat-treatment temperature increased, while the melting point of sPVA-H remained almost unchanged as the heat treatment temperature was increased. This indicates that crystals showing a high melting point have already been formed in sPVA-H. The heat-treatment causes a change in crystallinity, but the crystal structure itself shows little change. In the case of aPVA-H, it can be inferred that the crystal structure is changed to a crystal structure showing a high melting point by heat-treatment.

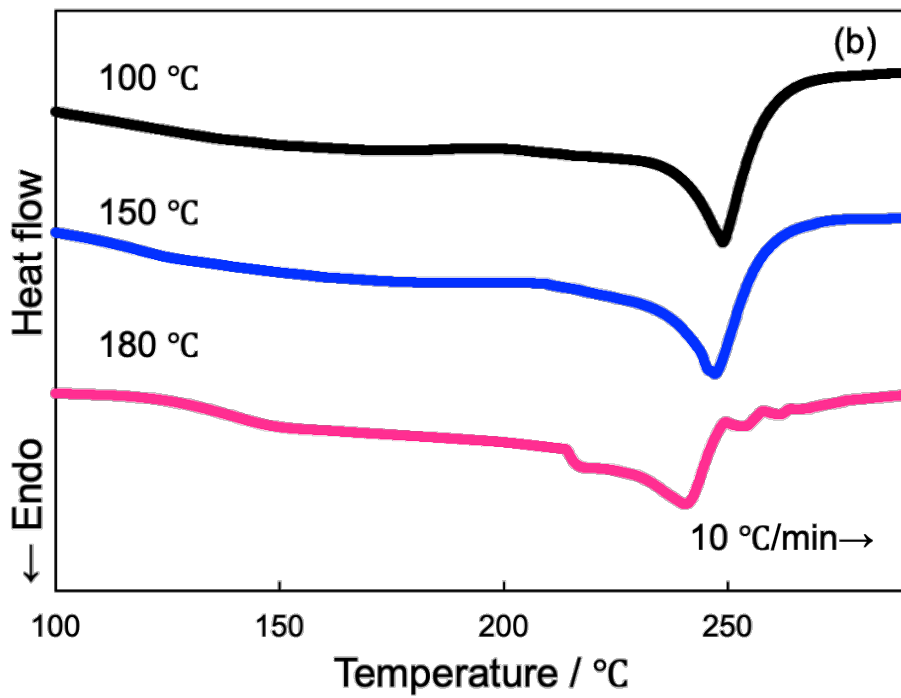
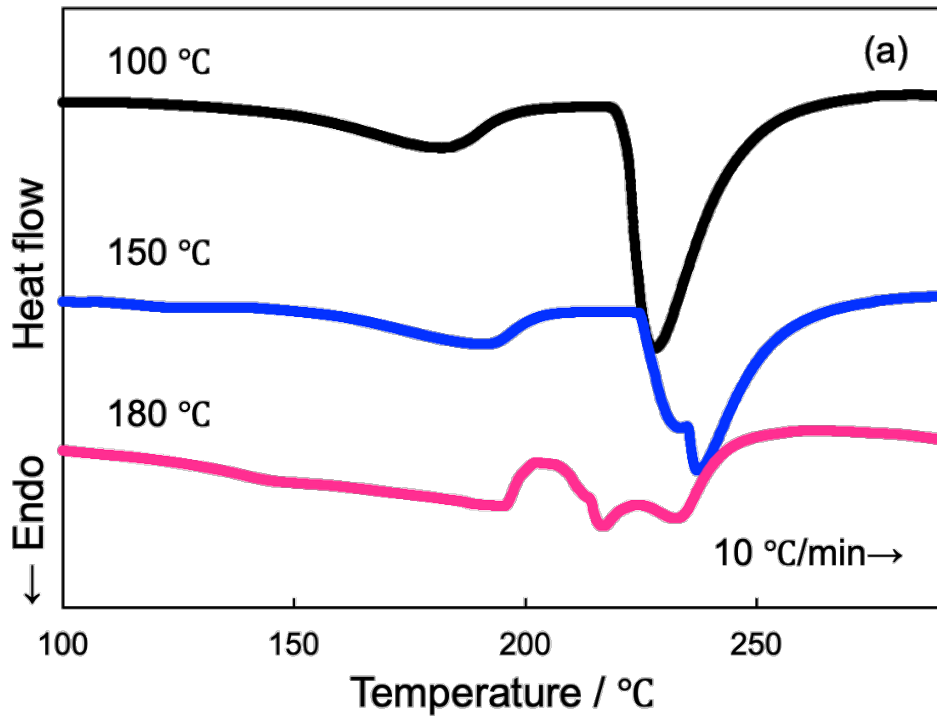


Figure 4-9 DSC heating curves. (a) aPVA-H, and (b) sPVA-H

#### 4-3-5. Tensile test

Figure 4-10 shows the Young's modulus results obtained from the tensile test. Compared to aPVA-H, sPVA-H shows some higher Young's modulus even at lower heat-treatment temperatures. In particular, sPVA180 showed the highest value of 58.8 MPa. This value is significantly higher than that of aPVA180. Even in the case of aPVA180, the value was lower than that of sPVA100. This indicates that sPVA-H has significantly higher mechanical properties than aPVA-H. In other words, Young's modulus improves with increasing heat treatment temperature in sPVA-H. The effect of this improvement is significantly higher than that of aPVA-H, and a level of high Young's modulus that cannot be achieved with aPVA-H can be achieved. However, although the sPVA exhibited a high Young's modulus, the amount of strain was very small, resulting in a hard and brittle gel state. This could possibly be improved by increasing the temperature and duration at the time of water impregnation, but in this case, there is also concern about a decrease in Young's modulus. There is also a possibility to control the Young's modulus of sPVA-H by changing the temperature and duration of heat-treatment.

Consideration is given to Young's modulus and water content obtained from tensile testing. In the case of sPVA100 and aPVA180, which had similar water content, sPVA100 showed a higher elastic modulus. This can be attributed to the fact that sPVA-H easily crystallizes at low heat treatment temperatures due to its excellent tacticity.

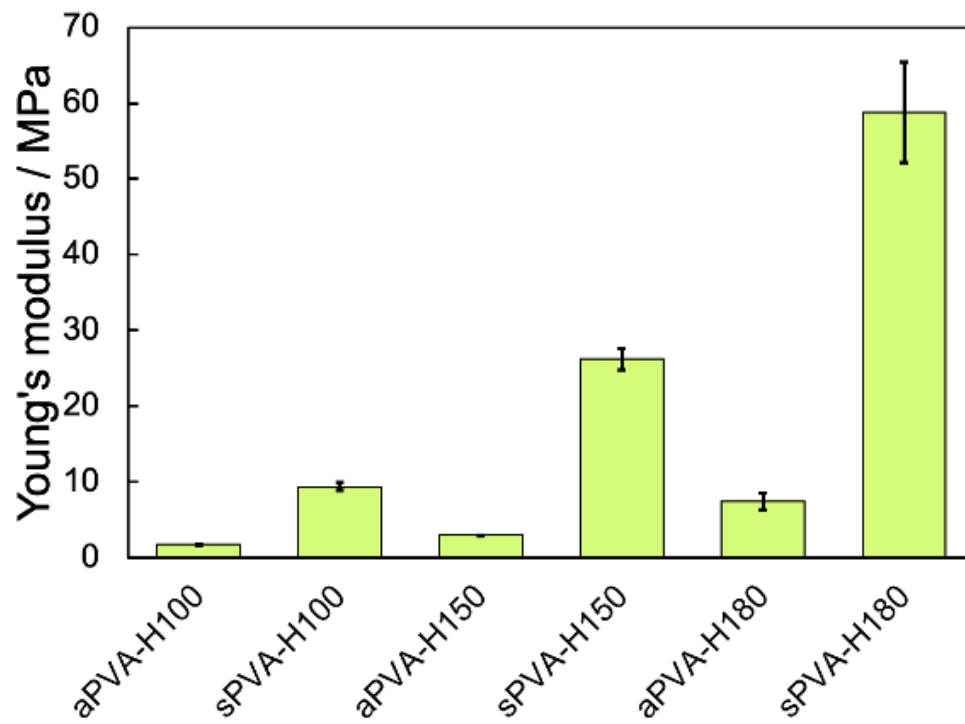


Figure 4-10 Young's modulus obtained by tensile testing.

#### 4-3-6. WAXD

Figure 4-11 shows the  $2\theta$  profiles at the equator of XRD of aPVA-H and sPVA-H measured in the dry state after heat treatment. For crystalline PVA there is a maximum peak at  $[10\bar{1}]$  ( $19.4^\circ$  ( $4.68 \text{ \AA}$ )) and a sharp crystalline reflection peak with a shoulder at  $[101]$  ( $20^\circ$  ( $4.43 \text{ \AA}$ )). In particular, the peak intensity at  $19.4^\circ$  depends on the crystalline amount of PVA; if it is broad, it indicates amorphous. These diffraction intensities are stronger when a larger amount of crystals are present. Clear peaks were observed for both aPVA-H and sPVA-H, suggesting that both have high crystallinity. In particular, the peak intensity is observed to be strongest for sPVA180, indicating that the amount of crystals is higher than for other hydrogels. However, the diffraction patterns are almost identical for aPVA and sPVA. In other words, the crystal structures of sPVA-H and aPVA-H are almost identical [24]. The crystal size distribution and other details need to be further investigated using small-angle X-ray scattering and neutron scattering methods.

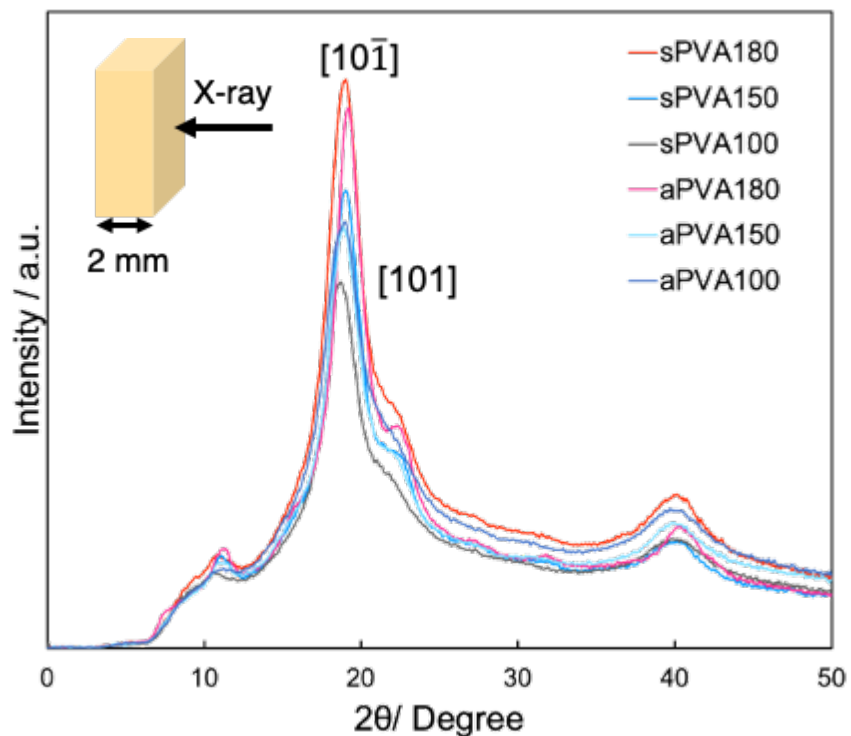


Figure 4-11  $2\theta$  profiles of aPVA-H and sPVA-H.

#### 4-3-7. SAXS

Figure 4-12 shows the SAXS profiles of aPVA-H and sPVA-H measured in the dry state after heat treatment. Broad scattering was observed at  $2\theta$  around  $0.9 \sim 1^\circ$ . This scattering indicates the average distance between microcrystalline structures. The value calculated from Bragg's law shown in Eq. (4-4) was 9 nm for aPVA. However, the value for sPVA100 was 9 nm, the same as that for aPVA, while sPVA150 and sPVA180 showed values of 10 nm or higher. In other words, the greater distance between the microcrystalline structures may be a factor in the gel's high elastic modulus but brittleness.

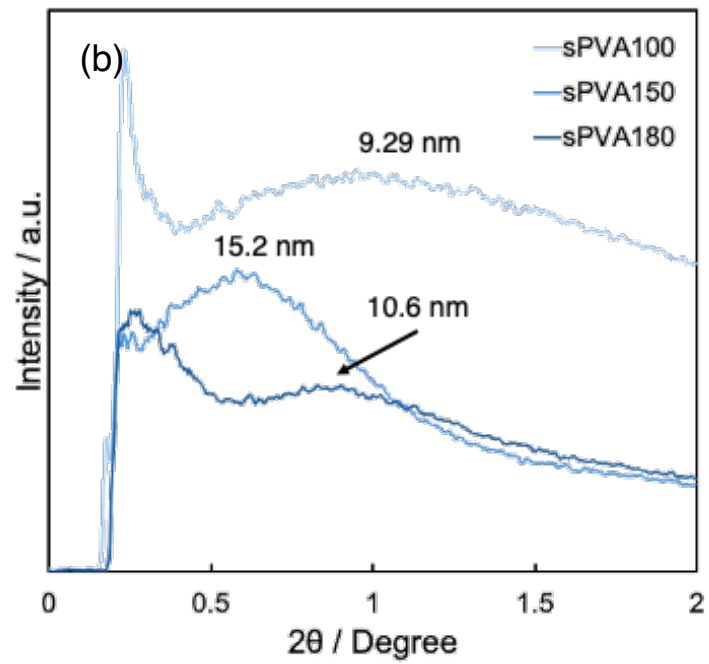
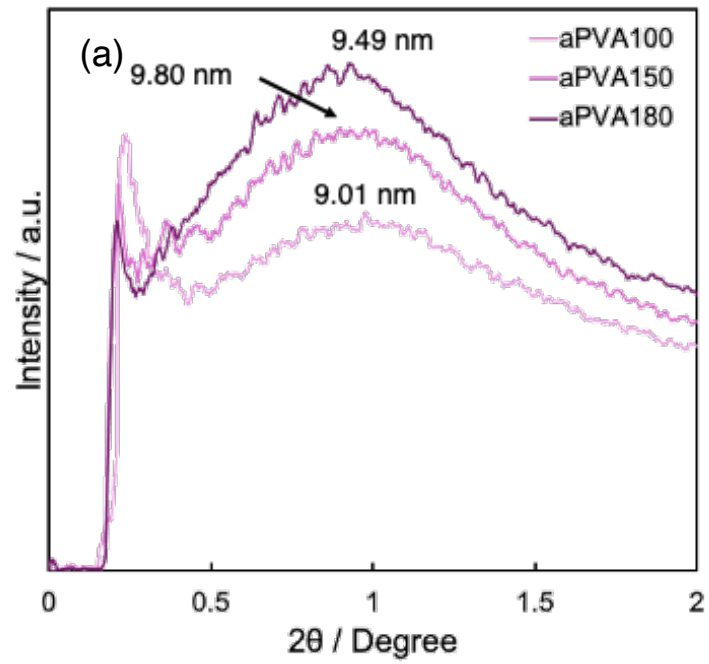


Figure 4-12 SAXS profiles of aPVA-H and sPVA-H.

(a) aPVA, (b) sPVA

$$n\lambda = 2d\sin\theta$$

(4 - 4)

#### **4-4. Conclusion**

sPVA-H was successfully formed by hot pressing. Hot-pressing is the best method for gelation of sPVA because it does not require dissolution in water. sPVA-H showed higher crystallinity with lower water content and higher Young's modulus than aPVA-H, even under the same heat treatment conditions. In other words, it was shown that sPVA-H had overwhelmingly better mechanical properties than aPVA-H, even though the hydrogels were prepared by the same method. This is presumably due to the superior tacticity (syndiotacticity) of sPVA compared to aPVA. Hydrogels made with sPVA exhibit mechanical properties that could not be achieved with aPVA, and are therefore expected to be used as artificial cartilage materials that are subjected to strong loads.

## 4-5. References

1. C.C. DeMerlis, D.R Schoneker, Review of the oral toxicity of polyvinyl alcohol (PVA), *Food and Chemical Toxicology*, Vol.41 (3) p319-326 (2003)
2. J. Ma, X. Ye, B. Jin, Structure and application of polarizer film for thin-film-transistor liquid crystal displays, *Displays*, Vol.32 (2) p49-57 (2011)
3. A.A. Oun, G.H. Shin, J.W. Rhim, J.T. Kim, Recent advances in polyvinyl alcohol-based composite films and their applications in food packaging, *Food Packaging and Shelf Life*, Vol.34 100991 (2022)
4. Y. Liu, S. Wang, W. Lan, Fabrication of antibacterial chitosan-PVA blended film using electrospray technique for food packaging applications, *International Journal of Biological Macromolecules*, Vol.107 (Part A) p848-854 (2018)
5. A. Karimi, M. Navidbakhsh, Mechanical properties of PVA material for tissue engineering applications, *Materials Technology*, Vol.29 (2) p90-100 (2014)
6. E. Chiellini, A. Corti, S. D'Antone, R. Solaro, Biodegradation of poly (vinyl alcohol) based materials, *Progress in Polymer Science*, Vol.28 (6) p963-1014 (2003)
7. T.S. Gaaz, A.B. Sulong, M.N. Akhtar, A.A.H. Kadhumj, A.B. Mohamad, A.A. Al-Amiery, Properties and Applications of Polyvinyl Alcohol, Halloysite Nanotubes and Their Nanocomposites, *Molecules*, Vol.29 (12) p22833-22847 (2015)
8. M. Aslam, M.A. Kalyar, Z.A. Raza, Polyvinyl alcohol: A review of research status and use of polyvinyl alcohol based nanocomposites, *Polymer Engineering and Science*, Vol.58 (12) p2119-2132 (2018)
9. N.B. Halima, Poly(vinyl alcohol): review of its promising applications and insights into biodegradation, *RSC Advances*, 6 p39823-39832 (2016)
10. M.I. Baker, S.P Walsh, Z. Schwartz, B.D. Boyan, A review of polyvinyl alcohol and its uses in

- cartilage and orthopedic applications, *Journal of Biomedical Materials Research Part B Applied Biomaterials*, Vol.100B (5) p1451-1457 (2012)
11. M. Teodorescu, M. Bercea, S. Morariu, Biomaterials of Poly(vinyl alcohol) and Natural Polymers, *Polymer Reviews*, Vol.58 (2) p247-287 (2018)
  12. M.H. Alves, B.E.B. Jansen, A.A.A. Smith, A.N. Zelikin, Poly(Vinyl Alcohol) Physical Hydrogels: New Vista on a Long Serving Biomaterial, *Macromolecular Bioscience*, Vol.11 (10) p1293-1313 (2011)
  13. P. Yusong, D. Jie, C. Yan, S. Qianqian, Study on mechanical and optical properties of poly(vinyl alcohol) hydrogel used as soft contact lens, *Materials Technology*, Vol.31 (5) p266-273 (2016)
  14. J.C. Bray, E.W. Merrill, Poly(vinyl alcohol) hydrogels for synthetic articular cartilage material, *Journal of Biomedical Materials Research*, Vol.7 (5) p421-443 (1973)
  15. H. Adelnia, R. Ensandoost, S.S. Moonshi, J.N. Gavгани, E.I. Vasafi, H.T. Ta, Freeze/thawed polyvinyl alcohol hydrogels: Present, past and future, *European Polymer Journal*, Vol.164 (5) 110974 (2022)
  16. C.M. Hassan, N.A. Peppas, Structure and Morphology of Freeze/Thawed PVA Hydrogels, *Macromolecules*, Vol.33 (7) p2472-2479 (2000)
  17. S.H. Hyon, W.I. Cha, Y. Ikeda, Preparation of transparent poly(vinyl alcohol) hydrogel, *Polymer Bulletin*, Vol.22 p119-122 (1989)
  18. T. Sakaguchi, S. Nagano, M. Hara, S.-H. Hyon, M. Patel, K. Matsumura, Facile preparation of transparent poly(vinyl alcohol) hydrogels with uniform microcrystalline structure by hot-pressing without using organic solvents, *Polymer Journal*, Vol.49 p535-542 (2017)
  19. Y. Zhang, M. Song, Y. Diao, B. Li, L. Shi, R. Ran, Preparation and properties of polyacrylamide/polyvinyl alcohol physical double network hydrogel, *RSC Advances*, Vol.6 (113) p112468-112476 (2016)

20. B. Hou, X. Li, M. Yan, O. Wang, High strength and toughness poly (vinyl alcohol)/gelatin double network hydrogel fabricated via Hofmeister effect for polymer electrolyte, *European Polymer Journal*, Vol.185 (17) 111826 (2023)
21. K. Yamada, T. Nakano, Y. Okamoto, Stereospecific polymerization of vinyl acetate in fluoroalcohols Synthesis of syndiotactic poly(vinyl alcohol), *Proceedings of the Japan Academy, Series B*, Vol.74 (3) p46-49 (1998)
22. Y. Nagara, K. Yamada, T. Nakano, Y. Okamoto, Stereospecific Polymerization of Vinyl Acetate in Fluoroalcohols and Synthesis of Syndiotactic Poly(vinyl alcohol), *Polymer Journal*, Vol.33 p534-539 (2001)
23. O.N. Tretinnikov, S.A. Zagorskaya, Determination of the degree of crystallinity of poly(vinyl alcohol) by FTIR spectroscopy, *Journal of Applied Spectroscopy*, Vol.79 (4) p521-526 (2012)
24. Y. Nagara, T. Nakano, Y. Okamoto, Y. Gotoh, M. Nagura, Properties of highly syndiotactic poly(vinyl alcohol), *Polymer*, Vol.42 (24) p9679-9686 (2001)
25. S.A. Zagorskaya, O.N. Tretinnikov, Infrared Spectra and Structure of Solid Polymer Electrolytes Based on Poly(vinyl alcohol) and Lithium Halides, *Polymer Science, Series A*, Vol.61 p21-28 (2019)
26. H. Tadokoro, S. Seki, I. Nitta, The Crystallinity of Solid High Polymers. I. The Crystallinity of Polyvinyl alcohol Film, *Bulletin of the Chemical Society of Japan*, Vol.28 (8) p559-564 (1955)

## *Chapter 5: General Conclusion*

## Chapter 5: General Conclusion

### 5-1. Conclusion

The high mechanical properties, biodegradability, and biocompatibility of PVA make it a polymeric material that will play an important role in achieving the Sustainable Development Goals (SDGs). PVA has hydroxyl groups and is water soluble. Therefore, there is no need to use organic solvents or other chemicals that pollute the environment or are toxic to the human body during processing. However, there are many problems with processing using only water as a solvent. In this thesis, I developed functional PVA materials with low environmental impact and low toxicity to living organisms without the use of organic solvents such as DMSO. In the following, I summarize what I have identified in each chapter.

In Chapter 2, I investigated the improvement of ductility and mechanical properties of PVA fibers obtained by wet spinning with the addition of lithium salts. LiI, which has been reported in previous studies, was employed as a lithium salt that is highly effective in inhibiting hydrogen bonding between PVA molecular chains; the stretchability of PVA fiber with LiI added was greatly improved. The improved stretchability allowed for stretching at higher drawing ratios and increased molecular orientation. The advanced molecular orientation significantly increased the Young's modulus and tensile stress of the PVA fiber. The enhancement of the stretchability leading to the improvement in molecular orientation is attributed to the suppression of hydrogen bonding by the addition of LiI, resulting in lower crystallinity. Almost all of the LiI can be removed during the wet spinning process and by washing. Subsequently, strong hydrogen bonds are formed again, resulting in excellent mechanical properties.

In Chapter 3, the effect of lithium salt (lithium halide) on PVA prepared by hot-pressing at a

high concentration (56 wt%) was investigated in terms of mechanical properties in the dry state and thermoplasticity due to a decrease in melting point. Lithium salts decreased the melting point and crystallinity of PVA. As a result, mechanical properties were also reduced. This may be due in part to the hydration power of the halide ions, with Cl<sup>-</sup> being particularly hydrophilic and retaining more water molecules. This suggests that more water remains in LiCl PVA. It was confirmed that the lithium salt added PVA is thermoplastic, as it can be remolded by hot press. It was also found that the physical properties of PVA before and after thermoforming were hardly affected. In other words, the addition of lithium salt is an effective means of improving the processability of PVA.

In Chapter 4, I established a gelation method using sPVA with high steric regularity, which is different from aPVA used so far, for application to artificial joint cartilage, and investigated the difference in physical properties between sPVA and aPVA. sPVA-H exhibited lower water content than aPVA-H. In addition, the higher melting point and crystallinity suggest a higher crystalline volume and thicker lamellar crystals. Even for hydrogels prepared by the same method, sPVA-H shows better mechanical properties. This is because sPVA-H has a structure that is easy to crystallize due to its superior tacticity. In other words, those that exhibit high mechanical properties, such as sPVA-H, are expected to be applied to artificial joint cartilage, which is subjected to strong loads over a long period of time.

## **5-2. Future scope**

Water soluble, biocompatible synthetic polymers such as PVA are versatile and play an important role in our lives. The high strength PVA fiber with the addition of lithium salt obtained in this thesis is expected to play an active role as a new reinforcing fiber in the field of composite materials. Furthermore, thermo-plasticization of PVA can improve its processability and is expected to be used in more fields. In addition, biomaterials that can be produced using PVA hydrogels could lead to better medical care for all. However, many issues were found in these studies. In particular, future detailed studies on the physical properties after thermoforming are essential for the addition of thermoplasticity by lithium salts. In addition, the effects of sPVA-H on cells and adhesion compared to aPVA-H must also be evaluated. Although PVA has been the subject of much research around the world, further studies are expected to lead to new applications of PVA as a new material.

# Achievements

## Publications

1. **Yusuke Taoka**, Riza Asmaa Saari, Takumitsu Kida, Masayuki Yamaguchi, Kazuaki Matsumura, Enhancing the Mechanical Properties of Poly (vinyl alcohol) Fibers by Lithium Iodide Addition, ACS Omega Volume 8, Issue 36, pp.32623-32634 (2023)

## Presentation

### International Conferences

1. **Yusuke Taoka**, Riza Asmaa Saari, Takumitsu Kida, Masayuki Yamaguchi, Kazuaki Matsumura, Spinning of high-strength Poly (vinyl alcohol) fiber with high orientation - Approach by addition of salt-, The 33rd Annual Conference of the European Society for Biomaterials, Davos, Switzerland, September 2023. (Poster)
2. **Yusuke Taoka**, Miyu Nakazawa, Kazuaki Matsumura, Facile preparation of hydrogel with high mechanical strength by syndiotactic rich Poly (vinyl alcohol), The 33rd Annual Conference of the European Society for Biomaterials, Davos, Switzerland, September 2023. (RAPID FIRE presentation (Poster))

### Domestic Conferences

1. **田岡裕輔**、山口政之、松村和明 「ヨウ化リチウム添加による PVA 繊維の延伸性向上」 第 70 回高分子討論会 オンライン 2021 年 9 月 (ポスター発表)
2. **田岡裕輔**、山口政之、松村和明 「ヨウ化リチウム添加による高強度 PVA 繊維の開発」 第 70 回高分子学会北陸支部研究発表会 オンライン 2021 年 11 月 (口頭発表)
3. **田岡裕輔**、山口政之、松村和明、「リチウム塩添加によるポリビニルアルコール(PVA)

高強度繊維の開発」、第46回複合材料シンポジウム、オンライン、2021年10月（口頭発表）

4. **田岡裕輔**、「無機塩を用いたポリビニルアルコールの高機能化」、第40回流体科学におけるバイオ・医療に関する講演会、東北大学流体科学研究所、2022年7月
5. **田岡裕輔**、木田拓充、山口政之、松村和明、「ヨウ化リチウムを用いたポリビニルアルコール高強度繊維の開発」、第71回高分子討論会、北海道、2022年9月（口頭発表）
6. **田岡裕輔**、中澤美佑、松村和明、「シンジオタクチックポリビニルアルコールのゲル化と物性評価」、第11回日本バイオマテリアル学会北陸信越ブロック若手研究発表会、長野、2022年12月（口頭発表）